

1-1-2006

# A thermal approach to the generation of stable diblock copolymer templates using thin films.

Julie M. Leiston-Belanger  
*University of Massachusetts Amherst*

Follow this and additional works at: [https://scholarworks.umass.edu/dissertations\\_1](https://scholarworks.umass.edu/dissertations_1)

---

## Recommended Citation

Leiston-Belanger, Julie M., "A thermal approach to the generation of stable diblock copolymer templates using thin films." (2006).  
*Doctoral Dissertations 1896 - February 2014*. 1085.  
[https://scholarworks.umass.edu/dissertations\\_1/1085](https://scholarworks.umass.edu/dissertations_1/1085)

This Open Access Dissertation is brought to you for free and open access by ScholarWorks@UMass Amherst. It has been accepted for inclusion in Doctoral Dissertations 1896 - February 2014 by an authorized administrator of ScholarWorks@UMass Amherst. For more information, please contact [scholarworks@library.umass.edu](mailto:scholarworks@library.umass.edu).

312066 0325 0279 2

A THERMAL APPROACH TO THE GENERATION OF  
STABLE DIBLOCK COPOLYMER TEMPLATES USING THIN FILMS

A Dissertation Presented

By

JULIE M. LEISTON-BELANGER

Submitted to the Graduate School of the  
University of Massachusetts Amherst in partial fulfillment  
of the requirements for the degree of

DOCTOR OF PHILOSOPHY

May 2006

Polymer Science and Engineering

© Copyright by Julie M. Leiston-Belanger 2006

All Rights Reserved

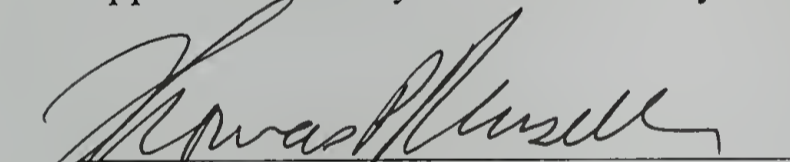
A THERMAL APPROACH TO THE GENERATION OF  
STABLE DIBLOCK COPOLYMER TEMPLATES USING THIN FILMS

A Dissertation Presented

By

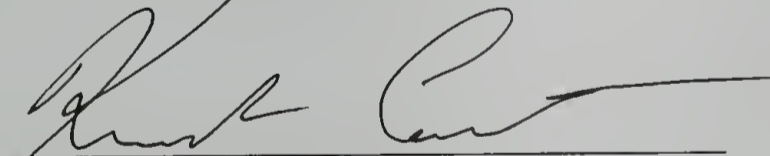
JULIE M. LEISTON-BELANGER

Approved as to style and content by:



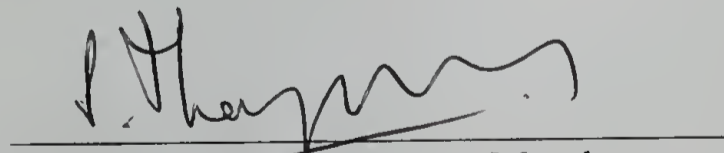
---

Thomas P. Russell, Chair



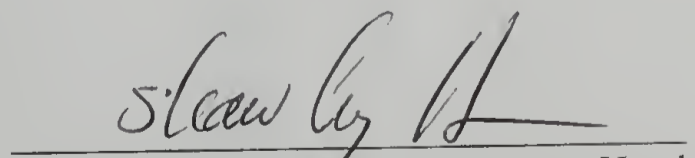
---

Kenneth Carter, Member



---

Sankaran Thayumanavan, Member



---

Shaw Ling Hsu, Department Head  
Polymer Science and Engineering

## DEDICATION

To my mother, Patricia, and brother, Michael.  
Thank you for your words of encouragement, support and  
humor when I needed them most.

To my loving husband, Jonathan, who has been very supportive of my scientific  
curiosities, and a constant source of motivation.

Also, to my late father, Lawrence, whom I know would be proud.

## ACKNOWLEDGMENTS

This thesis was reproduced in part with permission from:

Leiston-Belanger, J. M.; Russell, T. P.; Drockenmuller, E.; Hawker, C. J.  
*Macromolecules* **2005**, *38*, 7676-7683.

Leiston-Belanger, J. M.; Penelle, J.; Russell, T. P. *Macromolecules* **2006**, *ASAP*.

Copyright © 2005-2006 American Chemical Society

I would like to thank my funding sources, for without them my thesis would not have been possible. My funding was provided by the National Science Foundation sponsored Materials Research Science and Engineering Centers at the University of Massachusetts Amherst, Materials Research Laboratory at the University of California at Santa Barbara, and an NSF GOALI grant. I would also like to acknowledge the support of IBM through the IBM Fellowship Program.

The progress of my research was also influenced by several helpful collaborations. I am very grateful for the all the guidance and opportunities that were provided in collaboration with Professor Craig Hawker (UCSB), including the opportunity to work with Craig in his laboratories at IBM Almaden. I would like to thank Dr. Craig Silvis (DOW Chemical Company) for supplying the 3-bromobenzocyclobutene, and to Professor Eric Drockenmuller for the initial PSBCB polymer and the alkoxyamine initiator. Also, I would like to thank Professor Kevin Cavicchi for his help with the swelling experiments, Sally Swanson (IBM-Almaden) for the PM-IRRAS data, Jiayu Wang (UMass) for the electric field alignment data, and Suresh Gupta (UMass) for supplying the gold-coated silicon wafers. Many of the images in my dissertation were taken at the W.M. Keck Electron Microscopy

Laboratory that is part of the Materials Research Science and Engineering Center and the Silvio O. Conte National Center for Polymer Research at the University of Massachusetts Amherst. I would like to thank Lou Raboin and Evgenia Pekarskaya for their help with the TEM whenever it was needed. I also have a special thanks to Charlie Dickinson, who maintained and trained for all the NMRs here at UMass, and did a fantastic job doing so. I was fortunate enough to be an NMR czar and to be trained by Charlie on how to troubleshoot the software and hardware on the NMR. Thank you, Charlie, for your support and also for the fudge recipe. Many thanks, as well, to all of the PSE faculty and staff that I have not individually mentioned, for your passing words in the hallways, suggestions, and comments.

I have a special note of thanks to all of the secretaries and staff in the department for helping me to get through all of the paperwork (etc.) at UMass. Many thanks to Anne, Ann, Anita, Linda, Laurie, Sophie, and Vivien for helping to make sure the UMass system did not eat me alive, and thanks to Andre Melcuk for keeping the departmental server and computers up and running. I have a special thank you to Eileen for making my first years tolerable, especially during the time when paychecks were not coming and a cash advance was sorely needed.

While at the University of Massachusetts Amherst I had the opportunity to be a part of one of the largest groups in the department. I would like to thank all of my former and current group members for their support, both professionally and personally. I feel very fortunate to have such a diverse group, both culturally and scientifically. I would especially like to thank Kevin Cavicchi, Kris Lavery, Amanda Leach, Jiayu Wang, and Ting Xu for their positive attitudes and support throughout the years. Also, I



thank Jiun-tai Chen for his positive attitudes and motivation, especially towards his research project which has given new life to a project that I thought would disappear after I graduated. I also want to thank Matt Misner for many helpful discussions and free cups of quite excellent coffee. I could always count on Matt to help me out when I needed it, with support and his own special style of humor. James Sievert, a fellow Russell group member and classmate, has also been very helpful over the years. I appreciate all of the guidance, support and humor from all of the Russell group members, and even though I am not acknowledging in writing every single person, I recognize that everyone, as an individual, has made an impact during my years in the group, and I thank you.

In addition to the support I received from the Russell group, I also had the opportunity to interact with the Penelle group. During my first two years, I received useful synthetic chemistry advice from Professor Jacques Penelle and his group members. In particular, I would like to thank James Goldbach (a former group member of both Russell and Penelle groups) and Gabi Menges for supporting me through my first years, especially during the time when I was taking the cumulative examinations. Gabi always knew that a good shopping trip would cure all, even if it involved a random trip to Connecticut. I would also like to thank Sterling, the sole remaining Penelle group member, for his humor, kindness and support over the years. I could not imagine sharing a lab with a nicer person, or with better music. I only hope my next lab has a subwoofer. I am very grateful that I was able to continue my synthetic work in the Penelle group laboratories throughout my graduate studies.

Not only did I focus on my graduate work throughout grad school, but I also had the opportunity to work in the Outreach programs in the PSE department. I thank Greg Dabkowski, the outreach coordinator, for being a great friend and letting me try out all the new Outreach and ASPIRE toys. He let Joanna Pool and I have free range over the ASPIRE program, letting us revamp it and create new labs, such as the “fire-safe polymer” lab. It has been a great experience over the years and has helped me to realize that I really enjoy teaching.

In addition to my graduate work, I made a lot of friendships along the way. My close circle of friends, aka “the girls and some boys” or “the lunch crew”, have been extremely supportive. I seriously do not think I would have lasted the entire length of graduate school without them. My close friend and swim buddy Lachelle Arnt, who is now hiding in the toilet room at Clorox in California, has been helpful in keeping me sane. Her and her husband, Andy, always made things fun and interesting. Whether it was midday bread making, playing hooky to buy fish, or daily lunch conversations, I knew that if I were having a bad day, Lachelle would be there to cheer me up. Jen Craymer has also been immensely supportive. Jen, also my swim buddy, is one of the most positive, caring individuals I have ever met. She has been a constant source of encouragement and always knows the right things to say to help motivate me and to make me feel better. Melissa Light, now in sunny Oregon, is quite possibly one of the most energetic and motivated people that I know. We studied for the cumes together, passed them together, and in the process ate every snack imaginable to mankind. In addition, we made time for fun and entertainment, while also making sure that the outlet malls stayed in business. Ticora Jones has been a great friend, with Happy Bunny

wisdom and helpful insight. Whenever I needed to talk, she was there for me, chocolate in hand. Jessica McCoy has also been very supportive throughout these past few years. Jess has been very helpful and can always put things into perspective. Joanna Pool is also one of the most energetic people I know. She is caring, humorous, and never hesitant to help out a friend in need. Naomi Sanabria-Delong, her husband Chad, and Liz Glogowski have been constant sources of wit and humor. Both Naomi and Liz are closet DDR junkies, and size exclusion chromatography (SEC's) addicts. Their cheery attitudes, and helpfulness have been great. Jeremy Rathfon has been an entertaining friend, with many funny (and scary) stories about his antics out in the wilds of New Hampshire. I appreciate Jeremy's laid-back attitude; it is a nice change from my inevitable high-strung-ness. Steve Eyles has been a constant source of hilarious British humor and has made my entire experience with the upkeep of the SEC equipment entertaining. I know I could always count on Steve to put things into perspective and to make me laugh even when I wanted to throw the SEC equipment off the roof. I feel so lucky to have such good friends.

I would also like to thank my friends from back in Rochester, NY. We all grew up together and graduated from Churchville-Chili High School, class of '97. My good friend Tricia Murphy has always been there for me. Her generosity and kindness has helped me keep my sanity throughout my undergraduate and graduate studies. Jolene Hasseler and I have come a long way from those elementary school bus rides and Pound Purries. Jolene is one of the strongest people I know. She is the epitome of "falling off a horse and getting right back on" - literally. Barb Swartzfager has also been a source of support, with her kind and caring attitude. I would also like to thank Terry (Jo's

husband) and Scott (Barb's husband) for being such nice guys and supportive husbands. I'm very impressed with how far all of us have come, and I am happy to say that I have such loyal and caring friends. I would also like to thank all of my brothers from the Beta Sigma Chapter of the Alpha Chi Sigma Fraternity at RIT. A special thanks to my little brothers Jen and Sam, my big brother Kourtney, and my good friend Al.

In addition to my friends, I also have immense gratitude to my family for their support. My mom, Patricia, has been so supportive over the years. She is the strongest person that I know, and has done so much for my brother and I, so that we could pretty much do whatever we wanted to do. My baby brother, Michael and his wife Sandora, have been great friends. Mike, a mechanical engineer, also graduated from RIT. He has been so helpful and I know I could always call him if I needed a hand with anything. I also have a special note of thanks to my grandparents. I remember when my grandma and grandpa Fien used to have me over their house when I was a little girl. My grandma and I would spend hours making crafts and just chatting. I remember that my late grandfather would play solitaire on a wooden board in his La-Z-boy, loved his garden, and would shell nuts in the garage. My grandma Leiston and I would go garage-saling really early in the morning to get the best sales. My grandpa Leiston used to show me how to hit a golf ball and let me steal cherry tomatoes from his garden. I cherish the experiences I had with my grandparents and love them so much. My husband, Jonathan, has the best combination of laid-back attitude, humor, and understanding that I could ever ask for. We met at RIT and he has supported my career choices ever since. His support of my scientific curiosities and his technological perspectives has been a constant source of motivation. Jon, and his friend Rick Stone

have been a constant source of amusement. Rick, a fellow Ph.D. student, lesser known celebrity and world-traveler extraordinaire, has a unique view of the world, and an undying energy. Jon's family has also been a great source of support. I would especially like to mention my great-grandmother-in-law, Martha Elizabeth Pratt Waldo, who graduated from the Stockbridge School, an integral part of the Massachusetts Agricultural College, which is now the University of Massachusetts Amherst. Great-grandma Waldo graduated with a diploma in Home Economics/General Women's studies in 1927, which was the first agricultural program to include women at M.A.C. In 2006, at 101 yrs old, the Stockbridge School will be awarding her, and other Stockbridge School graduates, who before 1961 received Certificates of Commencement, an Associates of Applied Science degree.

I also have a huge appreciation to the support that I received throughout my training as a chemist. It all started in high school with John Prouty, my chemistry teacher. He was one of the most energetic teachers that I had, and always knew how to make chemistry fun. I think I did almost every extra credit assignment in that class, because it was fun and I could earn points towards my grade and the "drawer of goodies", filled with all sorts of chemistry-related toys. Between Count Von HOFBrINCl, and launching 2-liter soda bottles at the math teacher's door to show the importance of molarity (once with scary consequences!), I think I knew chemistry was for me. This continued over the years with the support I received as an undergraduate at RIT. Both of my advisors, Prof. Marvin Illingsworth and Prof. Andreas Langner, allowed me to play in their labs as an undergraduate; an experience that I now realize as extremely scientifically advantageous. They were very supportive and were there for

me whenever I needed help. Dr. Illingsworth took the risk to have a freshman in his labs, and entrusted me to Jon McCarney, Russell Stapleton and Derek Chow. I thank all of them for their help, especially Russ, who I am sure was a bit concerned when I had to ask what benzene was my first year, ruined a column he was running and burnt my first recrystallization. Dr. Langner helped me get through all the twists and turns of undergrad, and went out of his way to help me in many instances. He was one of the best advisors an undergraduate could ever hope for. I would also like to thank Dr. Jeff Leon (Kodak) and Prof. Coleen Pugh (UAKron) for keeping in touch over the years, and all of your support.

Last, but certainly not least, I'd like to thank my committee. Thai and Ken were kind enough to serve on my committee and to put up with my lengthy presentations. They have taken the time to understand my work, and to show a genuine interest in my research. Even when I defended my independent proposal about "Using Photo-responsive Polymer Beads for Tailored Size Exclusion Chromatography", they took the time to read it through and ask informed questions. I would like to thank Tom for all of the above and, in addition, for his professional and emotional support over the years. When I chose Tom as an advisor, I knew he was going to be very busy, making sure everyone in the group had whatever they needed funding-wise, but I also knew that he would make time for his students. Tom has been especially helpful, and supportive, especially when I thought my first project was "scooped", and has made time for me whenever I needed extra guidance. Thank you, Tom, for all of your help and support over the years.

[Exeunt]

## ABSTRACT

### A THERMAL APPROACH TO THE GENERATION OF STABLE DIBLOCK COPOLYMER TEMPLATES USING THIN FILMS

MAY 2006

JULIE M. LEISTON-BELANGER, B.S., ROCHESTER INSTITUTE OF  
TECHNOLOGY

M.S., UNIVERSITY OF MASSACHUSETTS AMHERST

Ph.D., UNIVERSITY OF MASSACHUSETTS AMHERST

Directed by: Professor Thomas P. Russell

Thermally crosslinkable diblock copolymers were studied for their ability to self-assemble and microphase separate, creating polymeric domains on the order of nanometers that could be stabilized with the application of heat. Selective degradation of the uncrosslinked phase afforded a nanoporous template. The stability of these phase-separated structures is crucial for subsequent device fabrication, especially when one of the components is removed to create a nanoporous structure. Nanoporous structures can be used for the fabrication of nanoscopic materials, lithographic templates, and selective filtration on the nanometer size-scale. This dissertation focuses on the synthesis and characterization of novel diblock copolymers and their use in the creation of stable nanoporous templates via thermal crosslinking.

Two methods were used to this end. The first involved the use of benzocyclobutene chemistry to create thermally crosslinkable styrenic polymers, namely poly(styrene-*r*-vinyl benzocyclobutene) (PSBCB). PSBCB was synthesized via living free radical polymerization using a hydroxy-functionalized alkoyamine initiator. This polymer was used to initiate D,L-lactide via ring-opening polymerization, to create

a diblock copolymer with a base degradable poly(lactic acid) (PLA) block. Thin films (~30 nm) of PSBCB-*b*-PLA polymer, on a gold-coated substrate, were shown to microphase separate with cylindrical domains of PLA oriented perpendicular to the substrate. Annealing the polymeric thin films, followed by subsequent thermal crosslinking, stabilized the microphase-separated structure. The PLA cylinders were removed using base to afford a nanoporous template. These nanoporous templates were shown to be thermally and solvent stable, unlike their uncrosslinked PS-*b*-PLA analogs.

The second method to generate thermally stable nanoporous templates, used polystyrene (PS) as the uncrosslinked block and polyacrylonitrile (PAN) as the thermally crosslinkable block. Polystyrene macroinitiator with a bromine end-group (PS-Br) was synthesized using living anionic polymerization techniques. The PAN block was synthesized using atom transfer radical polymerization (ATRP), with the PS-Br as the initiator. These polymers were used to create carbonaceous replicas of the microphase separated structure using a completely thermal process. The PAN block, when heated to 250 °C, undergoes stabilization and crosslinking to create a ladder-like polymeric network. Further heating to 600 °C under nitrogen, leads to the pyrolysis of the microphase-separated structure, creating nanoporous carbon templates.



# TABLE OF CONTENTS

	Page
ACKNOWLEDGMENTS .....	v
ABSTRACT.....	xiii
LIST OF TABLES.....	xvii
LIST OF FIGURES .....	xviii
CHAPTER	
1. DIBLOCK COPOLYMERS.....	1
1.1 Introduction.....	1
1.2 General Template Methodologies.....	3
1.3 Basic Diblock Copolymer Synthesis .....	5
1.4 Overview.....	10
2. BENZOCYCLOBUTENE-BASED TEMPLATES .....	12
2.1 Background .....	12
2.2 Synthesis .....	13
2.3 Instrumentation .....	18
2.4 Characterization .....	20
2.4.1 Microphase Separation Behavior.....	20
2.4.2 Crosslinking Experiments.....	23
2.5 Nanoporous Template Preparation.....	29
2.5.1 Thermal degradation .....	29
2.5.2 Base Degradation .....	33
2.5.3 Template Characterization.....	37
2.5.4 Template Stability.....	43
2.6 Conclusions.....	48
3. ACRYLONITRILE-BASED TEMPLATES .....	49
3.1 Background .....	49
3.2 Synthesis .....	52
3.3 Instrumentation .....	60

3.4 Characterization .....	61
3.4.1 Microphase Separation Behavior .....	61
3.4.2 Thermal Degradation .....	65
3.5 Nanoporous Template Preparation.....	68
3.5.1 Template Pyrolysis.....	68
3.5.2 Effect of Stabilization .....	73
3.6 Conclusions.....	75
4. APPLICATIONS AND FUTURE DIRECTIONS .....	76
4.1 PSBCB- <i>b</i> -PLA Project.....	76
4.2 PS- <i>b</i> -PAN Project .....	79
APPENDICES	
A.    EXPERIMENTAL SECTION .....	82
B.    HYDROXYL FUNCTIONALITY ACCESSIBILITY IN NANOPOROUS PSBCB- <i>B</i> -PLA FILMS.....	90
C.    SOLUTION BEHAVIOR OF ACRYLONITRILE DIBLOCK COPOLYMERS.....	98
REFERENCES .....	108
BIBLIOGRAPHY .....	113

## LIST OF TABLES

Table		Page
2.1.	Homopolymers and diblock copolymers studied. Number average molecular weight ( $M_n$ ) is given in kg/mol.....	18
2.2.	D-spacing values and corresponding calculated domain sizes determined from SAXS.....	21
2.3:	Crosslinking values calculated for homopolymer PSBCB thin films after different thermal treatments using the data from Figure 8 and Equation 1. ....	25
3.1.	PS- <i>b</i> -PAN polymers synthesized.....	57
3.2.	PS- <i>b</i> -PAN samples used in the microphase separation studies. ....	62

## LIST OF FIGURES

Figure	Page
1.1. Generalized Morphology diagram for diblock copolymer morphologies. Adapted from Hawker et al <sup>3</sup> and Matsen et al <sup>11</sup> .....	2
1.2. Nitroxide mediated polymerization (NMP) mechanism, shown here using TEMPO and an initiator fragment (I). Note that the equilibrium favors the dormant species.....	7
1.3. Ring-opening polymerization (ROP) of D,L-lactide using triethylaluminum(AlEt <sub>3</sub> ). <sup>46</sup> .....	8
1.4. Atom transfer radical polymerization (ATRP) of polyacrylonitrile. The ligand used to solubilize the copper species is not shown for clarity. ....	9
1.5. Living anionic polymerization of polystyrene and sample termination mechanisms.....	10
2.1. General schematic of nanoporous template formation. Magnified regions show the details of the crosslinking reaction and pore functionalization after degradation. ....	13
2.2. Synthesis of poly[(styrene- <i>r</i> - benzocyclobutene)- <i>b</i> -D,L-lactic acid]. ....	14
2.3. Synthesis of vinyl-benzocyclobutene.....	15
2.4. Polymerization tube and reaction set-up. ....	17
2.5. SAXS peaks from a bulk sample cast from chlorobenzene onto Kapton indicate a cylindrical morphology. Multiple temperatures were examined in situ from 120 °C to 220 °C. ....	22
2.6. Swelling experimental set-up.....	23
2.7. Swelling experiments in THF vapor using PSBCB homopolymer thin films (~140 nm) at various stages of thermal treatment. PSBCB homopolymer A, containing 26% BCB units (dark circles); PSBCB homopolymer B, containing 16% BCB units (open squares). ....	24

2.8.	SEC traces (UV detector at 254 nm) for the sol fraction of the thin films of polymer G extracted using THF at room temperature. Unheated sample (solid black line); Sample heated at 170 °C for 1 hour, cooled, and extracted with THF for 30 min (dotted gray line); sample heated additional 200 °C for 1 hour (solid gray line). The variation in intensity between curves corresponds to the amount of polymer extracted.....	26
2.9.	TGA studies of PSBCB- <i>b</i> -PLA and PS- <i>b</i> -PLA analog at 5 °C/min.....	29
2.10.	SEC studies of the degradation of PS- <i>b</i> -PLA under air.....	31
2.11.	SEC studies of the degradation of PS- <i>b</i> -PLA under nitrogen.....	32
2.12.	SEC traces (UV detector at 254 nm) of substrate supported non-crosslinked films after base degradation for different lengths of time, as specified, followed by dissolution in THF.....	35
2.13.	PM-IRRAS spectra of a) crosslinked sample and b) crosslinked sample after base degradation. The fraction of PLA degraded was determined from the disappearance of the carbonyl peak at 1763 cm <sup>-1</sup> . ....	36
2.14.	Degradation studies done using a commercially available developer, Rohm and Haas MF-319™, for various degradation times.....	37
2.15.	SFM images of PSBCB- <i>b</i> -PLA (a) as cast and (b) annealed at 170 °C for 2 hours then base degraded for 30 minutes. Annealed at 170 °C for 2 hours, crosslinked at 200 °C for 5 hours and then base degraded for (c) 90 minutes and (d) 11 hours. Scale bar = 100 nm. Left images are height, scale= 5 nm, and right images are phase, scale = 20° (for a and b), 30° (for c and d). ....	38
2.16.	Characterization of the thin film porosity. a) TEM looking down through a 30 nm crosslinked film with holes where the PLA was removed, inset is expanded region. b) SFM, height (left) and phase (right), of the bottom of a similar 30 nm film. Scale bars = 100 nm. ....	40
2.17.	Electric field alignment of PSBCB- <i>b</i> -PLA. a) as cast, b) and c) areas of mixed alignment after e-field, d) area of full alignment. Arrows indicate the direction of the electric field. Scale bars= 100 nm.....	42
2.18.	Insufficient crosslinking resulting in pore collapse. Films of polymer G, a) heated at 170 °C for 1 hour and base degraded for 30 min b) subsequent heating at 170 °C for 5 min.....	43

2.19.	Insufficient crosslinking resulting in pore collapse. Films of polymer G, a) heated at 170 °C for 2 hours plus 200 °C for 1 h and base degraded for 30 min b) subsequent heating at 200 °C for 5 min and c) 20 min. ....	44
2.20.	Insufficiently crosslinked porous films exposed to solvent. Films polymer G, a) heated at 170 °C for 2 hours plus 200 °C for 1 h and base degraded for 30 min b) subsequent THF soak for 30 min and c) 90 min. ....	45
2.21.	SFM images of porous films subjected to various thermal and solvent conditions. (a) base degraded for 11h then heated at 250 °C for 1 hour (b) base degraded for 30 minutes then heated at 200 °C for 11 hours (c) base degraded for 30 minutes, then soaked in THF at room temperature for 3 days (d) base degraded for 11 hours then submerged in refluxing benzene for 3 hours. Scale bars = 100 nm. ....	47
3.1.	Thermal degradation mechanisms of PAN. <sup>83,85,91</sup> Some of the reactions that occur during a) stabilization under air, b) pyrolysis. ....	50
3.2.	Carbonaceous template formation via stabilization and subsequent pyrolysis of PAN containing diblock copolymers. PAN is shown as the matrix in this diagram. The minor component is a sacrificial non-graphitic forming polymer which is removed during the pyrolysis step. ....	51
3.3.	Synthetic scheme for PS- <i>b</i> -PAN polymers. ....	54
3.4.	Reaction set-up for living anionic polymerization of styrene. a) Distillation set-up for styrene, b) Reaction vessel used for anionic polymerization. ....	55
3.5.	Kinetics data for the polymerization of acrylonitrile using a polystyrene macroinitiator. ....	58
3.6.	Difference in the number average molecular weight between NMR and SEC measurements using DMF with 0.01 M LiCl. ....	59
3.7.	Overlay of SAXS patterns for various PS- <i>b</i> -PAN diblocks. a) SANa3, b) SANb6, c) SANb3. Curves are offset for clarity. Inset is a representative 2D SAXS scattering pattern. ....	63

- 3.8. TEM images looking down through films of PS-*b*-PAN (SANA3), (a) as cast from DMF then stained with RuO<sub>4</sub>, and (b) Stabilized at 250 °C. The stained sample shows PS as the dark regions, and the stabilized sample shows PAN as the dark regions. Large dark spots are from contamination during the RuO<sub>4</sub> staining process. Overlays are “zoomed-in” regions of the underlying TEM images. Scale bars= 50 nm..... 64
- 3.9. TGA studies of PS-*b*-PAN and homopolymers heated at 5 °C/min, under a) nitrogen, b) air..... 66
- 3.10. SEC of the sol fraction of stabilized PS-*b*-PAN heated to 250 °C for 2 hours under nitrogen. PS-Br and PS-*b*-PAN were dissolved at 1 mg/mL in DMF, and the heated sample (2 mg) was extracted with 1 mL of DMF. Chromatograms are not normalized. .... 67
- 3.11. The effect of different casting solvents on the morphology of the carbonaceous films. Thin films were spin-coated using SANA2 from (a) DMF, and SANb5 from (b)DMAc and (b) DMSO solutions, all stabilized at 250 °C for 2 hours, and pyrolyzed. Insets are of expanded areas of the underlying TEM micrographs. Scale bars = 100 nm..... 69
- 3.12. Thermal annealing of PS-*b*-PAN polymers. SANA2 spin-coated using, a) 5% DMF, b) 1% DMF solutions, annealed, stabilized, then pyrolyzed. c) and d) are comparable films without annealing to a) and b) respectively. Insets are of expanded areas of the underlying TEM micrographs. Scale bars = 100 nm. .... 71
- 3.13. Optical microscopy images of thicker films of SANA2 cast from DMF onto 200 nm SiO. (a) as-cast (b) stabilized at 250 °C for 2 hours under air (c) pyrolyzed at 600 °C under nitrogen. The image shows a distinct color change due to the change in film thickness and no cracking of the films upon heating..... 73
- 3.14. Carbonaceous film formation using thin films of SANA2 cast from DMF (a) stabilized and pyrolyzed, (b) unstabilized and pyrolyzed. Overlays are “zoomed-in” regions of the underlying TEM images. Scale bars= 200 nm, inset scale bars= 100 nm. .... 74
- 3.15. Effect of increased stabilization time. Both films were spin-coated, then stabilized for 4 hours, and pyrolyzed. a) cast from DMF, b) cast from DMAC. .... 75

4.1.	Possible applications for modified nanoporous crosslinked templates. a) lithographic methods with or without pore functionalization, b) selective filtration via pore wall functionalization.....	78
4.2.	Introduction of diblock copolymers into confined geometries. Cross-sections shown are for the concentric cylinder morphology.....	80
B.1.	Attempts to address the hydroxyl functionality within the pores. List of reactions attempted and characterization used. All results were inconclusive. ....	91
B.2.	Cerium ammonium nitrate reaction to convert primary alcohols to aldehydes. <sup>126</sup> .....	94
B.3.	Challenges associated with the modification of nanoporous templates.....	96
C.1.	Comparison of PS- <i>b</i> -PAN behavior in DMSO- <i>d</i> <sub>6</sub> (gray line) and DMF- <i>d</i> <sub>7</sub> (black line). ....	99
C.2.	Representative DLS data for PS- <i>b</i> -PAN in a) DMF and b) DMSO. ....	100
C.3.	TEM of PS- <i>b</i> -PAN aggregates from a) DMF and b) DMSO solutions at various magnifications. Scale bars = 200 nm. ....	102
C.4.	Effect of water on the aggregation behavior of PS- <i>b</i> -PAN in solution. a) DMF- <i>d</i> <sub>7</sub> and b) DMSO- <i>d</i> <sub>6</sub> . Humid air was passed over the solutions for the times shown. Figures are offset vertically for clarity. ....	104
C.5.	Creation of carbon nanostructures from solution aggregates. a) PAN selective solvent, b) PS selective solvent.....	105
C.6.	Thermal treatment of PS- <i>b</i> -PAN aggregates from a)DMF and b) DMSO on carbon-coated TEM grids at 250 °C for 2 hours in air. ....	106



## CHAPTER 1

### DIBLOCK COPOLYMERS

#### 1.1 Introduction

Diblock copolymers, consisting of two chemically distinct polymers, joined at one end, can be used for a wide variety of applications such as surfactants, fillers, commercial polymers with tailored properties, and templates and scaffolds for the fabrication of nanoscopic objects. The latter of these uses holds promise as a means to overcome photolithographic limitations.<sup>1-3</sup> Diblock copolymers self-assemble into microphase-separated morphologies, where the domain size is dictated by the size of the polymer chain and, therefore, is nanoscopic in size. The microphase separation behavior of diblock copolymers is based on the segmental interaction parameter,  $\chi$ , and the total number of segments comprising the diblock copolymer.<sup>4-6</sup> Experimentally,  $\chi$  can be determined using methods such as small angle neutron scattering (SANS)<sup>7</sup>. Alternatively,  $\chi$  can be calculated<sup>8,9</sup> from the Hildebrand solubility parameters,  $\delta$ , and the average molar volume,  $v$ , of each of the blocks using equation 1.

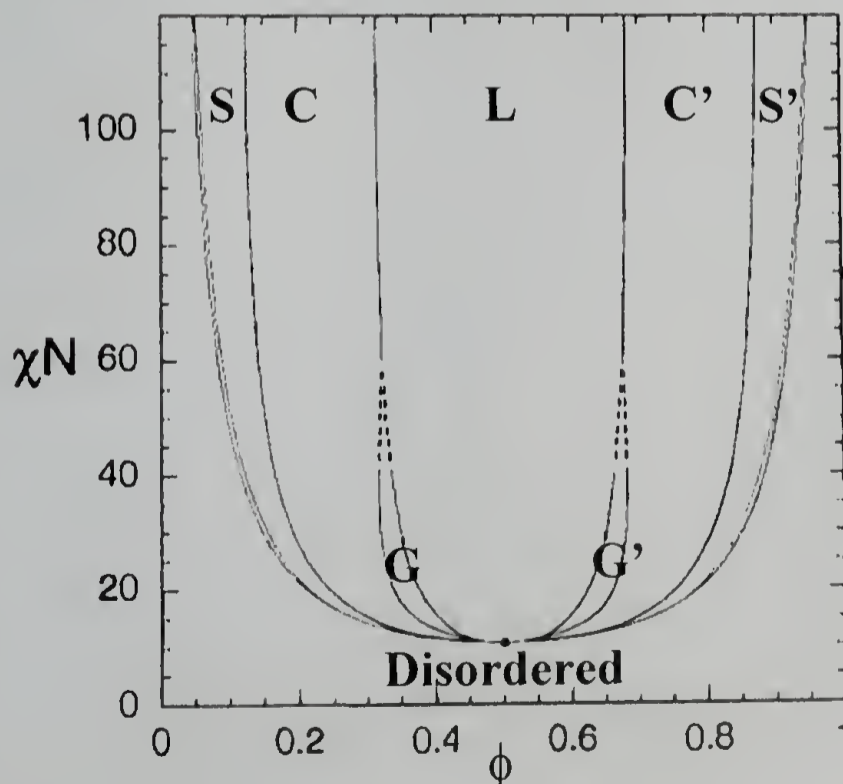
$$\chi \sim (v_A v_B)^{1/2} \frac{(\delta_A - \delta_B)^2}{kT} \quad (1)$$

$$\frac{\Delta G}{kT} = N_1 \ln \phi_1 + N_2 \ln \phi_2 + N_0 \phi_1 \phi_2 \chi \quad (2)$$

The interaction between the segments can further be described using the Flory-Huggins equation (see Equation 2), where  $\phi_i$  is the volume fraction of component  $i$ . The

phase diagram describes where phase separation or phase mixing occurs.<sup>5</sup> This diagram is an excellent first approximation for the phase separation behavior of incompressible systems. The interaction parameter,  $\chi$ , is only enthalpic in origin which limits this equation to the prediction of order-to-disorder transition (ODT) behavior, where mixing occurs with increasing temperature,  $T$ , where  $\chi \sim 1/T$ . Compressible systems, however, have to be treated separately, since entropy has a marked effect on the phase behavior. This type of system may exhibit lower disorder-to-order transition (LDOT) phase behavior that can be accurately approximated using a compressible regular solution theory (CRST). CRST takes into consideration the thermal expansion of each segment and volume changes associated with each block.<sup>9,10</sup>

**Figure 1.1. Generalized Morphology diagram for diblock copolymer morphologies.**  
Adapted from Hawker et al.<sup>3</sup> and Matsen et al.<sup>11</sup>.



Upon phase separation, diblock copolymers can exhibit a wide range of microphase separated morphologies, including spheres (S), cylinders (C), bicontinuous (or gyroid, G), and lamellae (L) (see Figure 1.1). The specific phase depends on the volume fraction of each block. For example, as the volume fraction of block A is lowered, the morphology varies sequentially from lamellar (equal blocks of A and B) to bicontinuous, to cylindrical, to spherical, and finally to a disordered state. The phases themselves arise from the curvature induced at the interfaces between the two blocks, such that the free energy is minimized. These self-assembled, microphase-separated morphologies have been explored for a variety of uses. This dissertation however, will only focus in detail on the use of diblock copolymers as nanoporous templates.

## 1.2 General Template Methodologies

Microphase separation, especially in thin films, is not without its own complexity. Once phase separation occurs, the ability to orient the phase-separated morphology and to create the long-range lateral order needed for templating applications can be challenging. The alignment of the microdomains of diblock copolymers using external fields such as shear, confinement, solvent annealing, electric fields, patterned substrates, and neutral brushes has been studied in detail.<sup>1,2,12-20</sup> Template formation using these aligned structures can be achieved by the removal of one of the components. Techniques such as UV, thermal, ozone, ion beam, and chemical etching processes have been developed to generate nanoporous films by removal of the minor component.<sup>21-26</sup> The resulting nanoporous films are finding applications as scaffolds and templates for the fabrication of nanostructured materials and advanced microelectronic devices.<sup>27-31</sup>

Removal of the minor component alone, however, is not sufficient. The surface area produced by the array of nanopores is large and the surface energy needs to be considered for the stability of the nanoporous structure. The energetic cost for producing the pores is significant such that, if the matrix were mobile, the pores would collapse. Consequently, the matrix must be immobilized to preserve the porosity. In the past, this has been accomplished by chemically crosslinking the matrix, crystallizing the matrix, or by keeping the matrix polymer below its glass transition temperature ( $T_g$ ). The chemical crosslinking of PS-*b*-PLA thin films using  $\text{RuO}_4$  has been explored with subsequent removal of the PLA to give a crosslinked nanoporous film.<sup>25</sup> Other studies have appeared on the use of dicumyl peroxide to crosslink PI-*b*-PDMS with subsequent removal of the PDMS phase.<sup>23,24</sup> P $\alpha$ MS-*b*-PHOST systems, using a photo-acid generator to promote small molecule crosslinking, have also been studied.<sup>32</sup> However, the addition of small molecules has limitations, including the incorporation of undesirable chemical functionality or metals associated with the crosslinking reaction. Selective degradation by ozone or reactive ion etching (RIE) has been used to produce nanoporous templates.<sup>21,22</sup> While being useful for nanolithographic templates, the resulting nanoporous polymer films may have unknown chemical functionalities, produced by the ozone or RIE process, that could limit subsequent chemical modification of the nanoporous polymer templates.

Diblock copolymers containing a high  $T_g$  block can be used to increase the allowable processing temperature before collapse of the porous template. Poly(cyclohexylethylene) (PCHE) containing diblock copolymers yield nanoporous

templates that resist collapse up to 136 °C, near the  $T_g$  of the PVCH block.<sup>33</sup> However, for temperatures above  $T_g$ , the pore structure collapses.

An attractive way to stabilize the matrix, while reducing the number of processing steps, is to incorporate thermally crosslinkable groups into the matrix block. This eliminates the need for small molecule crosslinking agents or the use of UV light. Additionally, the extent of crosslinking can be controlled by the number of crosslinkable groups incorporated into the chain during synthesis, which permits the physical and mechanical properties of the template to be controlled. From a manufacturing viewpoint, a purely thermal process streamlines the fabrication of the template, since crosslinking simply involves increasing the temperature following the standard thermal annealing used to orient and order the microdomain morphology. Thus, there is no additional handling of the film to produce a stable template.

### **1.3 Basic Diblock Copolymer Synthesis**

Diblock copolymers, created from vinylic monomers, are typically synthesized using living polymerization techniques, which give excellent control over the molecular weight distribution. Diblock copolymers of low polydispersity (PDI), typically  $<1.10$ , depending on the method of polymerization, are usually targeted for their reproducibility in fabrication and predictability of phase behavior. The effect of PDI has been studied and shown to have a mixed effect on the end morphology. Variations in PDI have a definite effect on the phase separation behavior, with an increase in the domain size with increasing PDI.<sup>34-36</sup> Some studies even indicate that a large PDI can result in a morphology different than that for a comparable low PDI diblock copolymer of the same volume fraction<sup>35</sup>, which is consistent with theoretical calculations.<sup>37,38</sup>

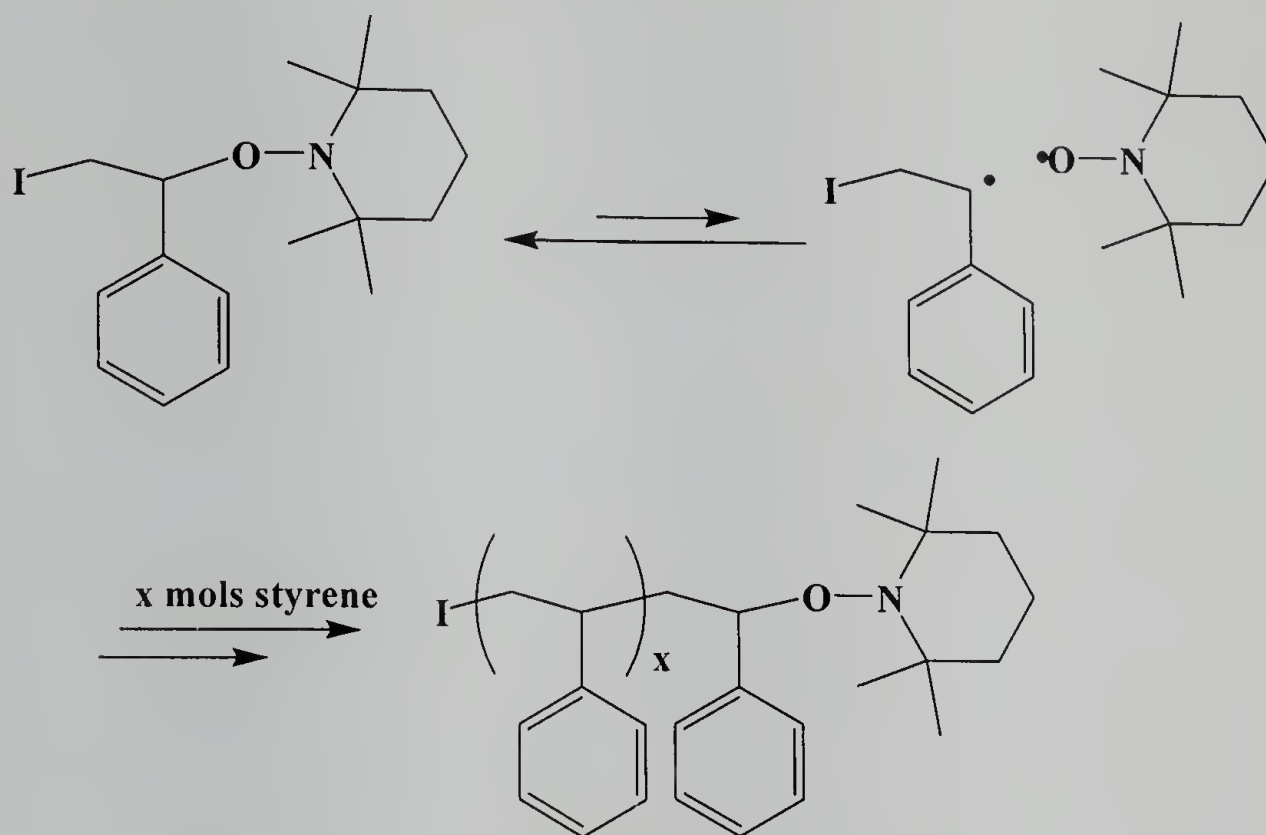
These studies indicate that a low PDI is not required to have microphase separation, providing the interaction between the two blocks is sufficiently unfavorable.

The basis for living polymerizations is that there is a fast initiation followed by propagation, without termination. In order for a polymerization to be considered living it has to meet certain criteria, including a narrow PDI, number average molecular weight ( $M_n$ ) that varies linearly with conversion, the number of polymer molecules is constant and the ability to continually add monomer to the growing chain.<sup>39,40</sup> Living polymerizations are typically done by anionic, free radical or cationic mechanisms. The first two will be the focus of the synthetic sections in Chapters 2 and 3 of this dissertation, and are described in detail in this section.

In Chapter 2 the polymeric materials were synthesized by a combination of living free radical and ring-opening polymerization techniques. Nitroxide-mediated polymerization (NMP)<sup>41,42</sup>, a living free radical polymerization, is one of many techniques used to polymerize styrene. In Chapter 2, an alkoxyamine initiator is used, which involves similar initiation and propagation events through homolytic cleavage of the carbon-oxygen bond. During nitroxide-mediated polymerization, the concentration of free radicals in solution is kept low to decrease the number of termination events. This is a result of the nitroxide-monomer “dormant” species being favored in the reaction equilibrium (see Figure 1.2). In addition, since the number of radicals is kept low, and the amount of “dormant species” is dominant, the reaction takes longer than a typical free radical polymerization (i.e. using azo- or peroxide-based initiators). Although these polymerizations are called “living” free radical, they are typically not

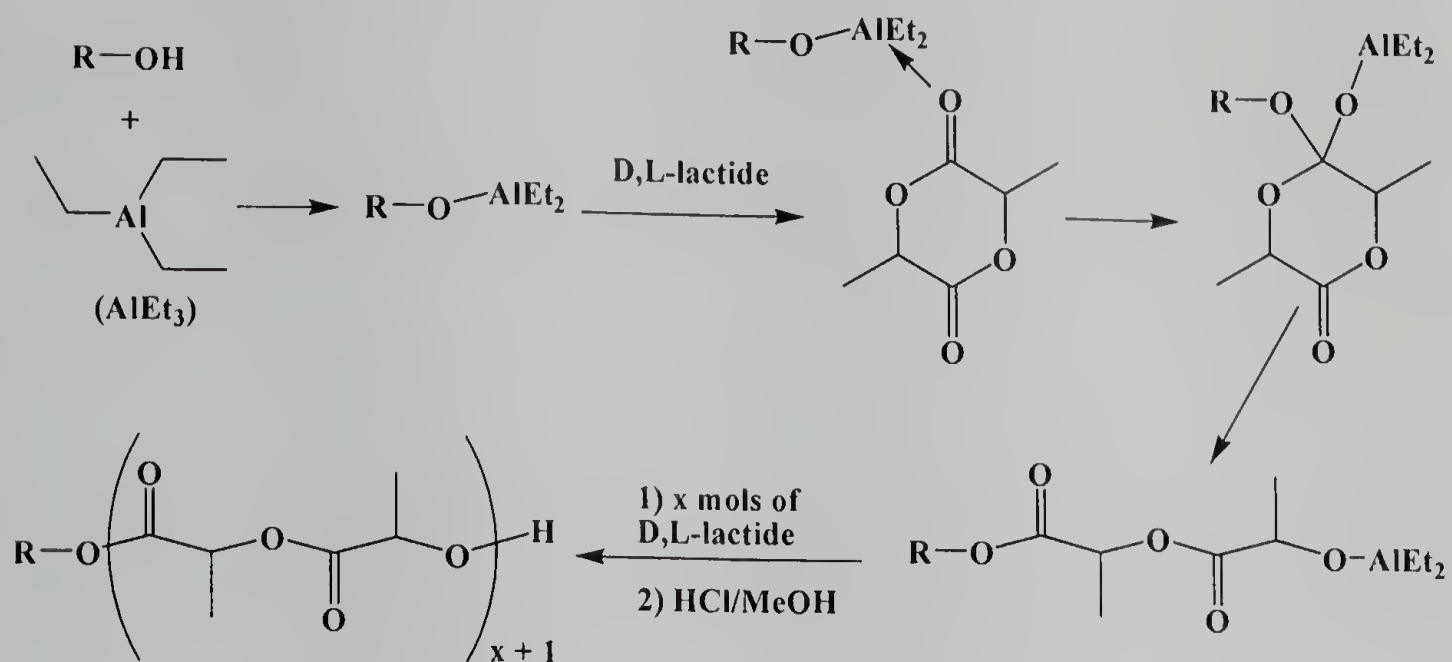
run to 100% conversion, since the higher the conversion, the greater the probability of termination or chain transfer events.

**Figure 1.2. Nitroxide mediated polymerization (NMP) mechanism, shown here using TEMPO and an initiator fragment (I). Note that the equilibrium favors the dormant species.**



Another type of living polymerization used in Chapter 2 involves the ring-opening polymerization (ROP) of D,L-lactide to create poly(D,L-lactic acid). This ROP can be done using organic-based (DMAP-derived) catalysts, tin catalysts, aluminum catalysts, as well as other transition metal catalysts.<sup>43-46</sup> The proposed mechanism works through the activation of the initiator (typically an alcohol) for attack on the carbonyl group of the lactide, to promote ring-opening (see Figure 1.3).

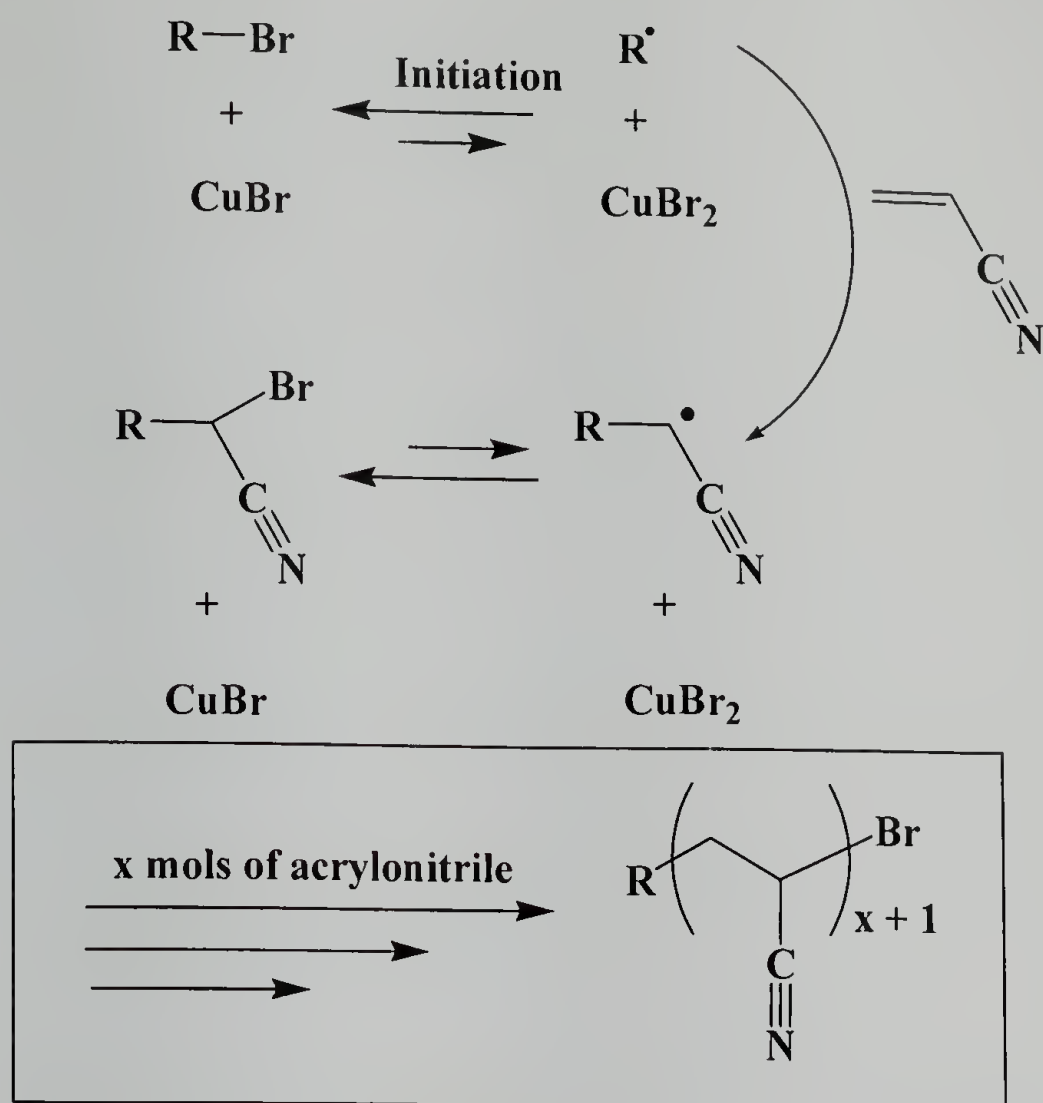
Figure 1.3. Ring-opening polymerization (ROP) of D,L-lactide using triethylaluminum ( $\text{AlEt}_3$ ).<sup>46</sup>



Another living free radical mechanism, used to create the PAN polymers in Chapter 3, uses atom transfer radical polymerization (ATRP). As in NMP, the concentration of free radicals is reduced to prevent termination, except this time the radical concentration is mediated through a reduction-oxidation reaction with a (typically) copper catalyst (see Figure 1.4). A variety of catalysts, ligands, initiators and monomers can be used for ATRP and are best described in a review by Matyjaszewski et al.<sup>47</sup>

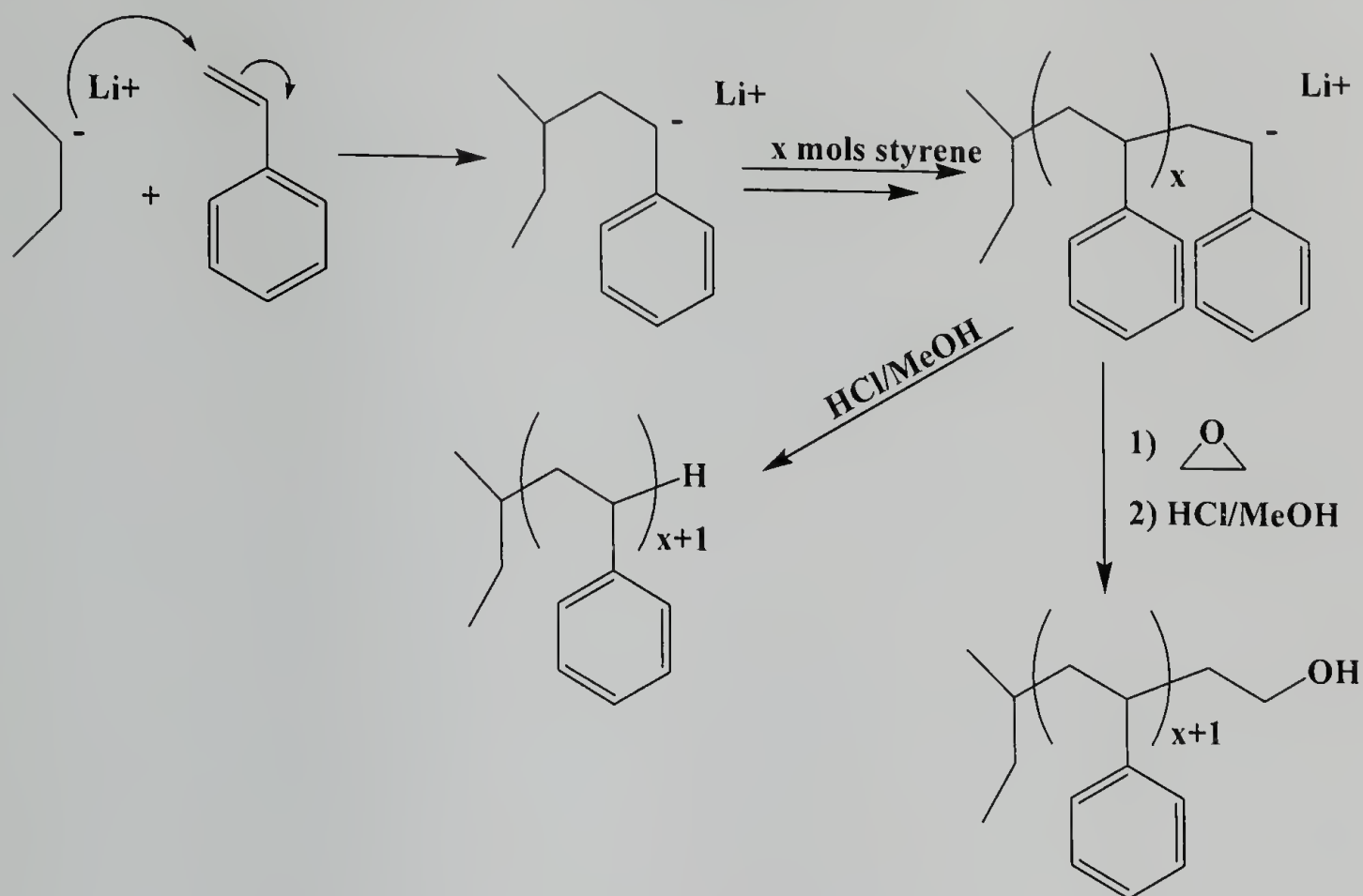


**Figure 1.4. Atom transfer radical polymerization (ATRP) of polyacrylonitrile. The ligand used to solubilize the copper species is not shown for clarity.**



The final polymerization technique utilized herein, to create bromine-functionalized polystyrene (PS-Br) in Chapter 3, involves a living anionic mechanism. Living anionic polymerization uses a propagating carbanion to create homopolymers and diblock copolymers.<sup>43,48,49</sup> There are a wide variety of anionic initiators that can be used to create these living polymers.<sup>50,51</sup> The control of a living anionic polymerization is due to the elimination of protic and electrophilic impurities that would cause termination. The rate of reaction depends strongly on the ion-pair separation, which can be tuned by the polarity of the solvent used for the reaction, and by the addition of salts. An example of the anionic polymerization of styrene is shown in Figure 1.5.

**Figure 1.5. Living anionic polymerization of polystyrene and sample termination mechanisms.**



#### 1.4 Overview

All of the aforementioned polymerization techniques were used to create the diblock copolymers in the following Chapters (2 and 3). These diblock copolymers were studied for their phase-separation behavior and were explored for the creation of nanoporous templates. Chapter 2 in this dissertation discusses a method by which a nanoporous template can be created using poly(styrene-*stat*-vinyl benzocyclobutene)-*b*-poly(D,L-lactic acid) (PSBCB-*b*-PLA) via a two step method. These two steps involve thermal crosslinking through the benzocyclobutene (BCB) pendent groups, and subsequent base degradation of the minor poly(lactic acid) (PLA) component. Chapter 3 focuses on a different polymeric system using polystyrene-*b*-polyacrylonitrile (PS-*b*-PAN), where a nanoporous thin film can be created using a purely thermal process to crosslink the film and degrade the minor PS phase. Exploration of the behavior of PS-

*b*-PAN in various solutions is briefly discussed in the Appendix. Chapter 4 discusses possible applications for the templates, designed in Chapters 2 and 3, as well as some ideas for future work.

## CHAPTER 2

### BENZOCYCLOBUTENE-BASED TEMPLATES

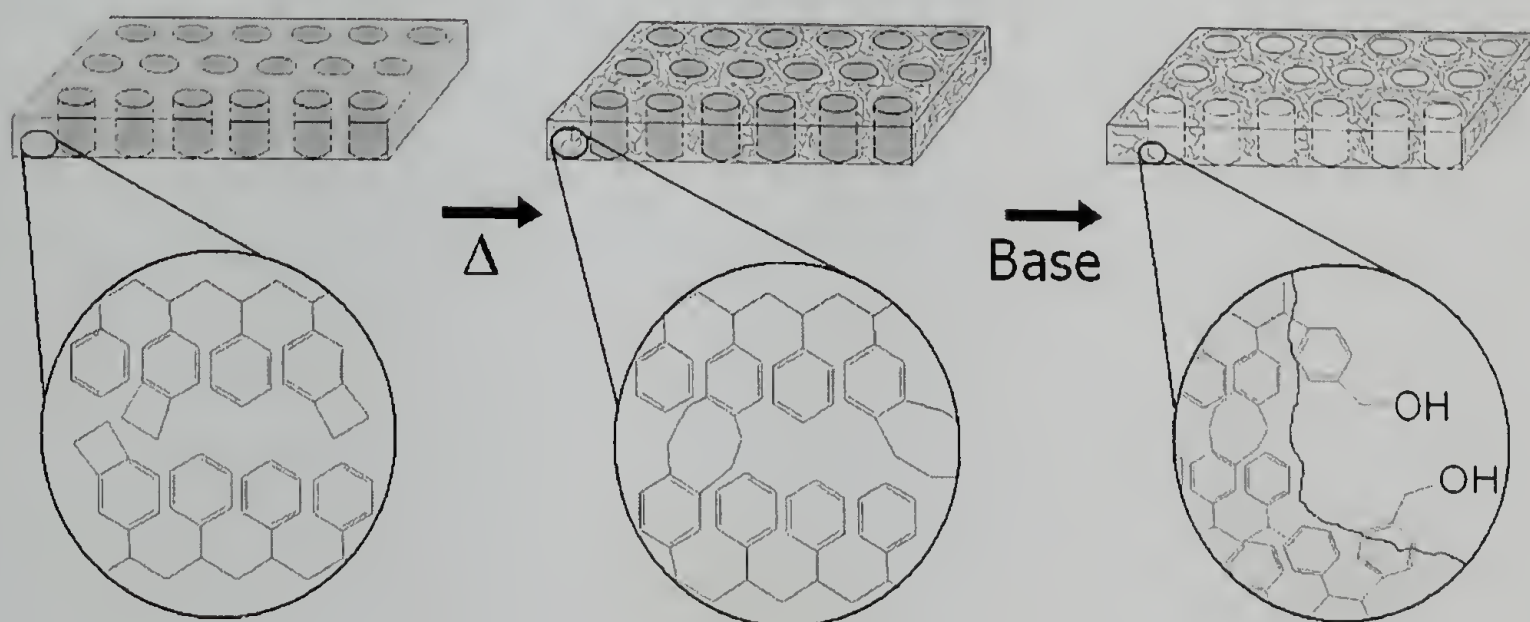
#### 2.1 Background

Benzocyclobutene has been explored for its ability to undergo crosslinking reactions with the application of heat, allowing for the generation and stabilization of polymeric structures. It has been used for the generation of low dielectric media<sup>52</sup>, crosslinked polymeric nanoparticles<sup>53</sup>, surface modifications<sup>20</sup>, and is commercially available in Dow's cylcotene™ electronic resins<sup>54-56</sup>. The temperature at which crosslinking occurs (above 170 °C) is well below the decomposition temperature of many polymers, such as polystyrene (PS) and poly(lactic acid) (PLA), yet is high enough for easy incorporation into copolymer backbones using radical polymerization mechanisms, without the worry of gelation during the reaction.

In this chapter, benzocyclobutene is used to create a diblock copolymer in which the major component is thermally crosslinked and the minor component is base-degraded to produce thin films with hydroxy-functionalized nanopores (see Figure 2.1). Specifically, BCB units were randomly placed along a PS chain, the major component, while PLA constituted the minor block. The thermal crosslinking of BCB has been shown to produce robust block copolymer templates when the minor component was PMMA.<sup>57</sup> Alternatively, with poly(styrene-*stat*-vinyl benzocyclobutene)-*block*-poly(lactic acid) (PSBCB-*b*-PLA), the PLA can be removed leaving hydroxyl-groups lining the pore walls (See Figure 2.1). Similar work using uncrosslinked PS-*b*-PLA nanoporous monoliths demonstrated that the alcohol groups lining the pore walls could be easily functionalized at conditions below the  $T_g$  of the matrix.<sup>26</sup> In our approach,

using PSBCB-*b*-PLA, the nanoporous templates are crosslinked and base degraded giving primary alcohol groups within the pores, potentially opening facile routes to post-functionalization, even at elevated temperatures.<sup>58</sup> This chapter focuses on the synthesis and characterization of these diblock copolymers and their corresponding thin films.

**Figure 2.1. General schematic of nanoporous template formation. Magnified regions show the details of the crosslinking reaction and pore functionalization after degradation.**

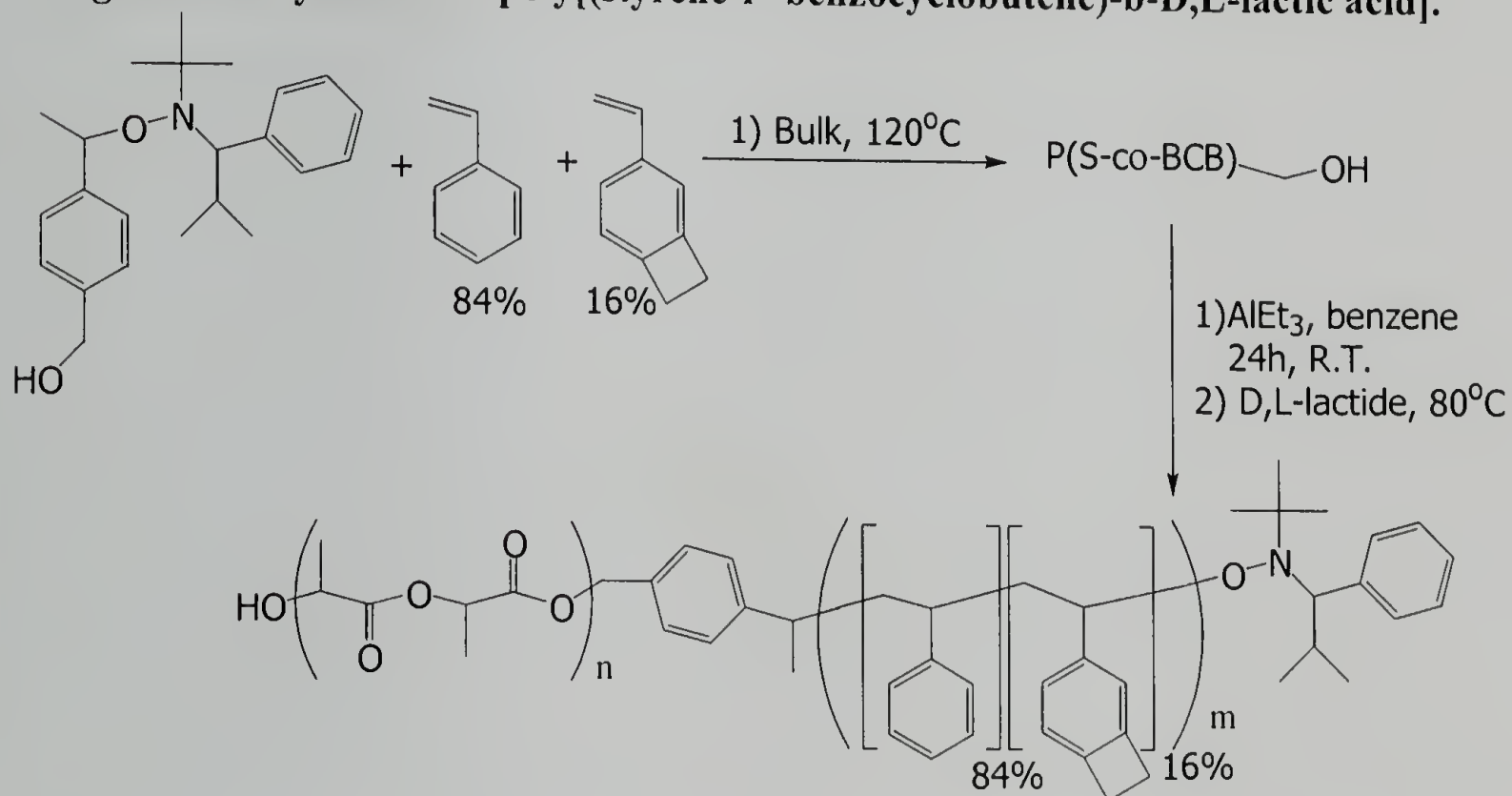


## 2.2 Synthesis

PSBCB-*b*-PLA was synthesized using a combination of nitroxide-mediated polymerization and ring-opening polymerization (ROP) techniques. A general outline of the complete reaction scheme is given in Figure 2.2. Initial studies used an alkoxyamine initiator with a protected hydroxyl end-group to create the PSBCB, which was deprotected prior to PLA polymerization. These polymers behaved in the same manner as their unprotected counterparts, therefore, protection of the hydroxyl functionality was deemed unnecessary. The protected polymer has been labeled within the text for clarity and consistency (see Table 2.1).

Initial studies used an 18 kg/mol diblock copolymer (PDI = 1.05) made using the protected PSBCB homopolymer, designated as polymer "G" (see Table 2.1). For this diblock copolymer, the tert-butyldimethylsilyl (TBDMS) protecting group was removed from the starting PSBCB homopolymer (polymer "A") using 1.0 M tetra-*n*-butyl ammonium fluoride (TBAF) in THF (see Appendix A). The synthesis of the diblock copolymer does not require protecting the hydroxyl group, so preparation of subsequent diblock copolymers were done without the protection/deprotection step.

**Figure 2.2. Synthesis of poly[(styrene-*r*- benzocyclobutene)-*b*-D,L-lactic acid].**



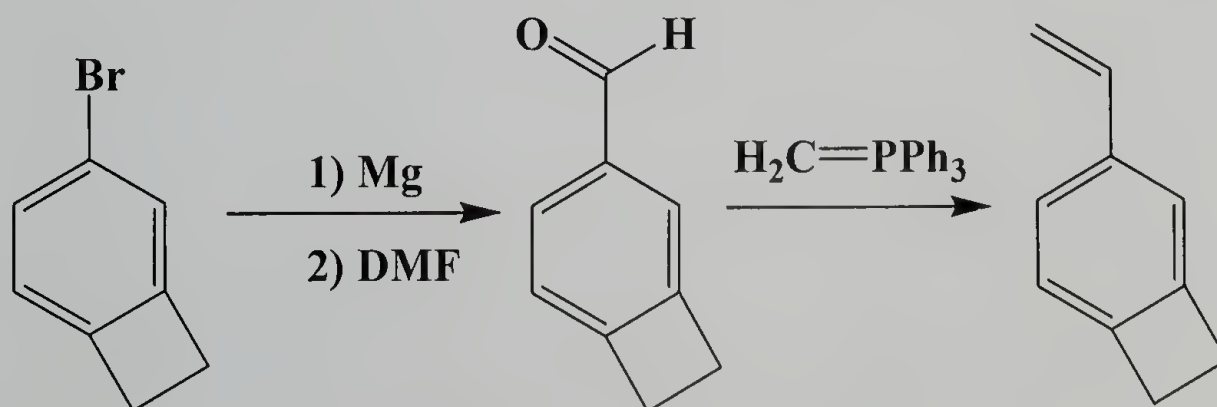
The hydroxy-functionalized alkoxyamine initiator was synthesized according to established procedures<sup>53</sup>, and provided by Dr. Eric Drockenmuller (IBM Almaden Research Center). The initiator was a sticky transparent brown solid, whose purity was verified through <sup>1</sup>H NMR.

The vinyl benzocyclobutene monomer was synthesized from the 3-bromocyclobutene precursor, which was provided by the Dow Chemical Company.

Synthesis of the benzocyclobutene precursor was initially attempted using various procedures<sup>59-62</sup>, such as the 1,1,2,2- (or 1,2)-dibromobenzocyclobutene intermediate followed by removal of the halogens, but met with very little to no yield. Another method using chlorine-substituted BCB was found, but not attempted.<sup>63,64</sup> A recent review published by Sadana et al.<sup>65</sup>, summarizes the various methods that can be used to create BCB and substituted BCB. The most reliable method, to date, to generate BCB materials is through flash vacuum pyrolysis procedures<sup>66</sup>, which were not explored in our laboratory since the supply from Dow chemical was enough for these studies.

The synthesis of the vinyl-BCB monomer was based on an established procedure<sup>53</sup>, using Grignard and Wittig reactions, as outlined in Figure 2.3 (see Appendix A for details). An attempt to use a tin reagent, via Stille coupling<sup>67-69</sup>, to convert the bromo-BCB directly to the vinyl-BCB monomer, met with mixed success, since both the starting material and target monomer have almost identical boiling points and have similar elution characteristics using column chromatography (tested with a variety of solvents).<sup>70</sup> The reaction was carried out, but the reaction mixture could not be easily purified. Therefore, the reaction as outlined in Figure 2.3 was used to create the vinyl-BCB monomer used in these studies.

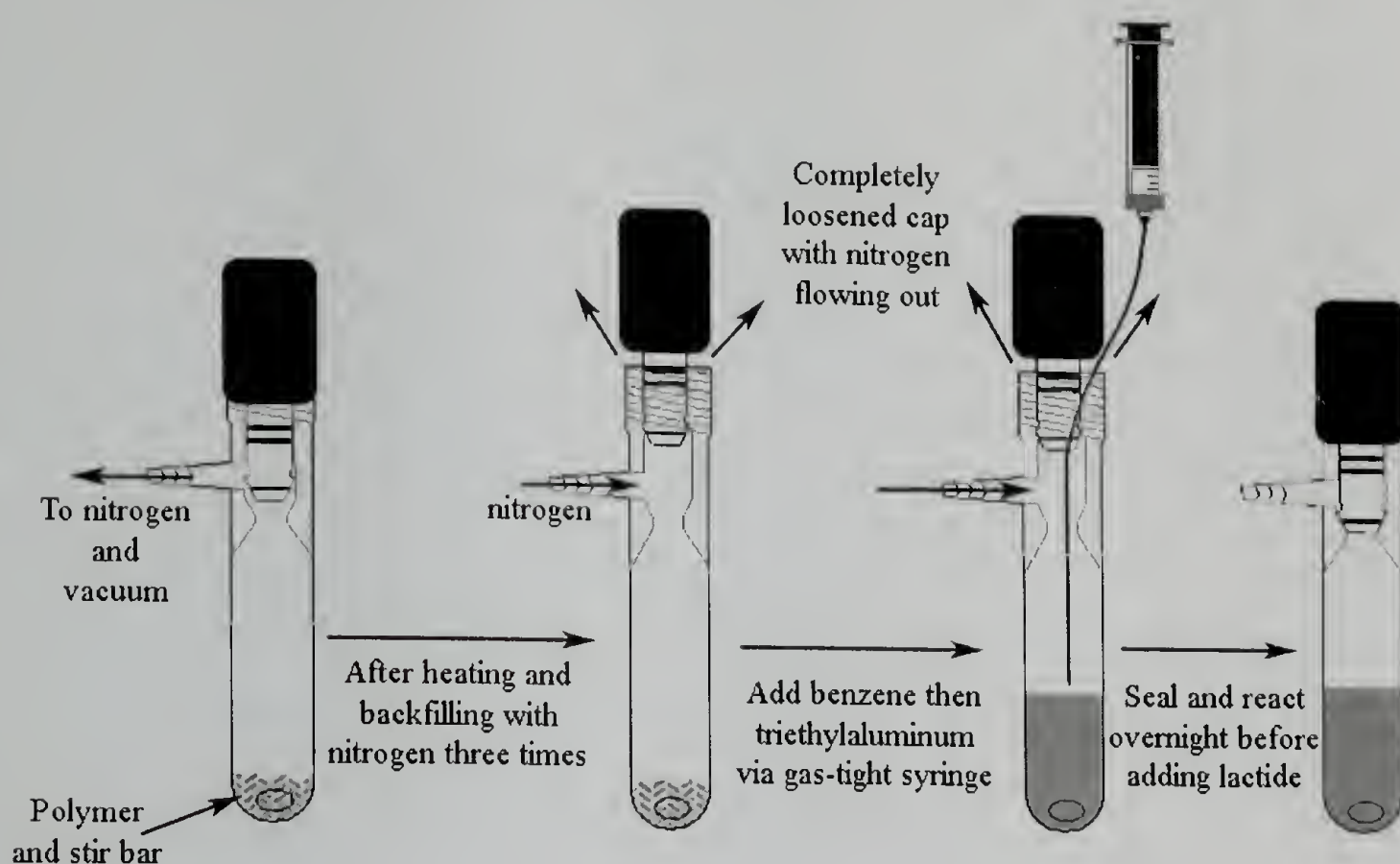
**Figure 2.3. Synthesis of vinyl-benzocyclobutene.**



Poly(styrene-*r*-benzocyclobutene) (PSBCB) was made using the hydroxy-functionalized initiator, styrene and vinyl-BCB in bulk at 120 °C (see Appendix A).<sup>53</sup> The styrene used for all the PSBCB homopolymers was used as received, without removing the inhibitor. The resulting PSBCB homopolymer was diluted with tetrahydrofuran, precipitated in methanol, then dried. These hydroxy-functionalized homopolymers were used to create the PSBCB-*b*-PLA diblock copolymers. The PLA blocks, on all the aforementioned diblock copolymers were grown using D,L-lactide and AlEt<sub>3</sub> in benzene, adapted from a previous procedure (see Appendix A).<sup>26</sup> For a typical reaction, a polymerization tube with a Teflon stopcock was charged with PSBCB-OH (0.3 g), heated briefly with a heat gun under vacuum, and then backfilled with nitrogen. This was repeated three times. Then under positive nitrogen flow, with the stopcock completely loosened, AlEt<sub>3</sub> and benzene were carefully added via gas-tight glass syringes. The polymerization tube was then quickly vented through a bubbler, sealed, covered in aluminum foil, and allowed to react overnight at room temperature (see Figure 2.4). This method was preferred over a septum-sealed flask, to prevent contamination from the septa, as well as to achieve a tighter seal to prevent the introduction of air or moisture. Keeping a septum-sealed flask under positive nitrogen pressure (vented through a bubbler) would be another route, but there would need to be an extra drying step of the nitrogen to eliminate water contamination.



**Figure 2.4. Polymerization tube and reaction set-up.**



The following day (~16 hours later), the reaction mixture typically appeared yellowish. This did not seem to affect the resulting diblock copolymer, and may very well be the color of the activated hydroxyl end-group, although studies were not done to confirm this. D,L-lactide was added to the polymerization tube in a glove bag under a nitrogen atmosphere. The tube was sealed, removed from the glove bag, and heated at 80 °C for 7 hours. The polymers were isolated by precipitation into acidic methanol (MeOH/HCl). Characterization of the diblocks was done using NMR and size exclusion chromatography (SEC).

The resulting homopolymers and diblock copolymers studied are summarized in Table 2.1. For clarity, throughout the remaining chapter, the polymers will be referred to by their letter designation. Multiple small batches of diblock copolymers with similar volume fractions of PLA were synthesized, as opposed to one large batch, due to the slow degradation of the copolymer over time. It was noticed that after > 6 months,

each batch of diblock copolymer behaved differently in microphase separation studies. No apparent change was noted in the NMR or SEC of these polymers, so the degradation occurring was minute, but enough to affect the results. Synthesis of a new batch of polymer every ~6 months produced consistent results.

**Table 2.1. Homopolymers and diblock copolymers studied. Number average molecular weight (Mn) is given in kg/mol.**

Notebook Number <sup>1</sup>	Polymer	PSBCB-OH			PSBCB- <i>b</i> -PLA		Vol fraction PLA <sup>5</sup>	Morphology <sup>6</sup>
		Mn	PDI	BCB <sup>3</sup>	Mn <sup>4</sup>	PDI		
JML-2-10	A <sup>2</sup>	13	1.06	0.26	-----	-----	0	N/A
JML-2-65	B	11	1.09	0.16	-----	-----	0	N/A
JML-2-32	C	3.4	1.09	0.26	-----	-----	0	N/A
JML-2-55	D	9.6	1.08	0.14	-----	-----	0	N/A
JML-2-57	E	11	1.08	0.22	-----	-----	0	N/A
JML-2-53	F	11	1.10	0	-----	-----	0	N/A
JML-2-21	G <sup>2</sup>	13	1.06	0.26	18	1.05	0.24	Cylinders
JML-2-70	H	11	1.09	0.16	19	1.08	0.36	Cylinders
JML-3-25	I	11	1.09	0.16	20	1.17	0.38	Cylinders
JML-3-26	K	11	1.09	0.16	19	1.13	0.36	Cylinders
JML-3-23	L	11	1.09	0.16	29	1.22	0.58	Lamellae
JML-3-28	M	11	1.09	0.16	13	1.09	0.13	Disordered
JML-2-43	O	3.4	1.09	0.26	1.2	1.13	0.23	Disordered
JML-2-59	P	11	1.10	0	14.7	1.17	0.22	Spheres/Cyl. <sup>7</sup>

<sup>1</sup> Notebook numbers are in the following format: JML-notebook number-page number

<sup>2</sup> This polymer was made using the TBDMS protected initiator followed by deprotection after the PSBCB homopolymer was made.

<sup>3</sup> Mole fraction of BCB in PSBCB homopolymer as determined by <sup>1</sup>H NMR.

<sup>4</sup> Mn of diblock determined from <sup>1</sup>H NMR

<sup>5</sup> Volume fractions determined using the densities: PS= 1.06 g/mL, PLA= 1.25 g/mL.

<sup>6</sup> Disordered structures were confirmed by SAXS and SFM. Further studies were not pursued.

<sup>7</sup> This sample did not show higher order reflections in SAXS, although SFM was consistent with either a cylindrical or spherical morphology.

### 2.3 Instrumentation

Size exclusion chromatography (SEC) measurements were used to characterize the homopolymers and diblock copolymers. SEC was also used for the degradation

studies, and to study the sol fraction in crosslinked films. SEC was done in THF at a flow rate of 1.0 mL/min, versus polystyrene standards, using three polymer laboratories PLGel 5  $\mu\text{m}$  Mixed-D columns, a Knauer K-501 HPLC pump, Knauer K-2301 RI detector, and Knauer D-2600 dual wavelength UV detector.

Bulk characterization of the morphology was done using small angle x-ray scattering (SAXS). SAXS measurements, as well as *in situ* temperature-dependent SAXS studies, were performed under vacuum using an Osmic MaxFlux x-ray (Cu  $K\alpha$ , 0.154 nm) source with a Molecular Metrology, Inc. camera consisting of a 3 pinhole collimation system, 150 cm sample-to-detector distance (calibrated using silver behenate), and a 2-dimensional, multiwire proportional detector (Molecular Metrology, Inc.).

All crosslinking studies were done using a hot plate in a glove bag. This allowed for the ability to crosslink the films under a dry, nitrogen atmosphere, or to vary the atmosphere's humidity as necessary.

Swelling studies were done on crosslinked homopolymer films to determine the number of crosslinks. Measurements of film thicknesses were taken *in situ*, using a Filometrics Interferometer Model F20 with FILMeasure v.2.4.3 software.

Base degradation studies on crosslinked thin films were done using polarization-modulation infrared reflection-absorption spectroscopy (PM-IRRAS)<sup>71</sup> PM-IRRAS was performed on a Thermo Nicolet Nexus 670 FT-IR Spectrometer equipped with a PEM module including a Hinds Instruments PEM-90 photoelastic modulator system and a liquid nitrogen cooled MCT-A detector. The difference reflectance measurements at 83° angle of incidence were collected for total of 1024 scans in the range of 4000-750

$\text{cm}^{-1}$  at a resolution of  $4 \text{ cm}^{-1}$ . The ratio taken between the spectra and those of previously scanned metal substrates was used to obtain the desired signal from the thin films.

Thin film images were taken using scanning force microscopy (SFM) and transmission force microscopy (TEM). SFM was done in both height and phase contrast modes using a Dimension TM3000 scanning force microscope. TEM images were obtained using a JEOL 2000KX transmission electron microscope at 200 kV.

Thermal degradation studies on the bulk powder were done using thermogravimetric analysis (TGA). TGA studies were done using a TA Instrument Series 2050 Thermogravimetric Analyzer. Polymer powder ( $\sim 2 - 5 \text{ mg}$ ) was heated at  $5 \text{ }^\circ\text{C}/\text{min}$  under either air or nitrogen.

## **2.4 Characterization**

### **2.4.1 Microphase Separation Behavior**

For each of the diblock copolymers in Table 2.2, small angle x-ray scattering (SAXS) was used to determine the bulk morphology. This was accomplished by drop casting films from chlorobenzene solutions ( $\sim 5\%$ ) onto Kapton films, allowing them to dry under a blanket of nitrogen for an hour, then drying them overnight *in vacuo*. For some polymers, the morphology was difficult to determine from SAXS, due to weak or missing higher order reflections. Instead, TEM was used to confirm microphase separation and to determine the morphology in the thin films. The d-spacing values from SAXS measurements, as measured using the first order reflection, are given in Table 2.2.

**Table 2.2. D-spacing values and corresponding calculated domain sizes determined from SAXS.**

Notebook Number <sup>1</sup>	Polymer	d-spacing (nm)	Calculated Domain Size (nm)	Observed Domain Size <sup>3</sup> (nm)	Vol fraction PLA <sup>4</sup>	Morphology <sup>5</sup>
JML-2-21	G <sup>2</sup>	18.5	11	10 (S)	0.24	Cylinders(X/T)
JML-2-70	H	18.9	14	14 (S)	0.36	Cylinders (T)
JML-3-25	I	22.5	17	19 (S)	0.38	Cylinders (T)
JML-3-26	K	19.2	14	14 (S)	0.36	Cylinders (T)
JML-3-23	L	15.1	8.8	-----	0.58	Lamellae (X)
JML-3-28	M	12.5	-----	-----	0.13	Disordered
JML-2-43	O	No peak	-----	-----	0.23	Disordered
JML-2-59	P	14.4	8.2 <sup>8</sup>	16 (S)	0.22	Spheres/Cyl. <sup>7</sup>

<sup>1</sup>Notebook numbers are in the following format: JML-notebook number-page number

<sup>3</sup> Domain size observed from SFM (S)

<sup>4</sup> Volume fractions determined using the densities: PS= 1.06 g/mL, PLA= 1.25 g/mL.

<sup>5</sup> Disordered structures were confirmed by SAXS and SFM. (X) designates that the morphology was determined from SAXS in bulk, and (T) is from TEM thin film studies.

<sup>7</sup>This sample did not show higher order reflections in SAXS, although SFM was consistent with either a cylindrical or spherical morphology.

<sup>8</sup>Calculated assuming a cylindrical morphology.

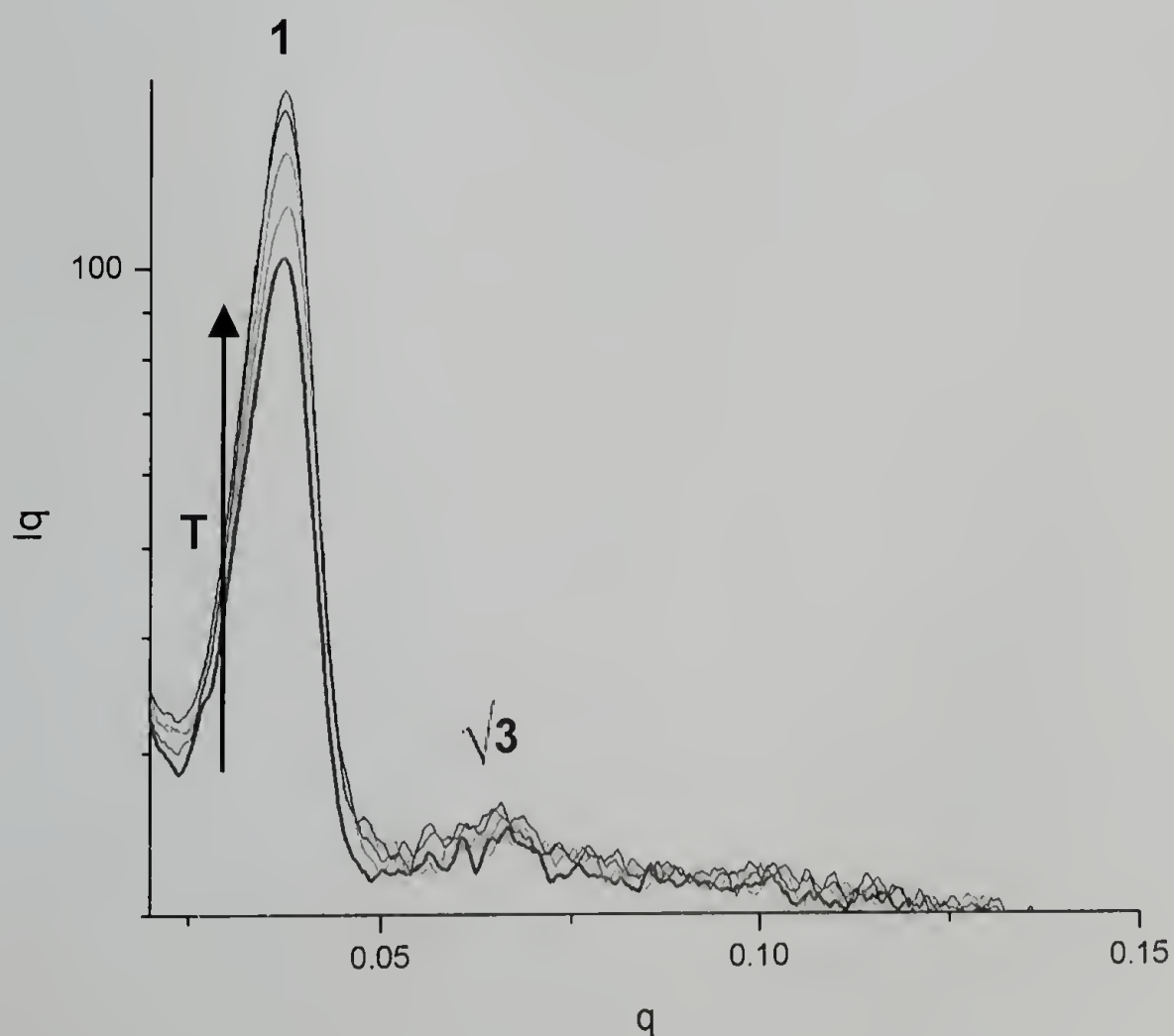
The corresponding domain sizes, as determined by SFM, are also given in Table 2.2. In the case of polymer L, the domain size was difficult to determine using SFM from the parallel orientation of the lamellae in the thin films. The domain sizes can also be calculated, assuming a sharp interface, using the SAXS first order reflection and volume fraction of PLA, also included in Table 2.2.

An *in situ* temperature study using SAXS was done to determine if the bulk morphology underwent an order-to-disorder transition (ODT) upon heating. If this were the case, then it would be difficult to stabilize the microphase-separated structure by thermal crosslinking due to the competing ODT transition. A sample of polymer G was studied and it did not undergo an ODT up to 220 °C (the limit of the instrument), which is above the temperature where the BCB groups undergo crosslinking (~170 °C) (see

Figure 2.5). The other polymers studied also did not undergo an ODT within the range used for annealing and thermal crosslinking.

The PSBCB-*b*-PLA copolymer that was studied in the SAXS temperature study (polymer G) was found to self-assemble into a cylindrical microdomain morphology in the bulk, where the first and second order scattering peaks were found at scattering vectors, relative to the first order reflection, of 1:  $\sqrt{3}$  (See Figure 2.5). The 2D SAXS pattern shows a diffuse ring, indicating the presence of many small grains of hexagonally-packed cylindrical microdomains with no long-range order. The other diblock copolymers (H, I, and K) only exhibited a first order peak, with no higher order reflections, but were also found to phase separate into cylindrical morphologies as well, as determined by SFM and TEM studies on thin films (see Table 2.2).

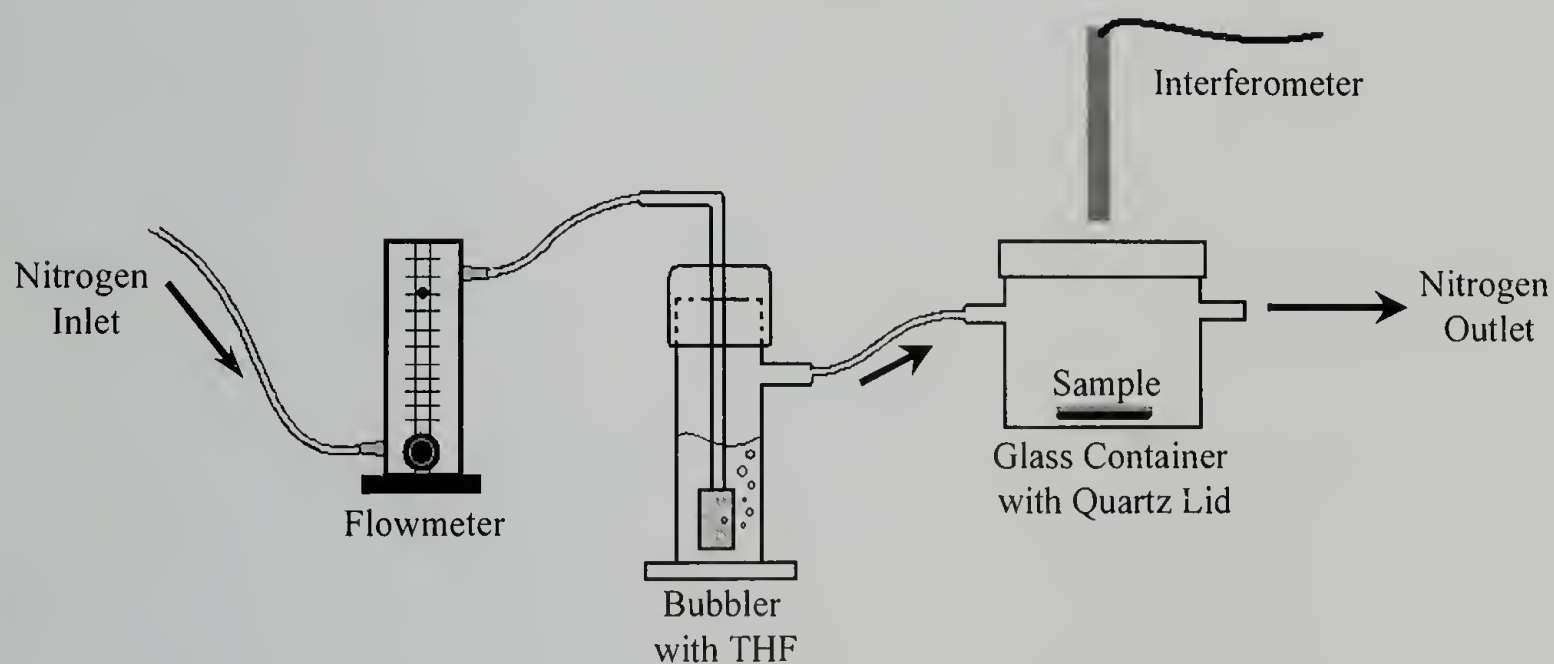
**Figure 2.5. SAXS peaks from a bulk sample cast from chlorobenzene onto Kapton indicate a cylindrical morphology. Multiple temperatures were examined in situ from 120 °C to 220 °C.**



## 2.4.2 Crosslinking Experiments

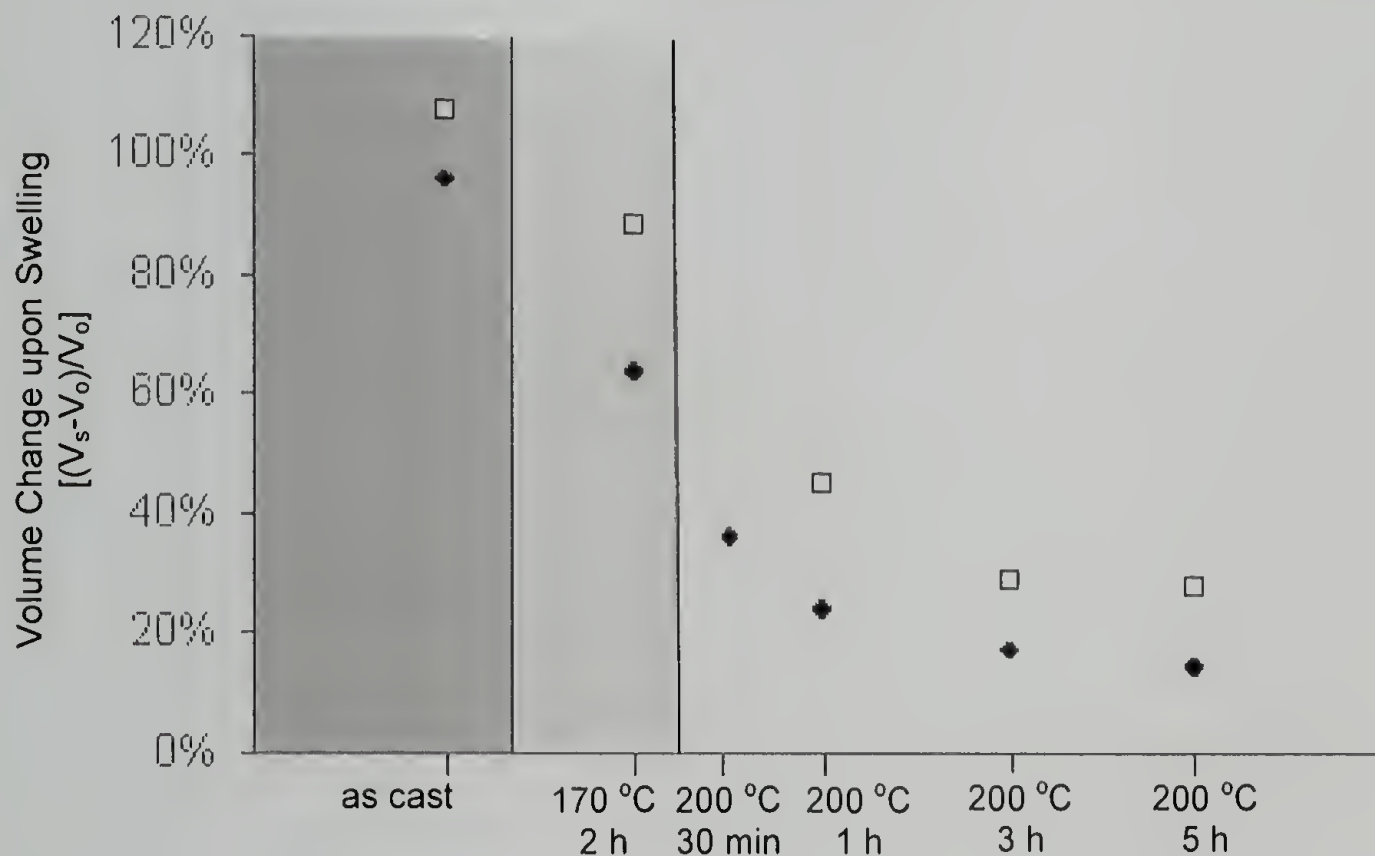
PSBCB homopolymer thin films ( $\sim 140$  nm) were cast from 5% chlorobenzene (3000 rpm) onto silicon wafers. Films using PSBCB homopolymers A and B, were studied under different thermal histories: unheated, heated to  $170$  °C for 2 h, heated to  $170$  °C for 2h +  $200$  °C for 30m, heated to  $170$  °C for 2h +  $200$  °C for 1h, heated to  $170$  °C for 2h +  $200$  °C for 3h, and heated to  $170$  °C for 2h +  $200$  °C for 5h. After thermal treatment, each film was introduced into a glass container with a quartz window. Nitrogen was bubbled through THF at a flow rate of 23 mL/min and passed over the thin film sample in the container (see Figure 2.6). Measurements of film thicknesses were taken *in situ*, prior to THF introduction and after reaching equilibrium at  $21$  °C, using an interferometer. The heated samples reached an equilibrium swelling thickness after  $\sim 7$  min, whereas the unheated films dewetted from the substrate after  $\sim 7$  min. The swelling measurements reported for the unheated films are prior to dewetting.

**Figure 2.6. Swelling experimental set-up.**



Measurements were taken using several similar film samples for each heat treatment, and normalizing them to the initial film thickness/film volume for comparison. The normalized change in volume was compared for each heat treatment (see Figure 2.7). The amount of swelling reached a plateau after heating for 170 °C for 2 h + 200 °C for 5 h. This indicates that the maximum amount of crosslinking obtainable for this system occurs after this heat treatment, and heating for longer periods of time will have little effect on the crosslinking density.

**Figure 2.7: Swelling experiments in THF vapor using PSBCB homopolymer thin films (~140 nm) at various stages of thermal treatment. PSBCB homopolymer A, containing 26% BCB units (dark circles); PSBCB homopolymer B, containing 16% BCB units (open squares).**



The swelling data can be used to calculate<sup>72</sup> the number of segments between crosslinks,  $N_c$ , using

$$N_c = \frac{(L_c/L_0)^3}{\phi^{(1/2 - \chi)}} \quad (3)$$

This equation is used for the uni-directional swelling behavior of surface-attached polymer networks, adapted from classical swelling arguments,<sup>73,74</sup> since the



polymer being swollen is immobilized on a substrate.  $N_c$  can be calculated using the volume fraction of polymer ( $\phi$ ) in the swollen network, the polymer-solvent interaction parameter ( $\chi$ ), the average swollen thickness ( $L_c$ ), and the thickness of the dry film ( $L_0$ ).<sup>72</sup> For our system,  $\chi$  is approximately 0.006 using the solubility parameters from the literature for THF and PS and Equation 1.<sup>75</sup> The average molecular weight between crosslinks ( $M_c$ ) can then be calculated using  $N_c$  and multiplying by the molecular weight for a styrene repeat (see Table 2.3).

**Table 2.3: Crosslinking values calculated for homopolymer PSBCB thin films after different thermal treatments using the data from Figure 8 and Equation 1.**

	Thermal Treatment	% Swelling	$N_c^a$	$M_c$ (g/mol)
26% BCB	170 °C 2 h	64%	23.5	2442
	170 °C 2 h + 200 °C 30 min	36%	12.0	1251
	170 °C 2 h + 200 °C 1 h	24%	8.6	894
	170 °C 2 h + 200 °C 3 h	17%	7.1	739
	170 °C 2 h + 200 °C 5 h	14%	6.5	673
	----	----	2.9 - 3.8 <sup>b</sup>	300 - 400 <sup>b</sup>
16% BCB	170 °C 2 h	89%	39.2	4079
	170 °C 2 h + 200 °C 1 h	45%	15.2	1582
	170 °C 2 h + 200 °C 3 h	29%	10.0	1041
	170 °C 2 h + 200 °C 5 h	28%	9.7	1012
	----	----	5.8 - 6.7 <sup>b</sup>	600 - 700 <sup>b</sup>

<sup>a</sup> Number of segments between crosslinks calculated using equation 3.

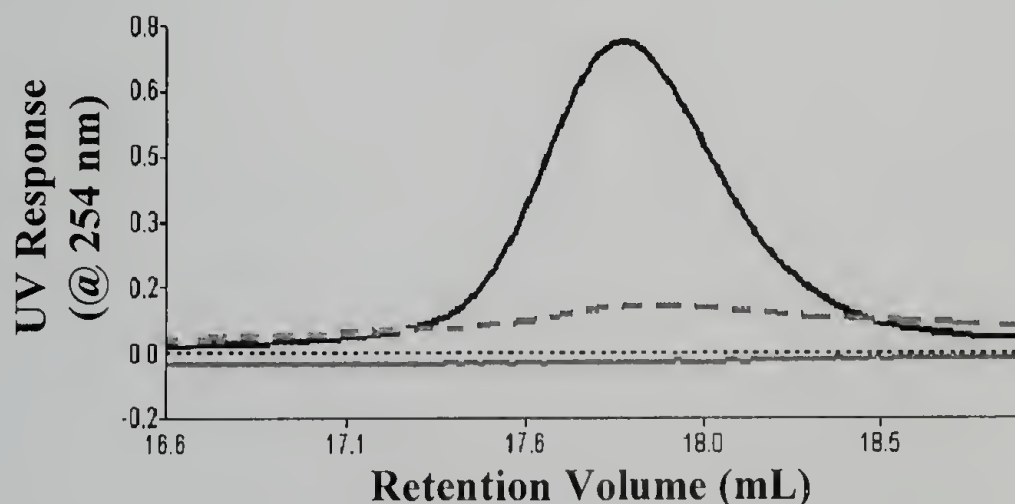
<sup>b</sup> Number of segments calculated assuming 100% crosslinking and uniform distribution of BCB groups along the chain

The average  $M_c$  for the templates after crosslinking at 170 °C for 2 hours + 200 °C for 5 hours is ~670 g/mol and ~1000 g/mol for the 26% and 16% BCB containing polymers, respectively. This is higher than the theoretical molecular weight between crosslinks calculated assuming complete BCB crosslinking and uniform placement of BCB groups. The higher  $M_c$  would indicate that the all the BCB groups

are not fully crosslinked, due to limited diffusion and availability of nearby BCB groups, since the BCB groups crosslink in pairs.

After crosslinking occurs, the amount of soluble material, or sol, decreases until all of the polymer chains have become part of the crosslinked matrix. Size exclusion chromatography (SEC) was used to determine the temperature conditions upon which no more sol could be extracted. Thin films (~30 nm) of polymer G were spun onto gold coated silicon wafers, ~1 cm x ~1 cm, heated and extracted in 1.0 mL of THF (see Figure 2.8). The unheated sample dissolved completely, whereas the sample heated at 170 °C for 1 hour, cooled, and extracted with THF for 30 minutes did not completely dissolve, indicating that the majority of the chains were crosslinked. Heating a similar film (not exposed to THF) an additional 200 °C for 1 hour, caused further crosslinking and no soluble polymer was extracted.

**Figure 2.8: SEC traces (UV detector at 254 nm) for the sol fraction of the thin films of polymer G extracted using THF at room temperature. Unheated sample (solid black line); Sample heated at 170 °C for 1 hour, cooled, and extracted with THF for 30 min (dotted gray line); sample heated additional 200 °C for 1 hour (solid gray line). The variation in intensity between curves corresponds to the amount of polymer extracted.**



Swelling studies on the homopolymer films, and evaluation of sol fractions in diblock copolymer thin films, indicated that heating at 170 °C for 2 hours + 200 °C for 1

hour was sufficient to crosslink the majority of the chains, where 200 °C for 5 hours was needed to achieve maximum crosslinking. When crosslinked PSBCB is used as the matrix in a nanoporous structure, it is important that the film does not collapse upon subsequent modification and processing of the nanoporous template. While heating the film results in enough crosslinks to cause the disappearance of the sol fraction, this number of crosslinks may not be enough to immobilize the nanoporous structure. The necessary number of crosslinks for pore stability can be determined from the modulus required for pore stability. The modulus of the matrix required to maintain the nanoporous structure in the films can be estimated from the surface area produced by pore formation, the surface energy, and pore diameter, using the arguments of Muralidharan et al.<sup>76</sup> The modulus required to stabilize a nanopore with a given radius (r) can be estimated using the surface tension ( $\gamma$ ) of the matrix, in this case, crosslinked polystyrene. Assuming the matrix behaves as an infinite elastic solid and the polymer behaves as an incompressible solid, then

$$\frac{2Er}{3\gamma} > 1 \quad (4)$$

The modulus can then be used to determine the molecular weight between crosslinks ( $M_c$ ) needed to keep the porous morphology from collapsing by

$$E = \frac{3\rho RT}{M_c} \quad (5)$$

While the nanoporous structure will not collapse below the glass transition temperature ( $T_g$ ) of PS, the concern is that subsequent modification of the nanoporous structure at higher temperatures may lead to pore collapse. Therefore the stability of the nanoporous matrix at a higher temperature (473 K), well above the  $T_g$  of PS, was

calculated using the above equations, to determine the number of crosslinks necessary for sufficient crosslinking. The density ( $\rho$ ) and surface tension of PS at 473 K were calculated to be  $0.9671 \text{ g/cm}^3$  and  $27.7 \text{ mN/m}$  using the bulk values for PS at  $200 \text{ }^\circ\text{C}$ .<sup>77</sup> Using the above equations, the modulus required to support a 14 nm diameter pore in a PS matrix at  $200 \text{ }^\circ\text{C}$  was calculated to be  $\sim 5.93 \text{ MPa}$ . This modulus can be achieved by having an  $M_c$  of  $\leq 2 \text{ kg/mol}$ . The  $M_c$  for the PS matrix with 16 mole percent BCB in the PS block (polymer H) is  $\sim 600\text{-}700 \text{ g/mol}$ , assuming 100% crosslinking of the BCB along the chain and a uniform distribution of BCB groups. For comparison, pores with a diameter of 10 nm, require an  $M_c \sim 1.4 \text{ kg/mol}$  to support the porous structure, which is much greater than the  $M_c \sim 300\text{-}400 \text{ g/mol}$  calculated for the PSBCB matrix used (polymer G), assuming complete crosslinking of the 26 mole percent BCB groups.

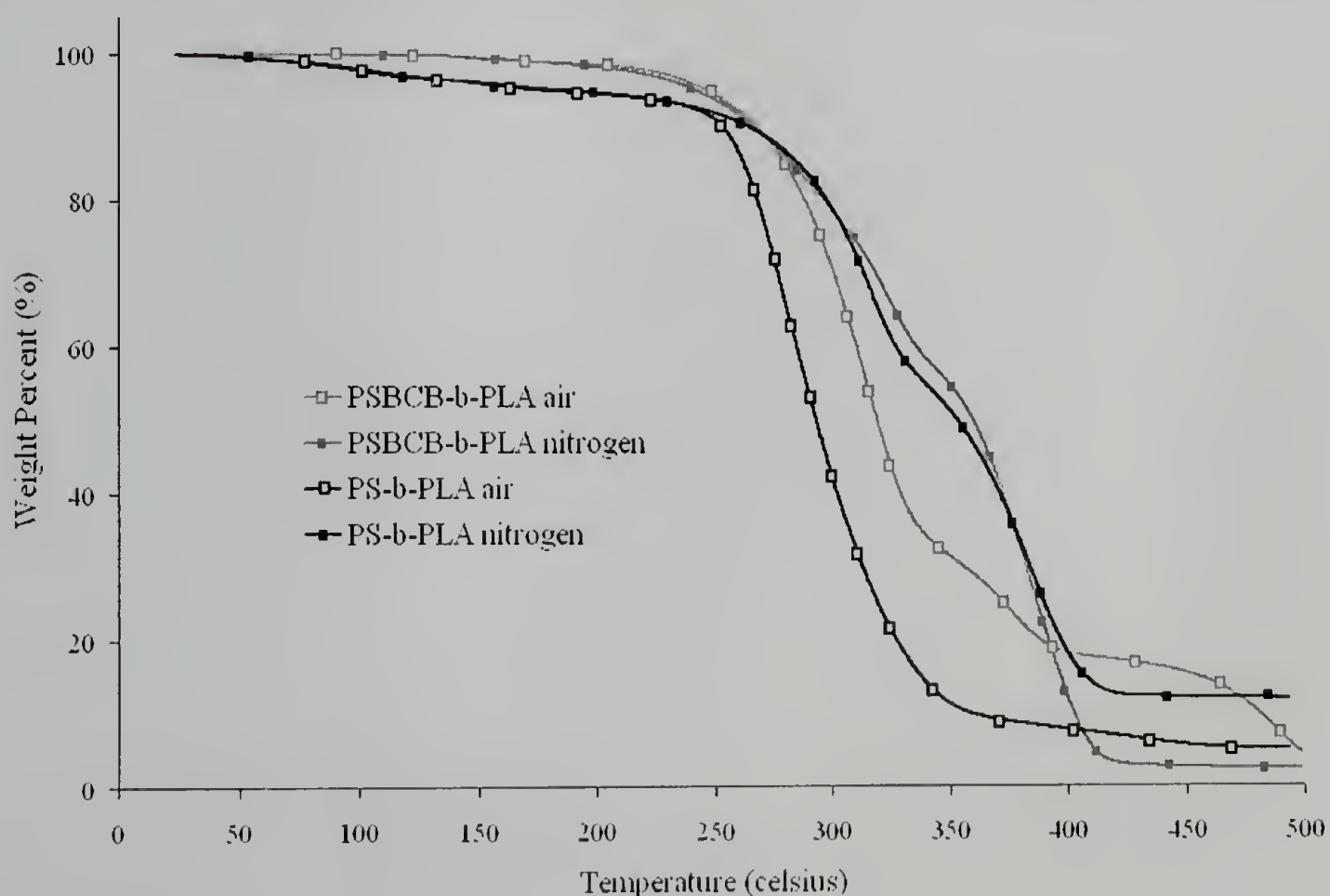
According to Table 2.3, the experimental  $M_c$  obtained by heating the film for  $170 \text{ }^\circ\text{C}$  for 2 hours +  $200 \text{ }^\circ\text{C}$  for just *30 minutes* should create enough crosslinks to stabilize the porous structures, when compared to the theoretical calculations using Equations 4 and 5. This however is not the case as will be discussed in the “Template Stability” section. In order to maintain the nanoporous structure without collapse, the film must be crosslinked at  $170 \text{ }^\circ\text{C}$  for 2 hours +  $200 \text{ }^\circ\text{C}$  for 5 hours. With this heat treatment followed by PLA degradation (discussed in section 2.5), SFM and TEM observations confirm the retention of the pores in the films well above the  $T_g$  of PS for the polymers studied (polymers G, H, I, K).

## 2.5 Nanoporous Template Preparation

### 2.5.1 Thermal degradation

Ideally, a completely thermal process for the creation of nanoporous templates is desired, where subsequent heating after crosslinking removes or degrades the minor component. To determine if a completely thermal route is possible using PSBCB-*b*-PLA, TGA and SEC were used to determine if the PLA degraded upon heating. TGA experiments (5 °C/min) done in air and under nitrogen, using PSBCB-*b*-PLA (polymer K) and PS-*b*-PLA (polymer P), are shown in Figure 2.9. The TGA data shows that there are no volatiles given off prior to the decomposition of the PS domain (~350 °C). This means that the PLA does not decompose via chain scission or unzipping mechanisms to release small molecules, so heating alone cannot be used to remove the PLA domains.

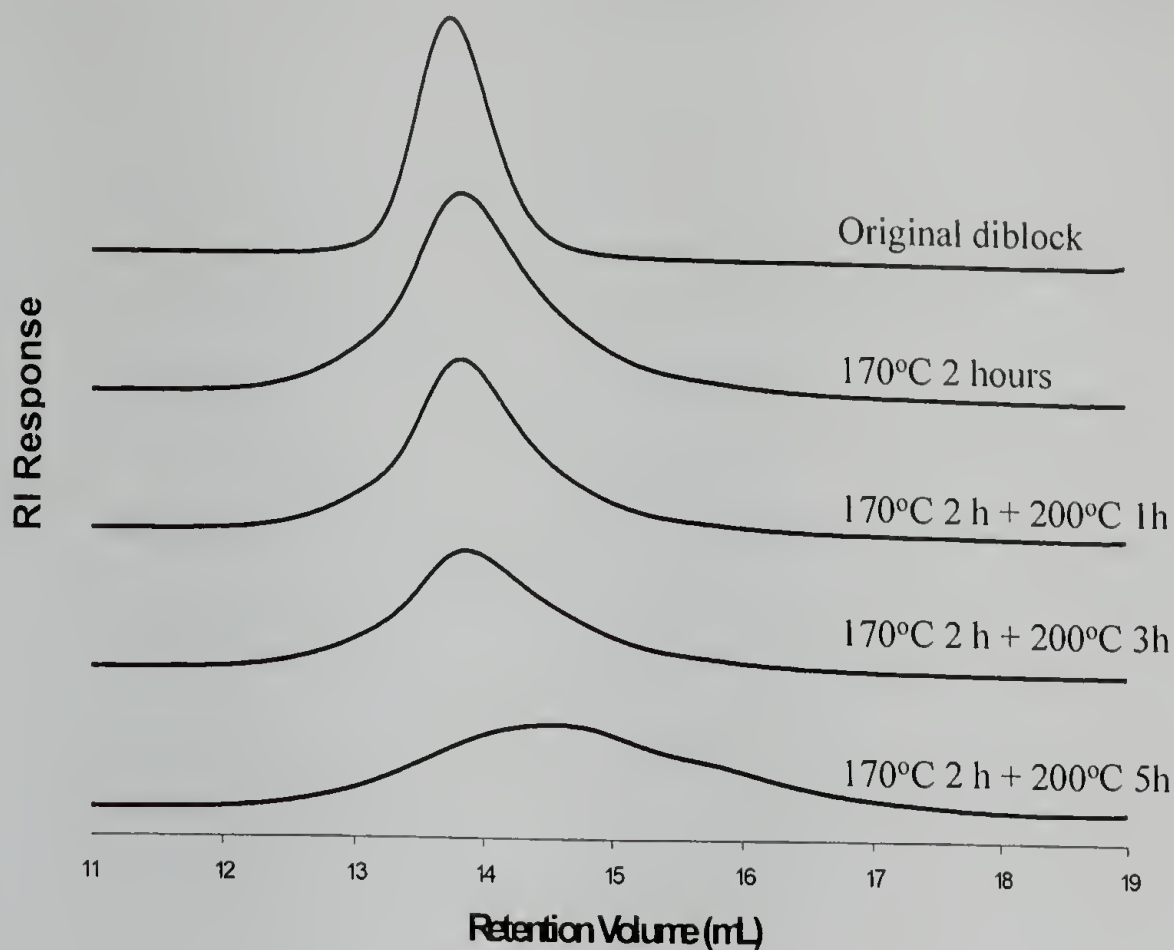
**Figure 2.9.** TGA studies of PSBCB-*b*-PLA and PS-*b*-PLA analog at 5 °C/min.



TGA data, however, is limited to mass loss, and therefore does not show if the PLA degrades by decomposing into non-volatile fragments, or if the PLA block simply cleaves at the junction point with the PS block. These two possibilities, nonvolatile fragments or cleavage, would not result in a completely thermal process for template formation (since the PLA would still need to be washed out). It would, however, cut down on the use of other unnecessary chemicals for degradation.

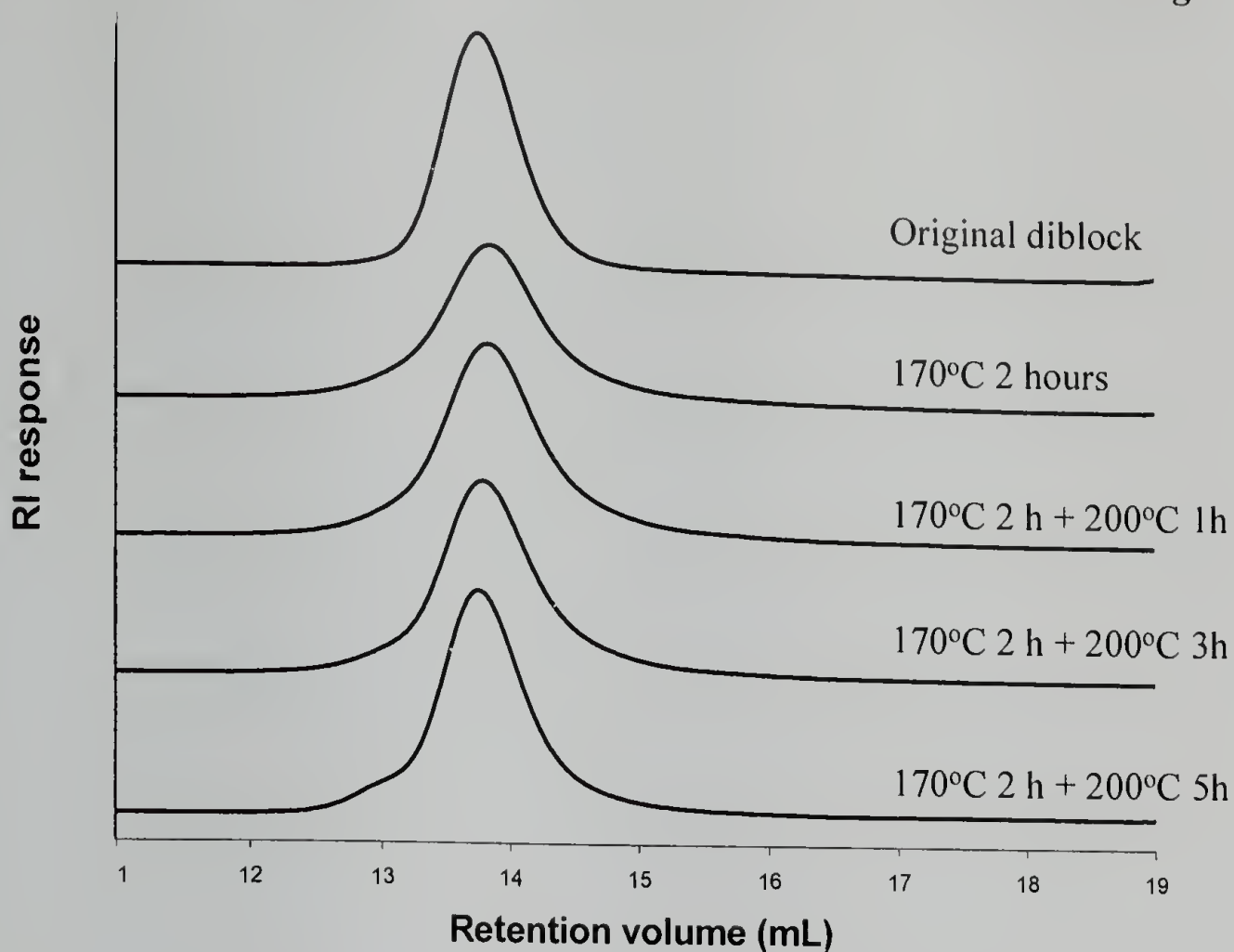
To determine if there was any degradation occurring, SEC studies were done on an uncrosslinked PS-*b*-PLA analog (polymer P) containing no BCB. The BCB containing polymers could not be used, since upon heat treatment they crosslink and become insoluble. Solutions of polymer P in chlorobenzene were drop cast under nitrogen, onto ~1 cm x ~1 cm silicon wafers, so that ~2-3 mg of a thick polymer film was on each wafer. These wafers were then dried overnight under a stream of nitrogen prior to heat treatment. The resulting films were several microns thick. When the PS-*b*-PLA films were heated for various times under an air atmosphere (ambient conditions), degradation did take place, as evidenced by SEC (see Figure 2.10). This degradation, however, most likely resulted in the oxidation of the PS matrix, and may, therefore, introduce unwanted chemical functionality.

**Figure 2.10. SEC studies of the degradation of PS-b-PLA under air.**



Ideally, the decomposition of the PLA should be done under an inert atmosphere to prevent oxidation reactions. Similar films heated in a glove bag under dry nitrogen did not show any degradation (see Figure 2.11). This data does, however, show something very interesting. At higher molecular weights, there is the appearance of a small peak, corresponding to approximately twice the molecular weight of the diblock copolymer. This is most likely due to the recombination of radicals formed on the PS ends of the diblock copolymer, where the alkoxyamine is located. This does not offer any quantitative data, but it is interesting to see that at least some of the chain ends may still contain the alkoxyamine end group, consistent with previous studies.<sup>78</sup>

**Figure 2.11. SEC studies of the degradation of PS-b-PLA under nitrogen.**



The degradation studies shown above indicate that the PLA can only be removed in an environment where air is present. Since the experiment done in Figure 2.10, was done on a hot plate on the lab bench, there was a possibility that the degradation could also be due to moisture, since the environmental humidity was not controlled. A separate set of studies done under nitrogen at 40% humidity gave the same results as Figure 2.11, indicating that oxygen is responsible for the degradation seen in Figure 2.10, and not humidity alone.

Since the thermal degradation of PLA could not be done under a nitrogen atmosphere at the temperature ranges used, this was not a viable route for the preparation of the nanoporous templates. Instead, the removal of the PLA domains had to be done using chemical degradation with a basic solution.



## 2.5.2 Base Degradation

Because thermal degradation does not seem to be a useful route to the preparation of nanoporous templates, an alternate chemical etching method must be used. Previous work using PS-*b*-PLA polymers to create uncrosslinked porous monoliths, used a 0.5 M NaOH solution in 50:50 methanol:water to remove the PLA.<sup>25</sup> This approach was applied here to create nanoporous crosslinked templates.

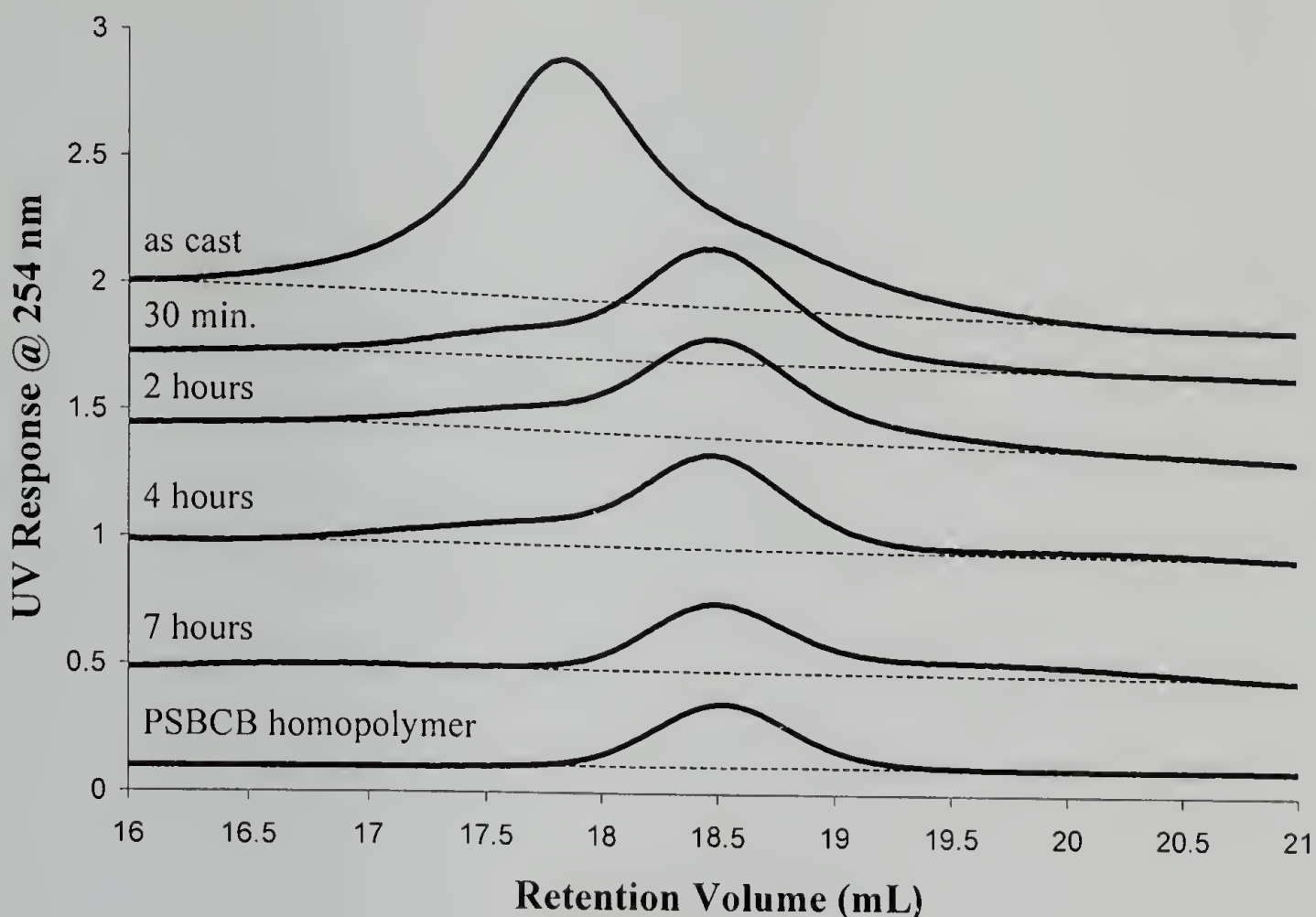
The template preparation involves first crosslinking the template, followed by degradation of the minor component (see Figure 2.1). The templates created herein were made from thin films (~30 nm) of the PSBCB-*b*-PLA diblock copolymers. Films were spin-coated from 1% chlorobenzene solutions onto a 35 nm gold surface. Gold coated silicon substrates (35 nm Au, on a 2 nm Cr adhesion layer) were prepared in-house on precleaned Si wafers. Crosslinked samples were prepared by annealing under nitrogen at 170 °C for 2 hours, then heating to 200 °C for 5 hours (unless otherwise noted). This temperature and time combination was determined from the swelling experiments to give the maximum degree of crosslinking, which is needed here for nanopore stability (as will be further discussed in the “template stability” section).

The thin film behavior of four PSBCB-*b*-PLA polymers, polymers G,H,I and K were studied in detail using SFM and TEM. All of these diblock copolymers microphase separated into cylindrical microdomains of PLA in thin films, despite the slight difference in volume fractions. This is consistent with the observations of Hillmyer and coworkers<sup>26</sup> for the non-BCB containing PS-*b*-PLA analogs. The majority of the template preparation studies were done using polymers G and H. where polymers I and K were used to confirm the results (not shown). The average center-to-

center distances of the PLA cylindrical microdomains were 21.4 nm (d-spacing= 18.5 nm) and 21.8 nm (d-spacing= 18.9 nm) for polymers G and H, respectively, as measured by SAXS, with cylinder diameters of 10 and 14 nm as measured by SFM, respectively (see Table 2.2).

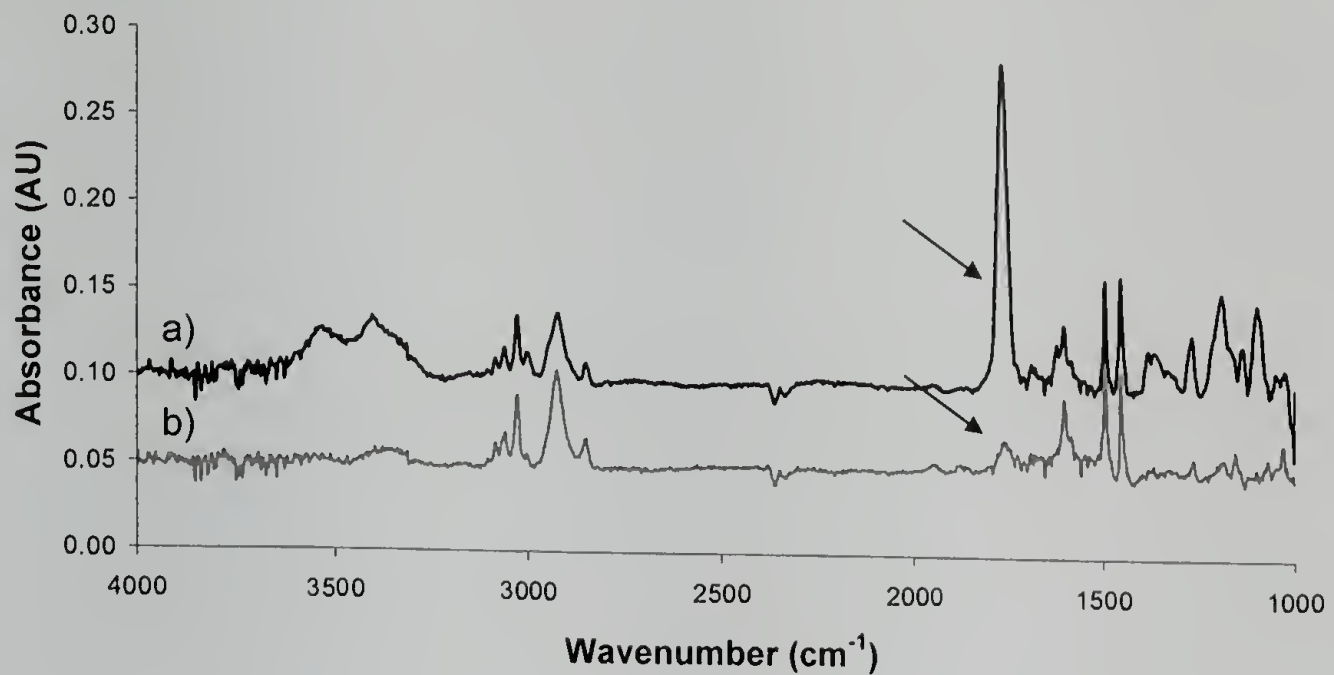
Studies were performed to determine the length of time needed in order to achieve maximum PLA removal. For this, SEC and polarization-modulation infrared reflection-absorption spectroscopy (PM-IRRAS) were used to monitor the removal of PLA from thin films on gold substrates. SEC studies were limited to uncrosslinked samples, due to insolubility of the crosslinked films. Uncrosslinked films of polymer H, were subjected to various base treatments and SEC was used to determine the extent of degradation (see Figure 2.9). It was found that the maximum amount of PLA was removed after 7 hours of degradation.

**Figure 2.12. SEC traces (UV detector at 254 nm) of substrate supported non-crosslinked films after base degradation for different lengths of time, as specified, followed by dissolution in THF.**



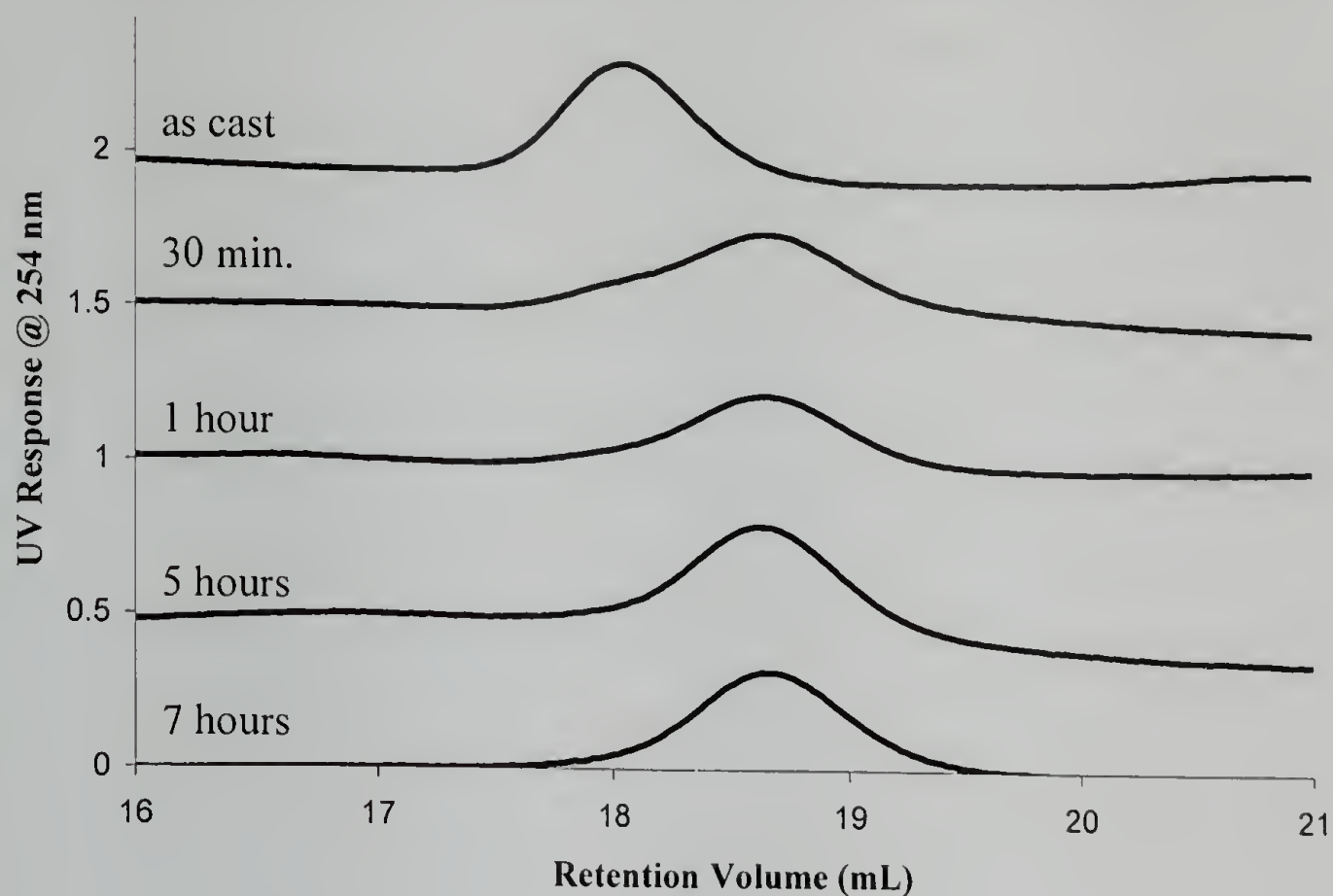
A similar 30 nm film of polymer H was crosslinked at 170 °C for 2 hours + 200 °C for 5 hours, and base degraded for 7 hours. PM-IRRAS studies on this film indicated that not all of the PLA was removed. This may be due to inaccessibility of the PLA within the pores, and is consistent with the blocked pores seen in TEM studies (see Figure 2.14). The IR data shows that 87% of the PLA is removed, as monitored by the disappearance of the carbonyl peak. As these base degradation results indicate, the optimal amount of time to remove the maximum amount of PLA is ~7 hours.

**Figure 2.13. PM-IRRAS spectra of a) crosslinked sample and b) crosslinked sample after base degradation. The fraction of PLA degraded was determined from the disappearance of the carbonyl peak at  $1763\text{ cm}^{-1}$ .**



Degradation of the PLA block can also be achieved using MF-319<sup>TM</sup> (Rohm and Haas), a commercially available chemical developer used in lithography that contains aqueous trimethylammonium hydroxide and surfactants. A similar base degradation study was done using this developer and it was found to completely degrade the PLA block, in a 30 nm thick film, after 5h as monitored by SEC (see Figure 2.14). The studies reported herein, however, used the sodium hydroxide solution, with 7 hours soak time, followed by a 50:50 methanol:water rinse, for the PLA degradation to create the nanoporous templates, unless otherwise noted.

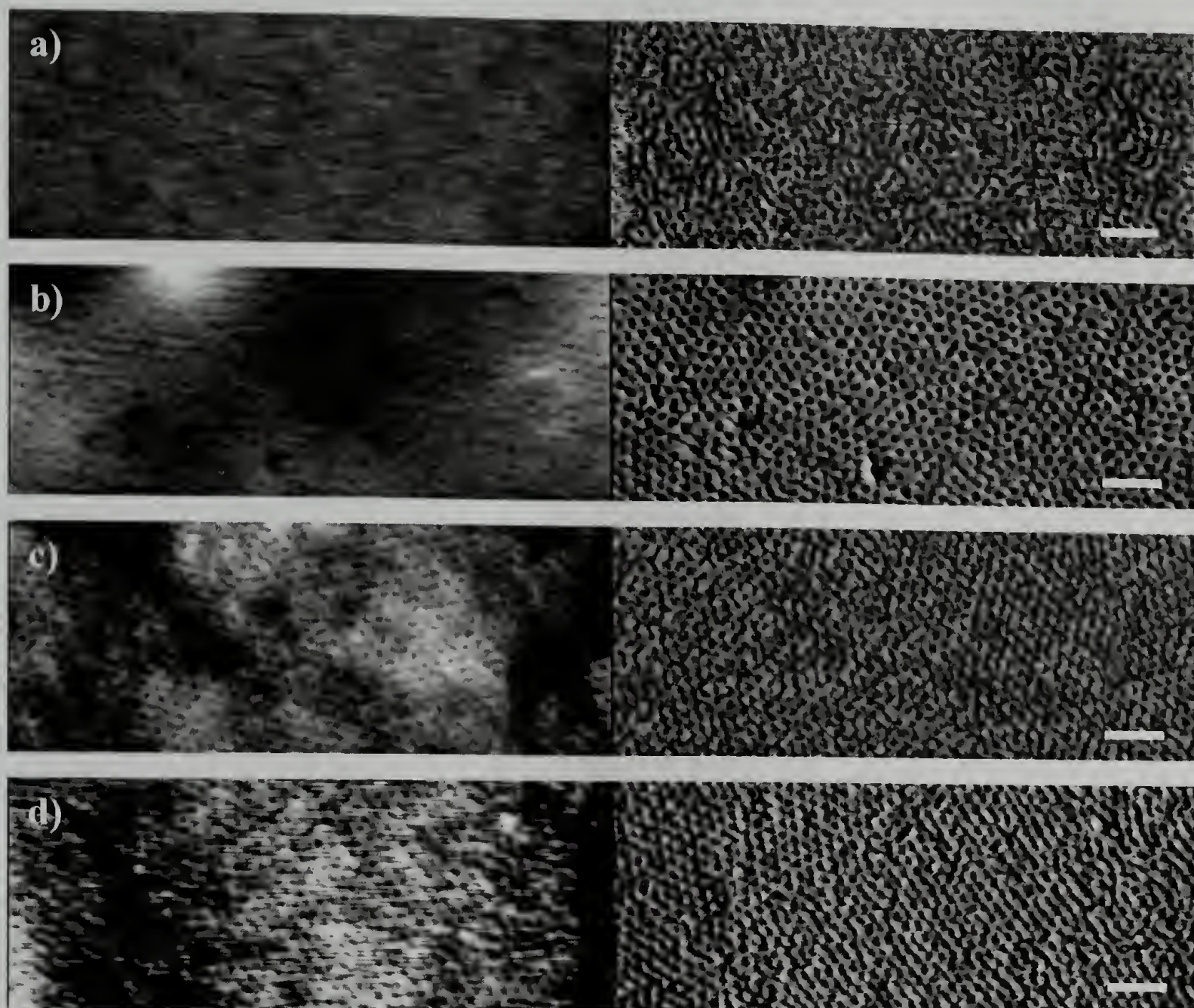
**Figure 2.14. Degradation studies done using a commercially available developer, Rohm and Haas MF-319™, for various degradation times.**



### 2.5.3 Template Characterization

The morphology of the nanoporous thin films, before and after base degradation, was characterized using scanning force microscopy (SFM). Degradation of the PLA using a sodium hydroxide solution produced nanoporous films (Figure 2.15) where the majority of the PLA could be removed by soaking the film (still on the substrate) in a basic solution for 30 minutes. Complete removal of the PLA required 7 hours of base degradation, as determined by SEC and PM-IRRAS (see Figures 2.12 and 2.13). SFM of films that were heated and base degraded for various times, showed the appearance of a porous morphology upon degradation as noted by the appearance of pores (dark spots) in the SFM height images (see Figure 2.15).

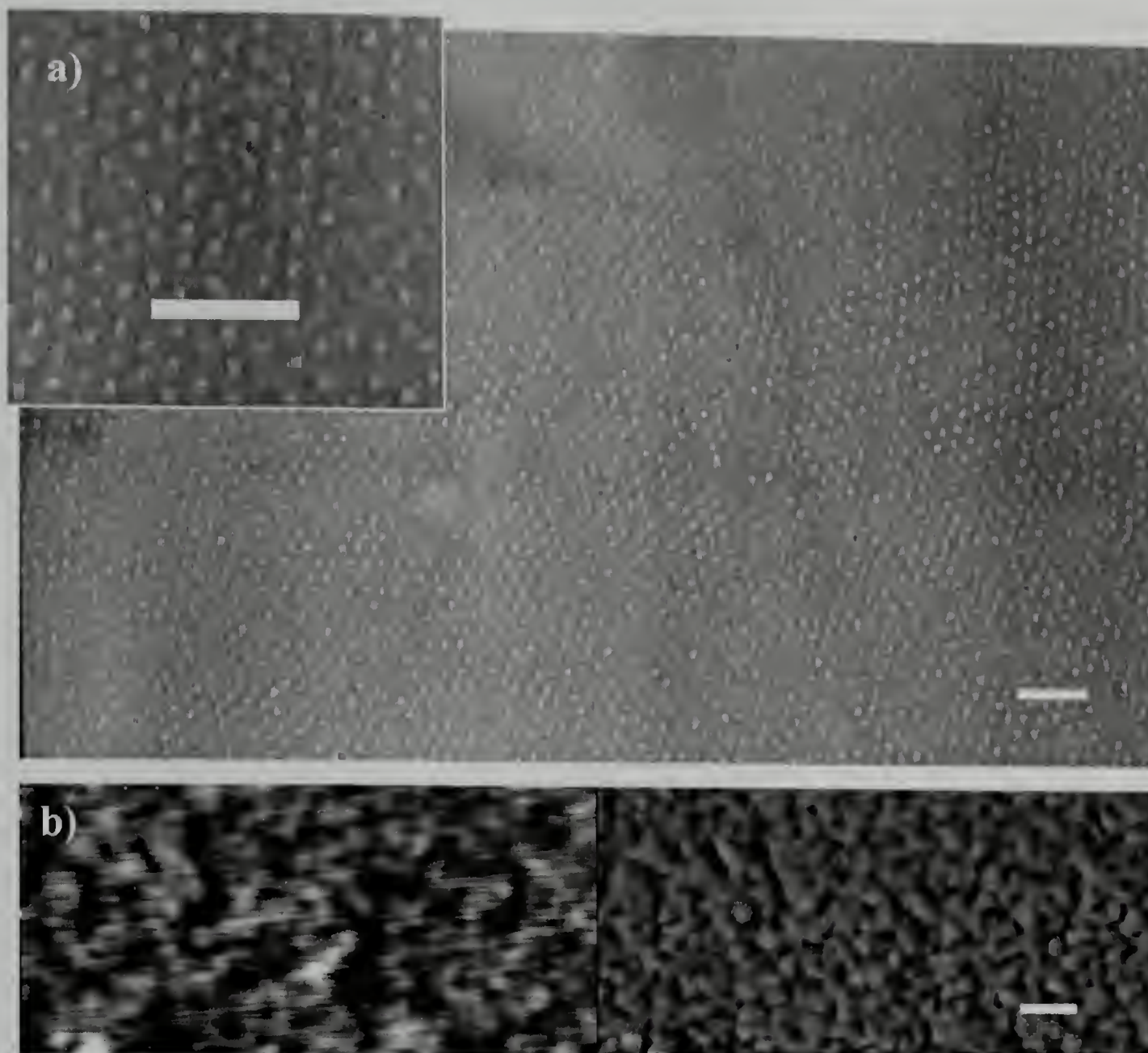
**Figure 2.15: SFM images of PSBCB-*b*-PLA (a) as-cast and (b) annealed at 170 °C for 2 hours then base degraded for 30 minutes. Annealed at 170 °C for 2 hours, crosslinked at 200 °C for 5 hours and then base degraded for (c) 90 minutes and (d) 11 hours. Scale bar = 100 nm. Left images are height, scale= 5 nm, and right images are phase, scale = 20° (for a and b), 30° (for c and d).**



Although the SFM characterization shows that the microphase-separated structure is oriented perpendicular to the air surface, further characterization was needed to determine if the pores maintained their orientation and penetrated through the film. Transmission electron microscopy (TEM) was used to look through nanoporous thin films to confirm the pore orientation. Thin film samples used for TEM studies were removed from the gold surface by floating the film onto an aqueous solution of potassium iodide and iodine (40 g KI, 10 g I<sub>2</sub> and 400 mL water) and picking up the

films using copper grids. TEM results of the base degraded films indicated that the cylindrical microdomains were oriented normal to the surface over large areas and penetrated through the film (see Figure 2.16). Since the microdomain size of the PSBCB-*b*-PLA is  $\sim 1/2$  of the film thickness, TEM provided strong evidence of the orientation of the pores. For stronger evidence that the porous morphology penetrated through the films, a thin film was coated with carbon and embedded in epoxy to “flip” the sample, to allow SFM imaging of both the top and the bottom of the film. For embedding, films still on the substrate were coated with a few nanometers of evaporated carbon, then embedded into epoxy and cured at 60 °C overnight. The embedded films were removed from the substrates using liquid nitrogen, exposing the underside of the films. SFM done on the underside of base degraded films, indicated that the cylindrical microdomains spanned across the film, from the surface to the substrate (see Figure 2.16). There is an added surface roughness due to the embedding of the films.

**Figure 2.16. Characterization of the thin film porosity. a) TEM looking down through a 30 nm crosslinked film with holes where the PLA was removed, inset is expanded region. b) SFM, height (left) and phase (right), of the bottom of a similar 30 nm film. Scale bars = 100 nm.**

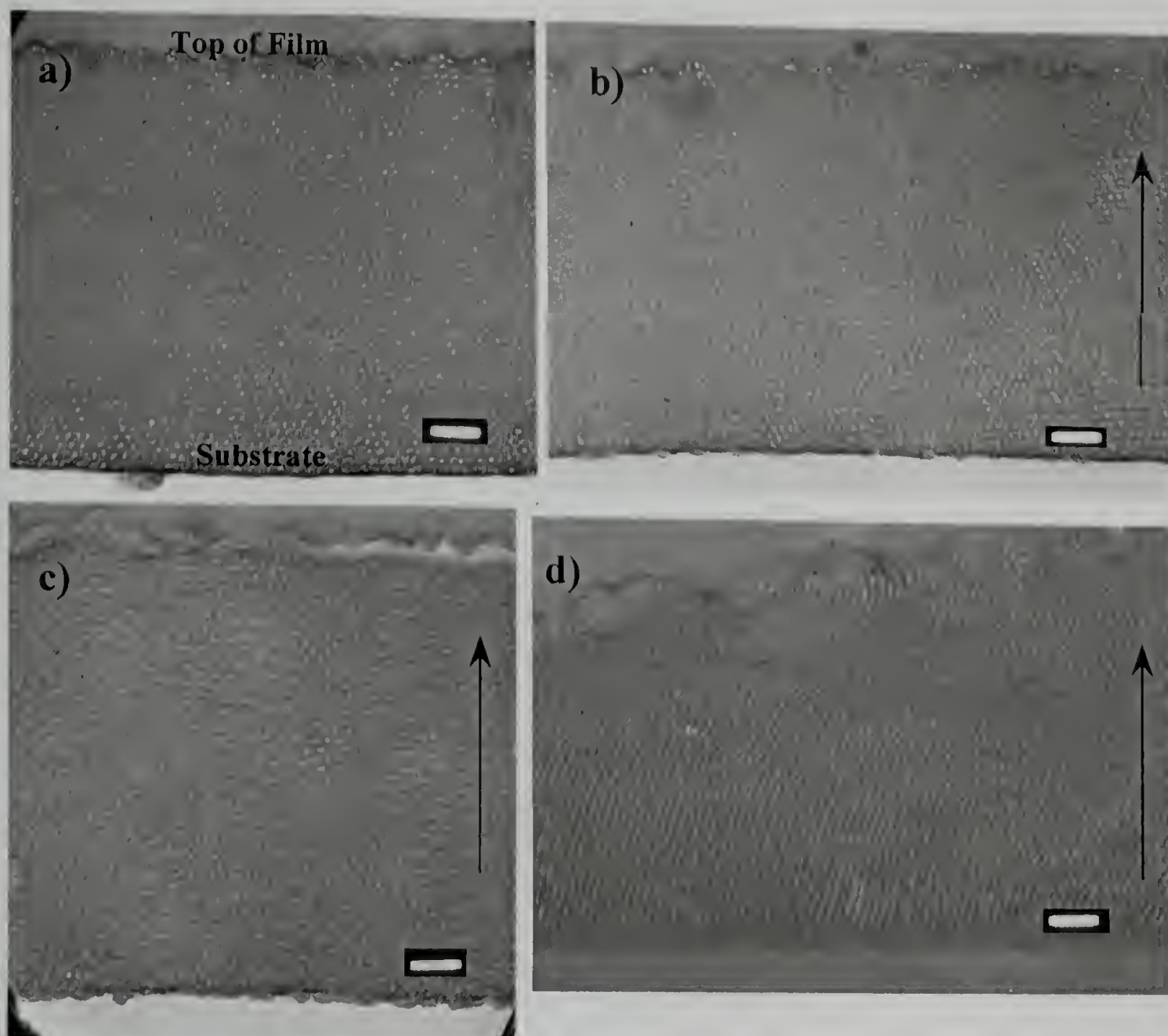


Confirmation of the perpendicular orientation of the nanoporous structure is important for possible templating strategies. The ability to control the orientation of the microphase separated morphology, either parallel or perpendicular, is an important tool for the reproducible fabrication of nanoporous templates. It is also important to have control over the lateral ordering of the morphology. Thermal and solvent annealing (with benzene, chlorobenzene, etc.) were attempted to improve the long-range ordering, but the attempts met with poor and inconsistent results, usually resulting in a mixed perpendicular and parallel orientation of the microdomains.



All the thin films studied favored a perpendicular orientation of the microphase-separated morphology on the gold substrates. A few studies done on thicker films indicated that films  $> 80$  nm thick on the gold substrate resulted in the parallel orientation of the morphology as measured by SFM. The ability to create templates of varying thickness, with consistent orientation of the morphology would be ideal for a variety of applications. One way to create perpendicular orientation of microphase separated morphologies is by the application of an electric field.<sup>16,18,19</sup> Preliminary studies using electric field alignment were done on thicker films of PSBCB-*b*-PLA, and show that perpendicular orientation is possible over  $\sim 1$  micron (see Figure 2.17). Films were prepared for the e-field alignment by spin-coating an 8% toluene solution onto a gold-coated silicon wafer. Subsequent electric field alignment was performed as previously described<sup>79</sup> using a  $50 \text{ V}/\mu\text{m}$  e-field. The TEM samples were prepared by coating the films with carbon, embedding them in epoxy, and microtoming thin slices. These slices were then placed on copper grids and the PS domains were selectively stained using ruthenium tetroxide. The as-cast sample (no heat applied) and the sample heated at  $170^\circ\text{C}$  for 2 hours (not shown) both exhibit parallel orientation of the microdomains with the substrate. The perpendicular alignment of the microdomains was not seen until the film was heated between  $170^\circ\text{C}$  and  $200^\circ\text{C}$  over several hours. It is not clear when the alignment actually began to take place, but it is clear that full alignment over the entire film was not possible (under these conditions) due to the competing crosslinking reaction of the BCB groups.

**Figure 2.17. Electric field alignment of PSBCB-*b*-PLA. a) as-cast, b) and c) areas of mixed alignment after e-field, d) area of full alignment. Arrows indicate the direction of the electric field. Scale bars= 100 nm.**



Further studies are needed to determine the ideal conditions for the electric field alignment of PSBCB-*b*-PLA. Previous work showed that the addition of salts to diblock copolymers can enhance the ability to orient the domains using an electric field, through an increase in the dielectric constant difference between the two blocks.<sup>80,81</sup> This method is currently being explored by the same group to enhance PS-*b*-PLA orientation. The results reported herein, however, focus on thin film behavior on gold substrates, since the thin films consistently exhibited perpendicular orientation without

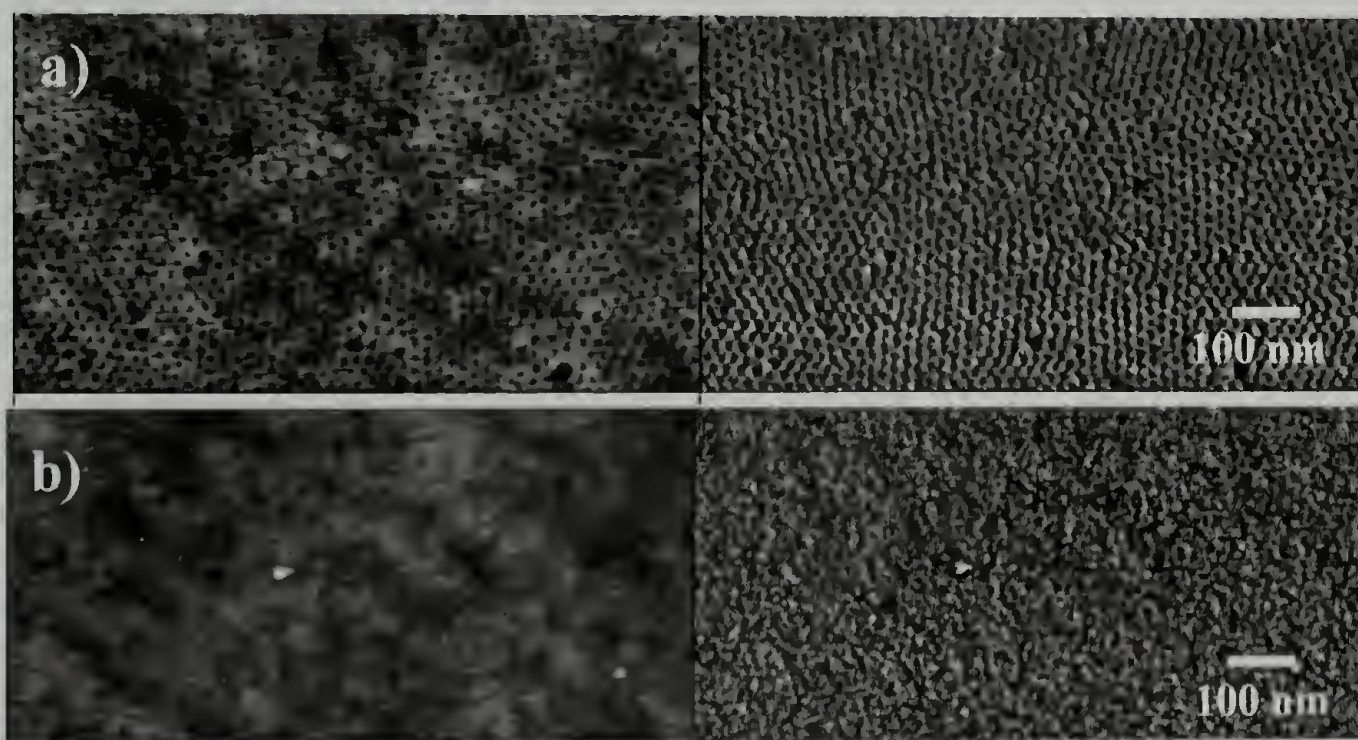
the need for added external fields. Therefore, the films used in the following studies were  $\sim 30$  nm thick to ensure perpendicular orientation of the domains.

#### 2.5.4 Template Stability

The thermal crosslinking of the matrix is, as would be expected, critical. With PS-*b*-PLA the porous film, produced by removal of the PLA, is not stable upon heating. Pore collapse is seen when the films are heated to 200 °C. Even with PSBCB-*b*-PLA, where there are BCB groups present for crosslinking, the crosslinking must be performed before removal of the PLA to prevent collapse of the pores.

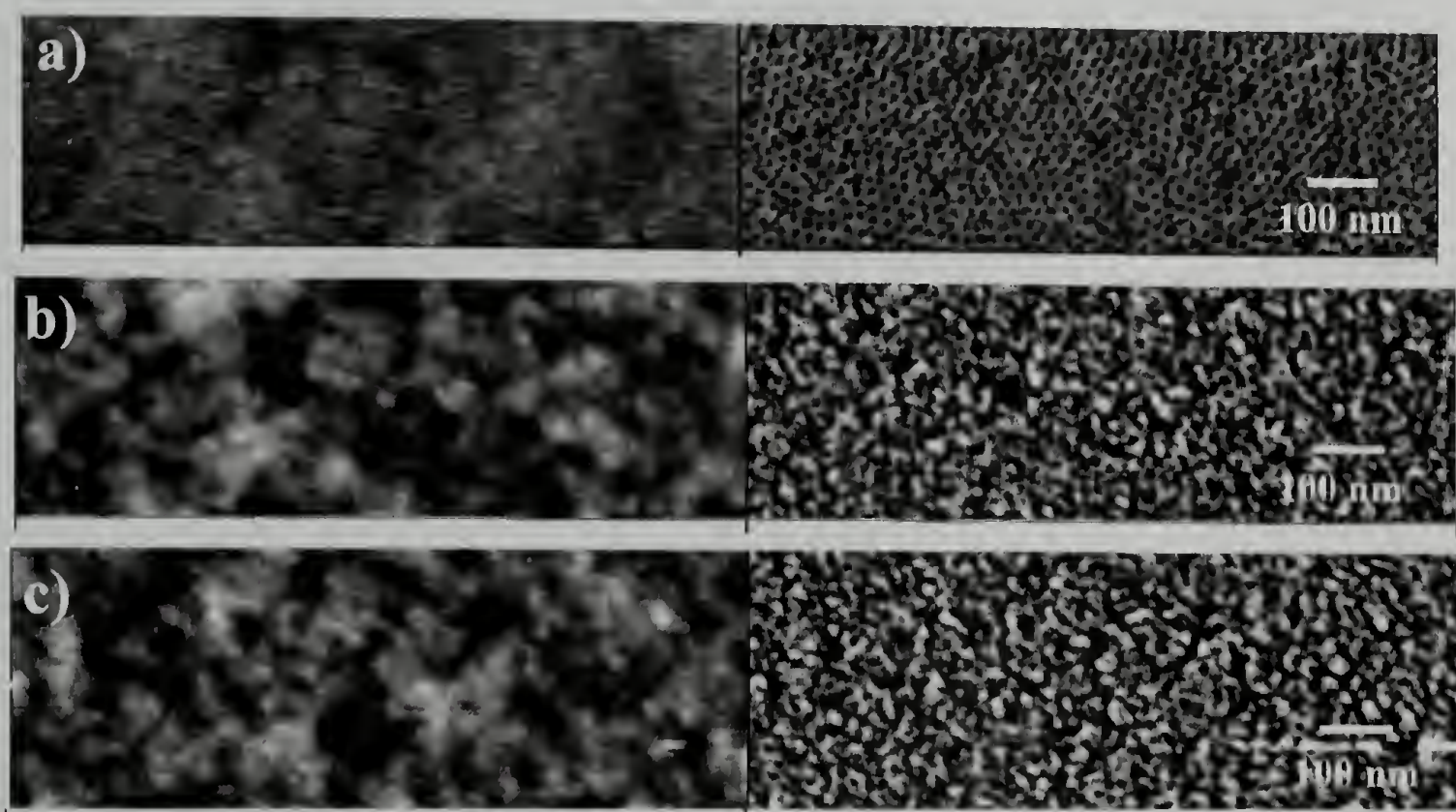
Insufficient crosslinking quickly leads to the collapse of the porous structure as seen in Figure 2.18. Heating the film to 170 °C for one hour, followed by base degradation, is not enough to stabilize the nanoporous morphology. Subsequent heating at 170 °C for just 5 minutes results in complete pore collapse.

**Figure 2.18. Insufficient crosslinking resulting in pore collapse. Films of polymer G, a) heated at 170 °C for 1 hour and base degraded for 30 min b) subsequent heating at 170 °C for 5 min.**



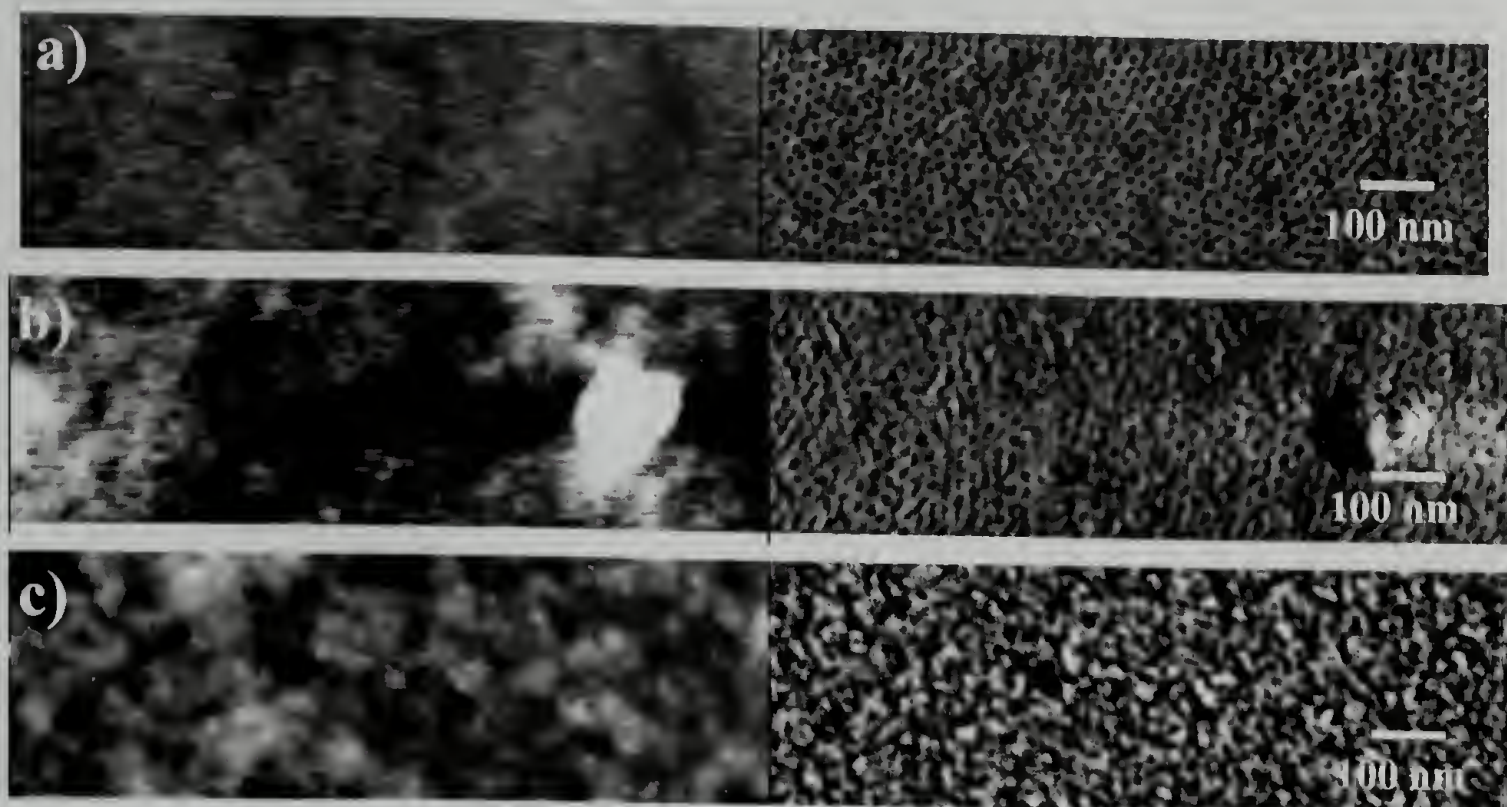
In order to prevent pore collapse, the amount of crosslinking needs to result in a modulus that will support the porous structure, as was calculated using equations 4 and 5. Although SEC (see Figure 2.8) indicates that the sol fraction is minimal after heating the films for 1 hour at 200 °C, the film is not sufficiently crosslinked after this time. SFM studies of the stability of the porous films after crosslinking for 1 hour show the destruction of the porous morphology (see Figure 2.19). Without adequate crosslinking, although some pores are still evident, fissures and cracks develop.

**Figure 2.19. Insufficient crosslinking resulting in pore collapse. Films of polymer G, a) heated at 170 °C for 2 hours plus 200 °C for 1 h and base degraded for 30 min b) subsequent heating at 200 °C for 5 min and c) 20 min.**



Also, a similar result is seen when insufficiently crosslinked films are exposed to solvent (see Figure 2.20). While there are enough crosslinks so that the majority of the film does not dissolve, there is the appearance of cracks similar to those seen in Figure 2.19. This indicates that the  $M_c$  is too large to support the porous structure.

**Figure 2.20. Insufficiently crosslinked porous films exposed to solvent. Films polymer G, a) heated at 170 °C for 2 hours plus 200 °C for 1 h and base degraded for 30 min b) subsequent THF soak for 30 min and c) 90 min.**

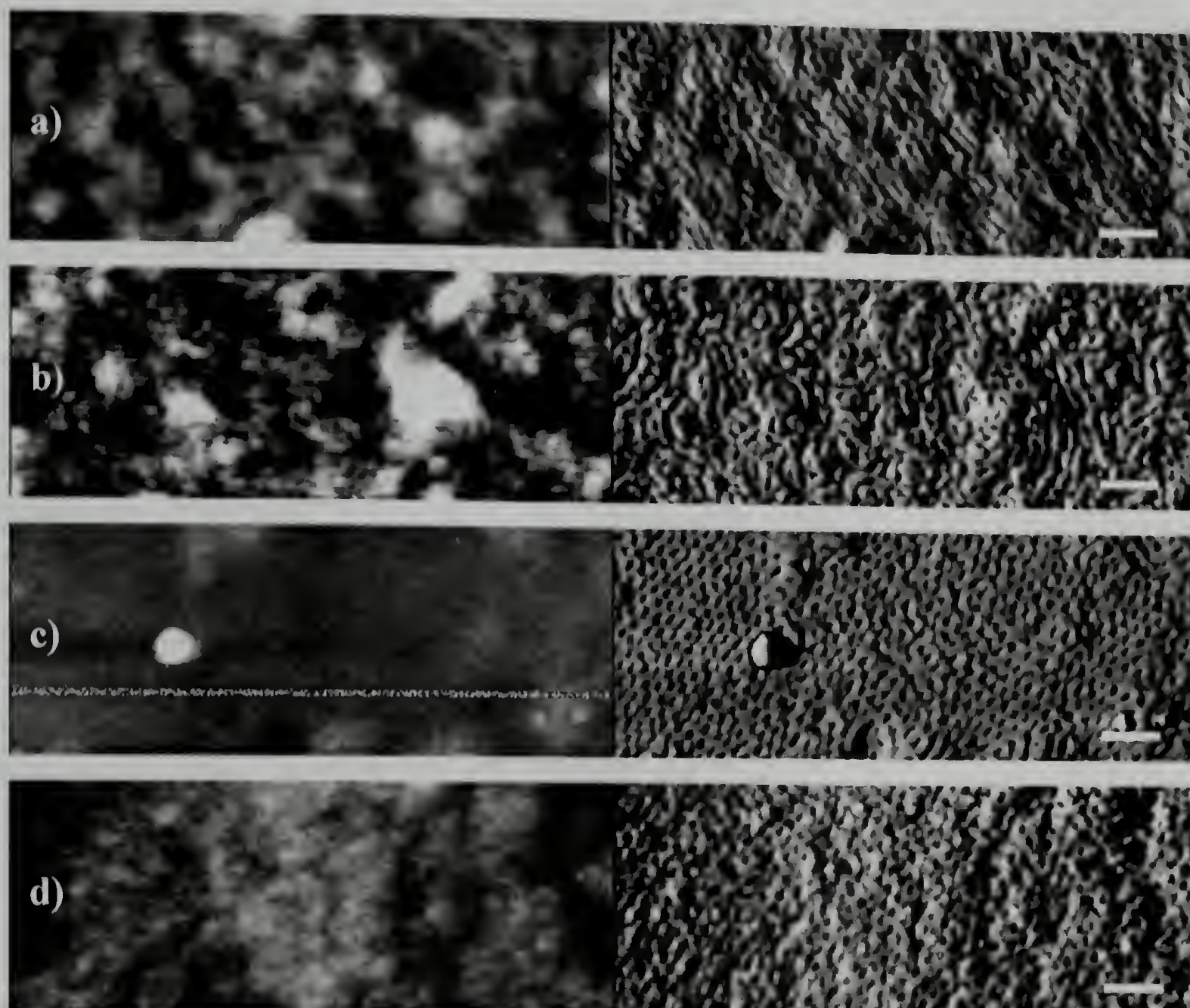


According to the calculations using equations 4 and 5, however, pore collapse would not be expected. When the calculations for the molecular weight between crosslinks needed for pore stability is compared to the experimental values obtained in Table 2.3, the porous structure should be stable after heating for 170 °C for 2 hours + 200 °C for 1 hour since this heat treatment yields a lower  $M_c$  than should be needed. However, this is not the case as evidenced in Figures 2.19 and 2.20. This is most likely due to the assumptions made in the calculations for pore stability, which do not take into account the presence of the sol fraction, nor the possibility for unequal distribution of the BCB groups as they crosslink.

These results indicate that using equations 4 and 5 for this system, give a poor representation of the  $M_c$  needed to maintain the porous structure. Based on the assumptions made for the calculation, it overestimates the  $M_c$  needed for pore stability. Therefore, the thermal treatment that was used, 170 °C for 2 hours + 200 °C for 5 hours,

was determined from the swelling experiments to give the maximum amount of crosslinks for the system (see Figure 2.7). This amount of crosslinks was sufficient to maintain the structural integrity of the pores, even when they were exposed to harsh thermal and solvent conditions (see Figure 2.21). These porous films are solvent resistant and do not dissolve or delaminate from the substrate upon soaking. Films soaked in THF at room temperature for 3 days, or treated more harshly by placing in refluxing benzene for 3 hours, maintained the porous structure, as evidenced by SFM. Heating studies done on the porous films show minimal collapse of the porous structure, in that the pores are maintained but show a slight rounding of the edges.

**Figure 2.21: SFM images of porous films subjected to various thermal and solvent conditions. (a) base degraded for 11h then heated at 250 °C for 1 hour (b) base degraded for 30 minutes then heated at 200 °C for 11 hours (c) base degraded for 30 minutes, then soaked in THF at room temperature for 3 days (d) base degraded for 11 hours then submerged in refluxing benzene for 3 hours. Scale bars = 100 nm.**



Therefore, to sufficiently crosslink the thin films for solvent and thermal resistance, the films were annealed at 170 °C for 2 h, and then crosslinked at 200 °C for 5h under a nitrogen atmosphere. Since the nanoporous films have hydroxyl functionality within the pores, the ability to withstand harsh reaction conditions opens up a wide range of possibilities for subsequent pore modification.

## 2.6 Conclusions

In summary, a crosslinkable diblock copolymer, PSBCB-*b*-PLA, was synthesized and used to create nanoporous thin films. The PSBCB block, containing a thermally crosslinkable group, was used to immobilize the microphase-separated morphology, while the minor PLA block was base degraded. The ideal conditions for crosslinking were determined to be 170 °C for 2 hours + 200 °C for 5 hours, while base degradation using 0.5 M NaOH was done in 7 hours. These conditions afforded a nanoporous template with cylindrical pores oriented perpendicular to the substrate that were stable to subsequent thermal and solvent conditions. The process presented here for the fabrication of nanoporous templates is simple, requiring minimal handling of the film and eliminating the need for UV irradiation, ion etching or secondary chemical modification to remove the minor component.



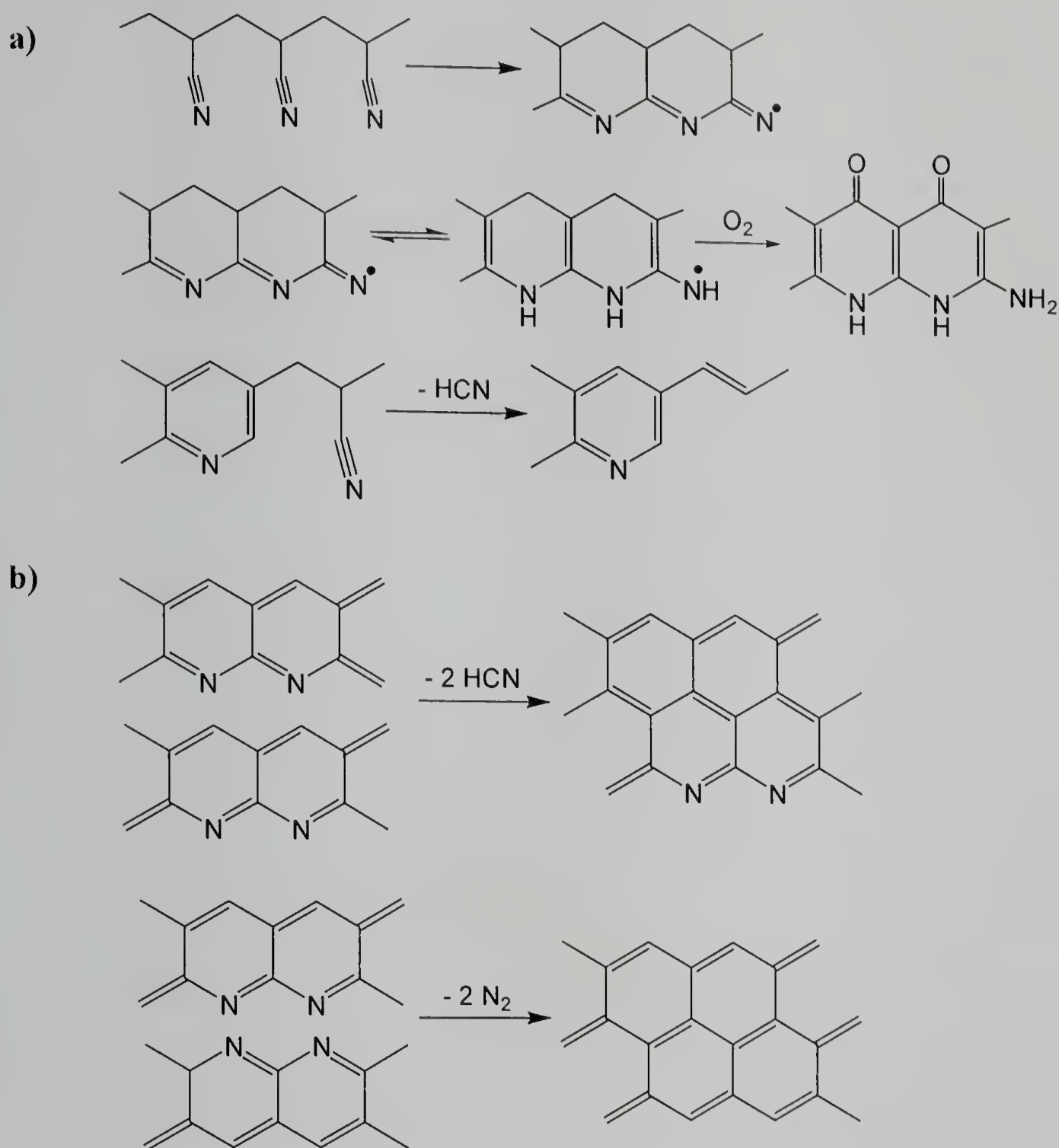
## CHAPTER 3

### ACRYLONITRILE-BASED TEMPLATES

#### 3.1 Background

Acrylonitrile-based materials have been used extensively as carbon precursors, especially for the formation of carbon fibers. Poly(acrylonitrile) (PAN), and related acrylic copolymers, undergo thermal stabilization and can be subsequently heated to form thermally stable carbonaceous structures.<sup>82,83</sup> This thermal behavior of PAN has been heavily characterized over the past several decades using techniques such as pyrolysis gas chromatography, solid-state NMR, IR, mass spectrometry, TGA, XRD and elemental analysis.<sup>83-90</sup> Some of the reactions that occur during PAN degradation are shown in Figure 3.1. When PAN is heated between 250 °C–300 °C it decomposes by cyclization and aromatization of the nitrile side groups, resulting in the formation of short cyclized ladder-like sequences.<sup>83</sup> This stabilization is typically done in an air atmosphere which aids in the intermolecular crosslinking reactions. After this stabilization step, the PAN can then be pyrolyzed at temperatures > 600 °C, where further intermolecular crosslinking occurs, resulting in the formation of honeycomb-like carbonaceous structures. These carbonaceous structures still contain heteroatoms, that are not completely removed until the sample is heated to >1600 °C, yielding a graphitic structure.

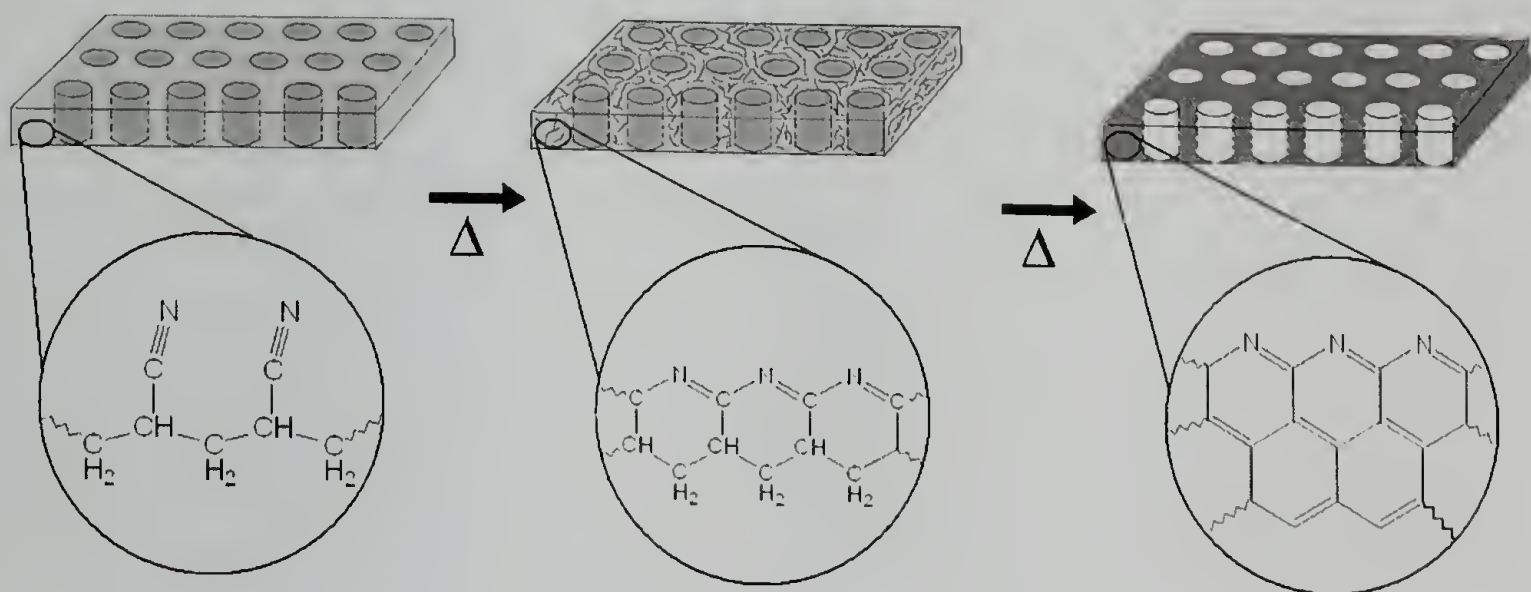
**Figure 3.1. Thermal degradation mechanisms of PAN.**<sup>83,85,91</sup> Some of the reactions that occur during a) stabilization under air, b) pyrolysis.



Diblock copolymers containing PAN can be used to create carbonaceous replicas of microphase separated morphologies. Here, polystyrene-*block*-polyacrylonitrile (PS-*b*-PAN) was used to create carbonaceous nanoporous templates. During the pyrolysis step, the PAN converts to carbon and the sacrificial PS domains undergo degradation, generating pores in place of the PS domains (see Figure 3.2). Unlike the BCB-containing diblock copolymers discussed in the Chapter 2, PS-*b*-PAN

can be used to create a completely thermal route for the generation of nanoporous templates.

**Figure 3.2. Carbonaceous template formation via stabilization and subsequent pyrolysis of PAN containing diblock copolymers. PAN is shown as the matrix in this diagram. The minor component is a sacrificial non-graphitic forming polymer which is removed during the pyrolysis step.**



Diblock copolymers containing PAN have been studied previously, and have been explored for their ability to form carbonaceous structures.<sup>92-94</sup> Another clever method for the creation of nanoporous carbon structures was demonstrated by Dai et al.<sup>95</sup>, where a resorcinol-formaldehyde resin was polymerized within a microphase-separated PS-*b*-PVP template, and subsequent carbonization lead to an ordered nanoporous carbon film.

PS-*b*-PAN copolymers, however, have not been studied in detail, nor has the limit for  $\chi_N$  been explored, with many groups focusing on larger diblock copolymers (>20 kg/mol) for their phase separation studies.<sup>92,93,95</sup> Diblock copolymers of PS and PAN are particularly interesting due to the strong non-favorable segmental interactions,  $\chi$ , between styrene and acrylonitrile. Since the order-to-disorder transition depends on the product,  $\chi_N$ , where N is the total number of segments in the copolymer, then N can

be made small while maintaining the block copolymer in the microphase separated state. This, of course, means that the microdomains and resulting carbonaceous structures can be made smaller, with dimensions of  $\sim 10$  nm readily achieved. This chapter focuses on the generation of carbonaceous templates from PS-*b*-PAN diblock copolymers, of relatively low molecular weight, to generate nanoporous materials with features  $\sim 10$  nm.

### 3.2 Synthesis

Previous attempts to synthesize poly(styrene-*b*-acrylonitrile) were done using anionic or free-radical methods using dialkylphosphines. These met with mixed results.<sup>96-100</sup> Poly(ethylene oxide-*b*-acrylonitrile)<sup>101</sup>, poly(vinyl alcohol-*b*-acrylonitrile)<sup>102</sup>, and poly(2-ethylhexyl methacrylate-*b*-acrylonitrile)<sup>103</sup>, have also been synthesized using different polymerization methods. The synthesis of diblocks containing polyacrylonitrile is challenging, due to the limited number of solvents that dissolve PAN. Controlled bulk polymerizations are difficult because PAN is not soluble in its own monomer, causing gelation and loss of control over the reaction. Bulk ATRP of PAN has been done to create diblocks, where PAN is the minor component ( $<10\%$ ) and has a molecular weight  $<3000$  g/mol.<sup>92</sup> The reaction is usually aided by the addition of a solvent such as ethylene carbonate or dimethylformamide (DMF).<sup>94,103</sup> Recently, PAN-*b*-PS polymers were synthesized by atom transfer radical polymerization (ATRP) techniques, using a polar aprotic solvent, to overcome the challenges associated with the instability of the propagating PS-Br end groups.<sup>104</sup> In the synthetic scheme described herein, the styryl bromide end group was avoided, allowing

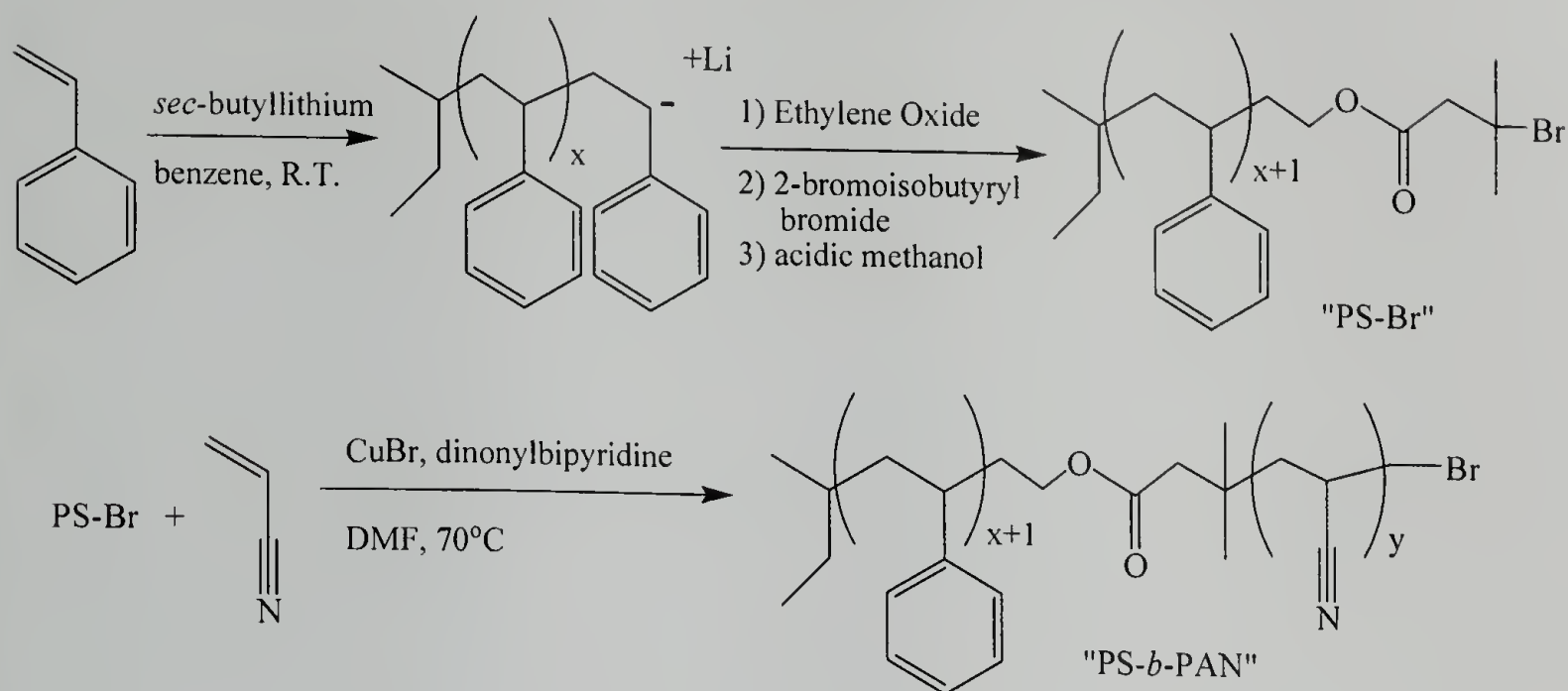
for the successful initiation of acrylonitrile by ATRP polymerization in a polar protic solvent.

For the creation of PS-*b*-PAN diblock copolymers, the limited solubility of PAN in common solvents is further complicated by the even smaller number of solvents that dissolve both PS and PAN. Ideally, a random copolymer of PS and PAN in place of the PAN block could be used to overcome solubility issues. However, these acrylonitrile containing random copolymers cannot be pyrolyzed to graphitic structures. When acrylonitrile is copolymerized with styrene, it loses its ability to crosslink into a graphitic structure due to chain scission at the styrene-acrylonitrile bonds.<sup>105</sup> Therefore, attempts to pyrolyze the structure results in the decomposition of the polymer.

With the advent of ATRP, certain polar monomers that could not be polymerized using typical living anionic procedures, can now be polymerized in a “controlled” fashion, enabling the synthesis of multiblock materials. Acrylonitrile has been shown to polymerize under ATRP conditions yielding polymers with polydispersities as low as  $M_w/M_n \sim 1.1$ , with molecular weights ranging from 1,000–10,000 g/mol.<sup>47,106</sup>

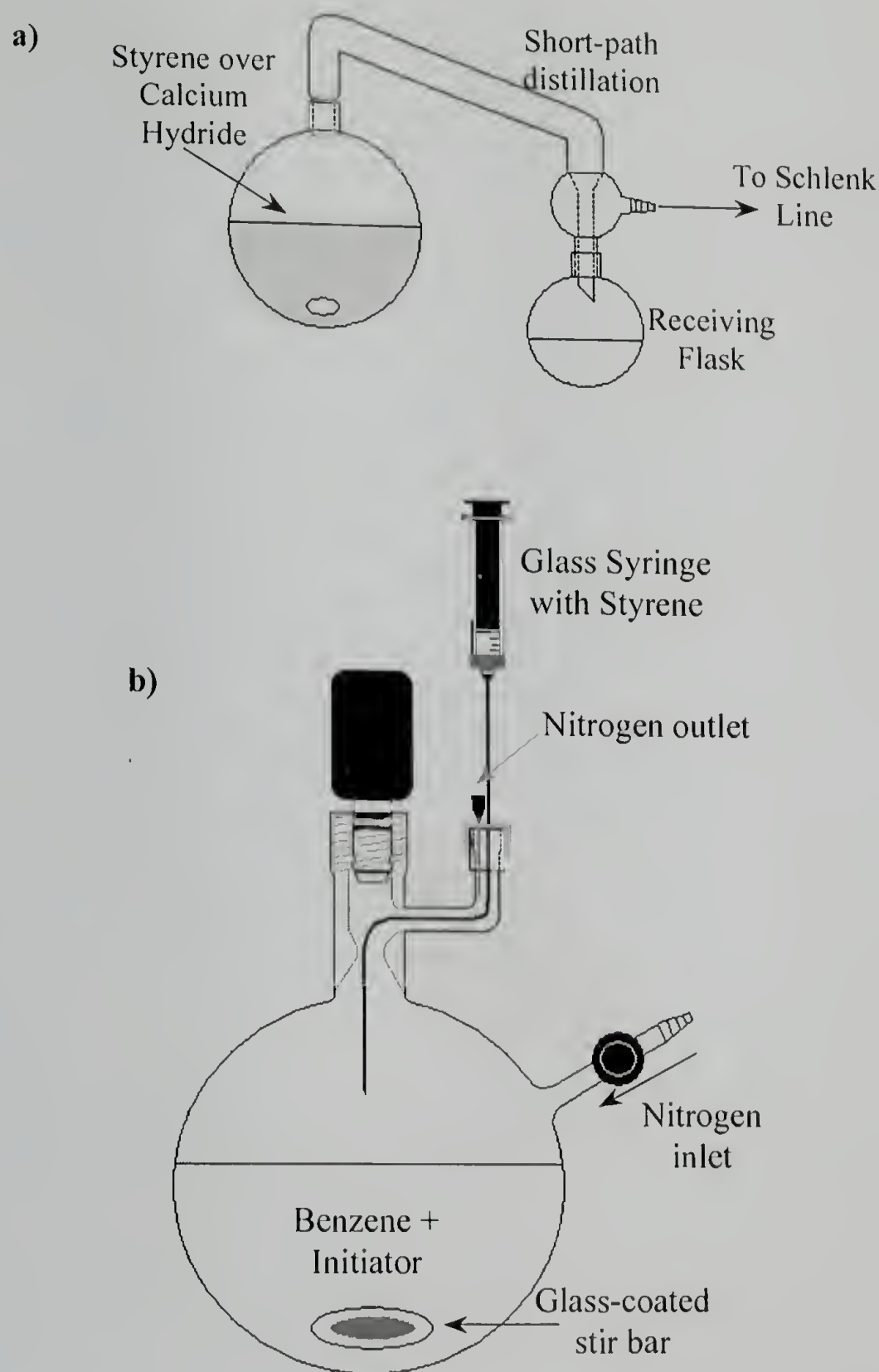
In this chapter, a combination of ATRP and living anionic polymerizations were used to synthesize a series of PS-*b*-PAN diblock copolymers. A bromine-functionalized PS macroinitiator<sup>107</sup> was used to grow PAN by ATRP using a copper catalyst (see Figure 3.3).

**Figure 3.3. Synthetic scheme for PS-*b*-PAN polymers.**



Typically, rigorous conditions are used for anionic polymerizations, involving the use of break-seals or the transfer of reactants in the gas phase, through a Schlenk line to the reaction vessel.<sup>108</sup> These rigorous conditions are necessary for targeting high molecular weight polymers (>200 kg/mol), but is not necessary for lower molecular weight polymers where minute impurities are tolerable due to the large concentration of initiator used. The technique used herein has been described previously for the synthesis of PS-*b*-PMMA diblock copolymers.<sup>109</sup> However, a major limitation of this technique involves the use of gas-tight glass syringes, which can introduce atmospheric moisture contaminants to the reaction flask causing the reaction to terminate. The reaction vessel for the living anionic polymerization is shown in Figure 3.4.

**Figure 3.4. Reaction set-up for living anionic polymerization of styrene. a) Distillation set-up for styrene, b) Reaction vessel used for anionic polymerization.**



The PS-Br macroinitiator was synthesized at room temperature in benzene (see Appendix A for details). All of the glassware used for the living polymerization (with the exception of the benzene still) were flame-dried prior to use to remove any adsorbed water. The benzene was stirred over sodium and benzophenone and distilled just prior to use. Benzene was added directly from the still head to an evacuated flame-dried

flask equipped with a glass stir bar, nitrogen inlet/outlet and Teflon stopcock (as shown in Figure 3.4). The flask was then placed on a stir-plate under a positive nitrogen flow. The benzene was titrated with a small amount of a mixture of sec-butyllithium and styrene, until the orange color just barely persisted. Then, the calculated amount of sec-butyllithium solution was added via syringe to the stirring solution. Styrene, distilled over calcium hydride (see Figure 3.4) and stored under nitrogen just prior to use, was added via glass syringe to the reaction flask. The reaction flask was sealed and the reaction was allowed to proceed for 3 hours at room temperature. Ethylene oxide was added to the reaction until the color associated with the living anion vanished (~5 minutes). The reaction flask was then sealed, and stirred overnight (~16 hours). An excess of 2-bromoisobutyryl bromide was added to the reaction flask and the polymer was precipitated in methanol and dried under vacuum overnight. The macroinitiator was characterized by SEC in THF and NMR;  $M_w = 2.1 \times 10^3$ ,  $M_n = 2.0 \times 10^3$ , and PDI = 1.09.

This PS-Br initiator was then used to synthesize the PS-*b*-PAN diblock copolymer. In a typical polymerization, the polystyrene macroinitiator, CuBr and 4,4'-dinonyl-2,2'-dipyridyl (dNbpy) were added to an oven dried polymerization tube equipped with a Teflon stir bar. The polymerization tube was backfilled with nitrogen 3 times, and then dimethylformamide (DMF) and acrylonitrile (AN) were added. The acrylonitrile was purified through a plug of basic alumina to remove the inhibitor, just prior to polymerization. The tube was then freeze/pump/thawed 3 times, backfilled with nitrogen and reacted at 70 °C for varying times. Multiple reactions were done



using the same starting PS-Br (2.0 kg/mol), and aliquots were taken to monitor the growth of the PAN for reaction times up to 4 hours and 62% conversion (see Table 3.1).

**Table 3.1. PS-*b*-PAN polymers synthesized.**

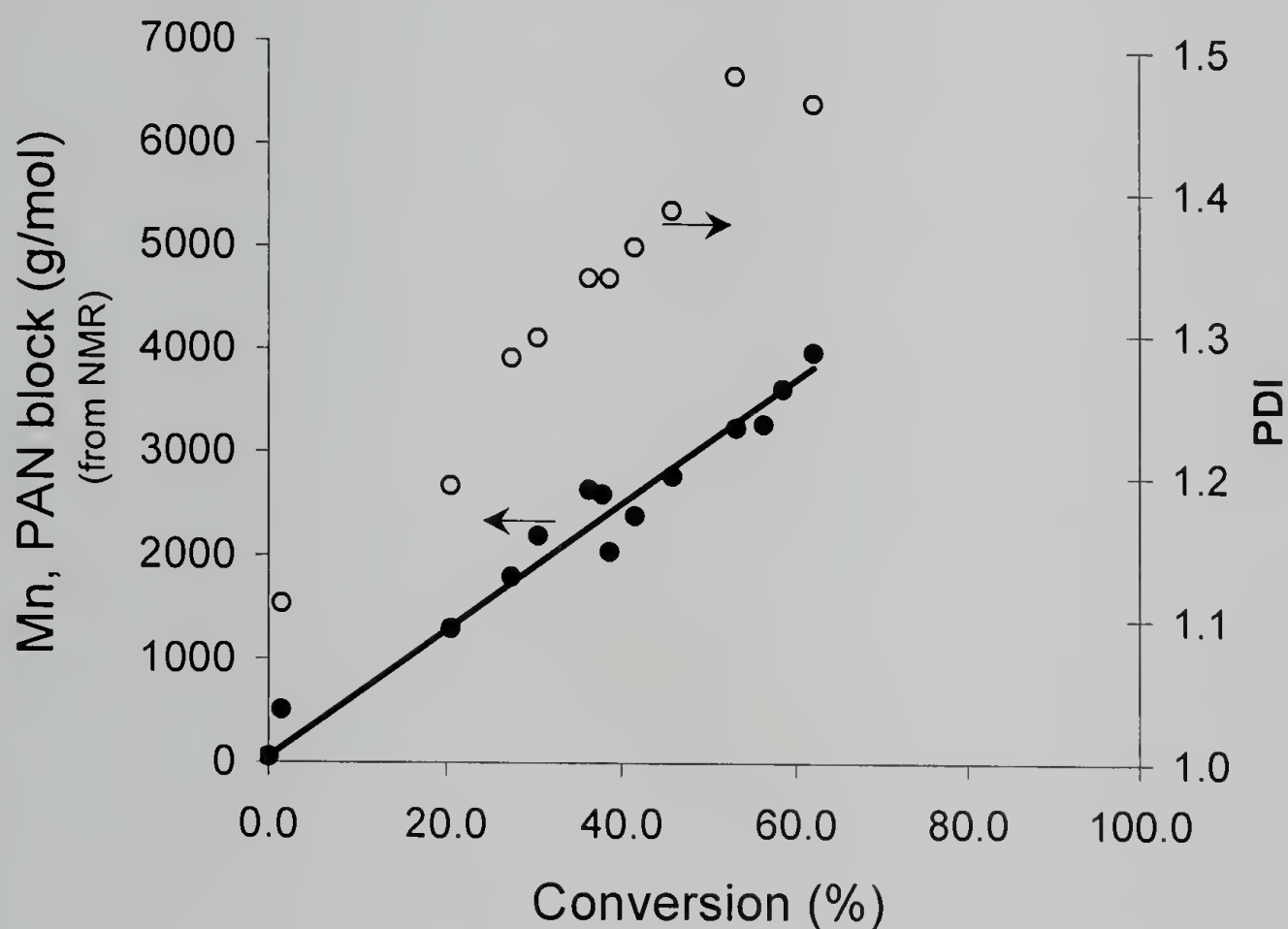
Notebook Designation <sup>a</sup>	Polymer	Reaction Time (min)	Total M <sub>n</sub>	M <sub>n</sub> PAN (NMR) <sup>b</sup>	Conversion <sup>c</sup>	Volume <sup>d</sup> % PAN	Total M <sub>n</sub> of diblock (GPC) <sup>e</sup>	PDI <sup>f</sup>
JML-2-20	SANa1	2	2510	510	1.4	18.7	11100	~1.11
JML-2-11	SANb1	10	3300	1300	20.5	37.1	18000	1.19
JML-2-11	SANb2	20	3800	1800	27.4	44.9	20000	1.28
JML-2-12	SANc1	30	4050	2050	38.7	48.1	21300	1.34
JML-2-11	SANb3	30	4200	2200	30.5	49.9	22600	1.30
JML-2-11	SANb4	40	4400	2400	41.6	52.1	22500	1.36
JML-2-11	SANb5	50	4650	2650	36.4	54.6	24800	1.34
JML-2-11	SANb6	60	5300	3300	N/A <sup>g</sup>	59.9	27700	1.26
JML-2-20	SANa2	60	4610	2610	37.9	54.1	N/A <sup>g</sup>	N/A <sup>g</sup>
JML-2-12	SANc2	60	4790	2790	45.9	55.8	25700	1.385
JML-2-12	SANc3	120	5260	3260	53.1	59.6	26000	1.48
JML-2-12	SANc4	150	5300	3300	56.3	59.9	N/A <sup>g</sup>	N/A <sup>g</sup>
JML-2-20	SANa3	180	5670	3670	54.1	62.4	N/A <sup>g</sup>	N/A <sup>g</sup>
JML-2-12	SANc5	180	5650	3650	58.5	62.3	25900	1.57
JML-2-12	SANc6	240	6000	4000	62.0	64.4	32600	1.46

**a** Notebook designation JML-notebook number-page number. Samples with same notebook numbers are different aliquots from same reaction. **b** M<sub>n</sub> was determined using the dried polymer sample in DMSO-*d*<sub>6</sub>. **c** Conversion was measured using aliquots of the reactions (a, b, c) at different times and using the integration of the DMF peak at 7.95 ppm as an internal standard to measure the disappearance of the monomer peaks. **d** Volume fraction was calculated from the NMR data using  $d_{\text{PS}}=1.06$  g/ml and  $d_{\text{PAN}}=1.17$  g/mol. **e** Significantly higher M<sub>n</sub> using SEC is typical of PAN containing samples when compared to NMR; SEC relative to PS standards. **f** No correction was done to account for peak tailing from instrument, which may account for a broadening in PDI (see Figure 3). **g** Data is not available due to limited quantities of material.

The kinetics data, as a function of conversion, for the ATRP polymerization of the PAN block are given in Figure 3.5, using the data given in Table 3.1. The number average molecular weight, M<sub>n</sub>, is shown to be linear as a function of conversion, one

indication of a controlled reaction, and typical for an ATRP polymerization. The PDI increases as a function of conversion, possibly due to deactivation of the copper catalyst by the DMF, as suggested by Matyjaszewski et al.<sup>47</sup> Even with this increase in PDI, the diblock copolymers microphase separated in bulk and in thin films, as will be discussed in the “microphase separation” section.

**Figure 3.5. Kinetics data for the polymerization of acrylonitrile using a polystyrene macroinitiator.**

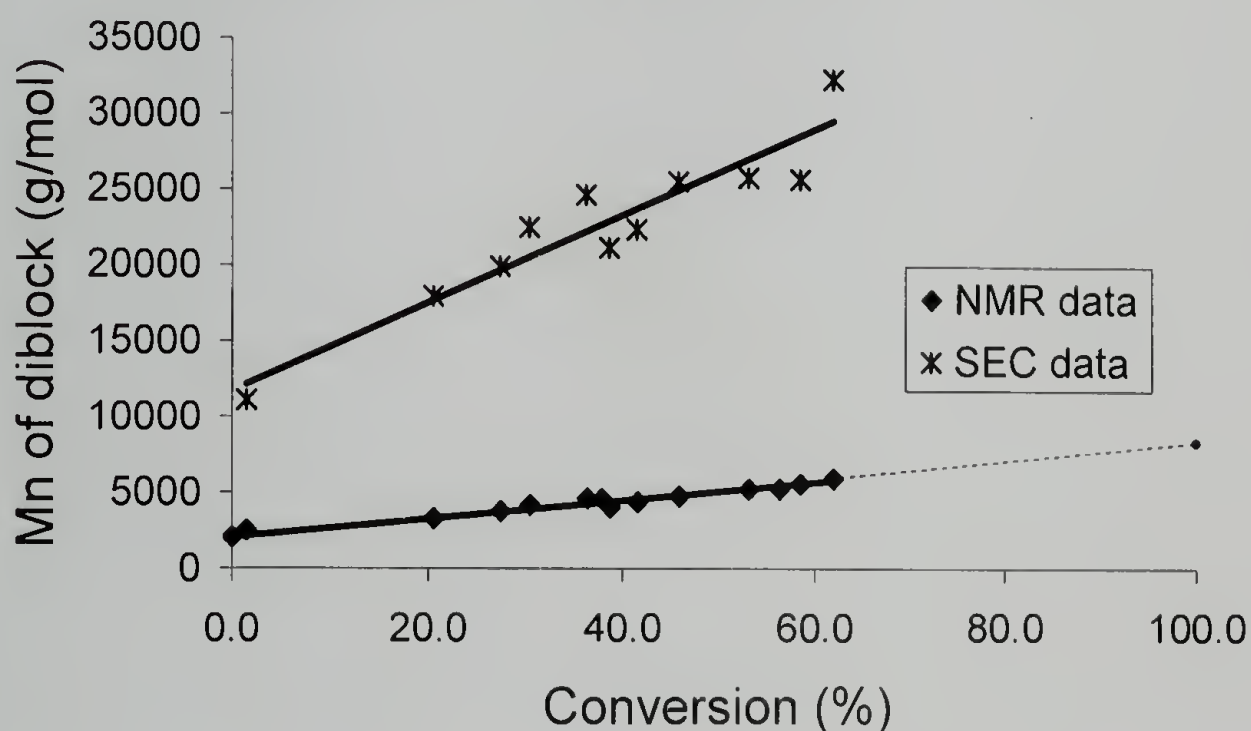


The values of  $M_n$  shown in Figure 3.5, determined using NMR, differ drastically from the molecular weights determined from SEC (see Table 3.1). Unfortunately, PAN-containing polymers interact with typical SEC column packing materials resulting in a broadening of the distribution by tailing, or odd peak shapes, that can be strongly influenced or screened by the addition of DMF soluble salts.<sup>110,111</sup> Even with the addition of salts to screen interactions, the peak shape can still be influenced by

impurities such as water, the type or brand of SEC packing material, and even the age of the columns (as per discussions with Polymer Lab technicians).

Also, when calibration standards such as PMMA or PS are used, the molecular weights corresponding to the PAN peaks can be off by an order of magnitude, which has been seen here (see Table 3.1 and Figure 3.6), and in other diblock copolymer studies where PAN is one of the blocks.<sup>92,94</sup> The  $M_n$  determined from NMR for the PAN block was the more reliable method for the characterization of the PS-*b*-PAN since the PS macroinitiator was well characterized before the polymerization of the PAN block.

**Figure 3.6. Difference in the number average molecular weight between NMR and SEC measurements using DMF with 0.01 M LiCl.**



The synthesis of PS-*b*-PAN polymers can also be extended to larger molecular weight polymers. However, since greater amounts of AN are needed to get higher molecular weight PAN, the issue of solubility in the reaction media plays a crucial role. While these higher molecular weight polymers provide some synthetic challenges, they also exhibit some interesting solution properties, as will be discussed in Appendix C.

The microphase separation behavior discussed in the rest of this chapter uses the lower molecular weight polymers from Table 3.1, unless otherwise noted.

### 3.3 Instrumentation

NMR was used to characterize the polymers using a 300 MHz Bruker spectrometer. Number average molecular weights ( $M_n$ ) were determined by  $^1\text{H}$  NMR in  $\text{CDCl}_3$  (for polystyrene samples),  $\text{DMSO-d}_6$  (for low molecular weight diblock samples made using the 2 kg/mol PS-Br), and  $\text{DMF-d}_7$  (for the higher molecular weight diblock samples). NMR was also used to determine AN conversion by taking aliquots of the reaction at different times and measuring the DMF to acrylonitrile peak ratio.

Size exclusion chromatography (SEC) measurements were used to characterize the starting PS-Br macroinitiators and diblock copolymers. SEC of the PS-Br was done in THF at a flow rate of 1.0 mL/min, versus polystyrene standards, using two polymer laboratories PLGel 5  $\mu\text{m}$  Mixed-D and one PLGel 5  $\mu\text{m}$  50A columns, a Knauer K-501 HPLC pump, Knauer K-2301 RI detector, and Knauer D-2600 dual wavelength UV detector. SEC of the PS-*b*-PAN diblock copolymers was done in DMF (0.01 M LiCl) at 0.5 mL/min flow rate using a Hewlett Packard (HP) series 1050 HPLC pump and a HP series 1047A RI detector, versus polystyrene standards.

Bulk characterization of the morphology was done using small angle x-ray scattering (SAXS). SAXS measurements were performed under vacuum using an Osmic MaxFlux x-ray ( $\text{Cu K}\alpha$ , 0.154 nm) source with a Molecular Metrology, Inc. camera consisting of a 3 pinhole collimation system, 150 cm sample-to-detector distance (calibrated using silver behenate), and a 2-dimensional, multiwire proportional detector (Molecular Metrology, Inc.).

PAN stabilization was done using a hot plate with an air inlet/outlet for in-house compressed air. This allowed for the ability to stabilize the films under a dry, air atmosphere.

Thin film images were taken using transmission force microscopy (TEM). TEM images were obtained using a JEOL 2000KX transmission electron microscope at 200 kV. Film thicknesses were measured using a Filmetrics Interferometer using a silicon oxide calibration wafer and also by SFM.

Thermal degradation studies on the bulk powder were done using thermogravimetric analysis (TGA). TGA studies were done using a TA Instrument Series 2050 Thermogravimetric Analyzer. Polymer powder (~2- 5 mg) or thin films still on the silicon substrate, were pyrolyzed (after stabilization) using TGA.

### **3.4 Characterization**

#### **3.4.1 Microphase Separation Behavior**

A few of the diblock copolymers synthesized were chosen for microphase separation studies (see Table 3.2). SAXS and TEM were used to study the microphase separation behavior of these diblock copolymers, in bulk and thin films. SFM was not used since the roughness of the spin-coated film varied drastically from sample to sample, and microphase separation was rarely seen in the micrographs. The roughness was most likely due to the inability to cast a perfectly smooth film due to the small amount of humidity present during the casting conditions.

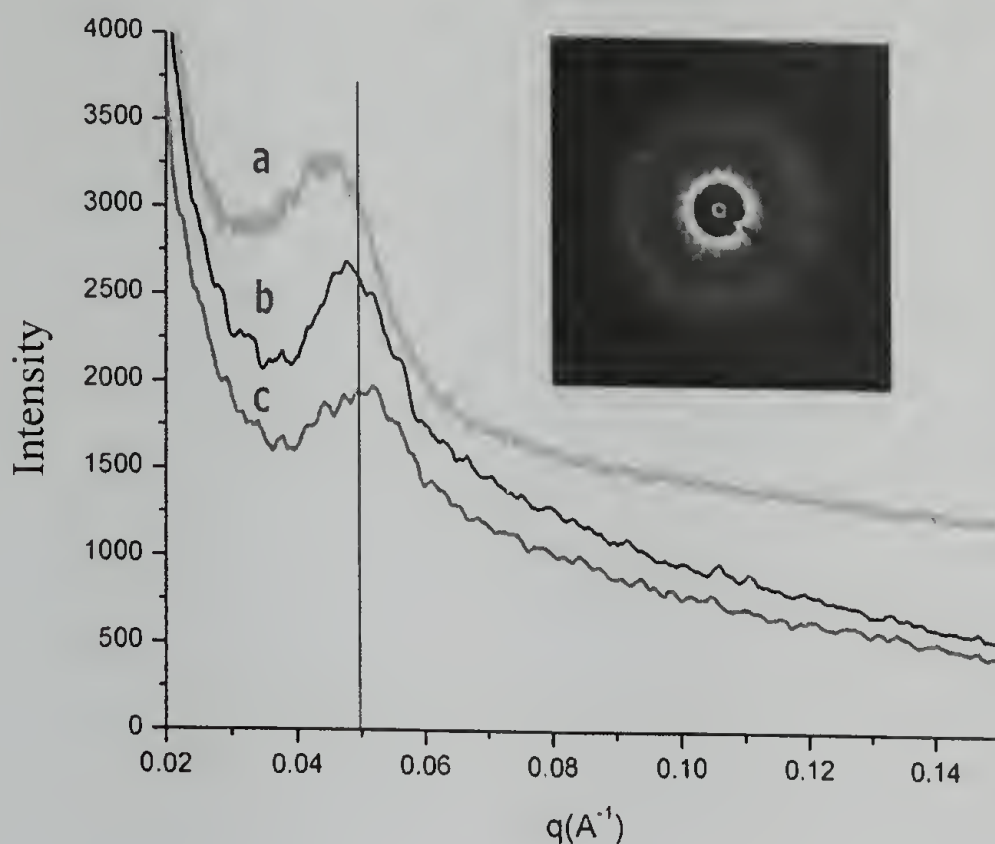
**Table 3.2. PS-*b*-PAN samples used in the microphase separation studies.**

Polymer	Reaction Time (min)	Total Mn	M <sub>n</sub> PAN (NMR) <sup>a</sup>	Conversion <sup>b</sup>	Volume <sup>c</sup> % PAN	PDI <sup>e</sup>
SANb3	30	4200	2200	30.5	49.9	1.30
SANb5	50	4650	2650	36.4	54.6	1.34
SANb6	60	5300	3300	N/A <sup>d</sup>	59.9	1.26
SANa2	60	4607	2610	37.9	54.1	N/A <sup>d</sup>
SANa3	180	5668	3670	54.1	62.4	N/A <sup>d</sup>

<sup>a</sup> M<sub>n</sub> was determined by NMR using the dried polymer sample in DMSO-d<sub>6</sub>. <sup>b</sup> Conversion was measured using aliquots of the reactions (a, b, e) at different times and using the integration of the DMF peak at 7.95 ppm as an internal standard to measure the disappearance of the monomer peaks. <sup>c</sup> Volume fraction was calculated from the NMR data using d<sub>PS</sub>=1.06 g/ml and d<sub>PAN</sub>=1.17 g/ml. <sup>d</sup> Data is not available due to limited quantities of material. <sup>e</sup> No correction was done to account for peak tailing from instrument, which may account for a broadening in PDI.

SAXS was performed on three representative samples; SANb3, SANa3 and SANb6. Bulk samples of these materials were prepared by drop casting from 5% DMF solutions onto a Kapton film and heating on a hot plate at 120 °C for several minutes to evaporate the majority of the DMF. The film was removed from the hot plate and further dried in a vacuum oven overnight prior to the SAXS measurements. The scattering peak in SAXS yielded d-spacings of 12.5 nm (for sample SANb3), 13.1 nm (SANb6), and 14.2 nm (SANa3). No preferred orientation or long-range order of the microphase-separated domains were seen in the data, as was evidenced by the diffuse rings seen in the 2D scattering patterns (see Figure 3.7). The SAXS data alone did not prove microphase separation, and TEM was needed to confirm microphase separation. It is important to note that the samples used for the TEM and SAXS studies were slightly different, with the exception of SANa3. The reason for using the different samples was due to the limited supply of SANb3 and SANb6. Consequently diblock copolymers with similar volume fractions were chosen to complete the studies.

**Figure 3.7. Overlay of SAXS patterns for various PS-*b*-PAN diblocks. a) SANa3, b) SANb6, c) SANb3. Curves are offset for clarity. Inset is a representative 2D SAXS scattering pattern.**

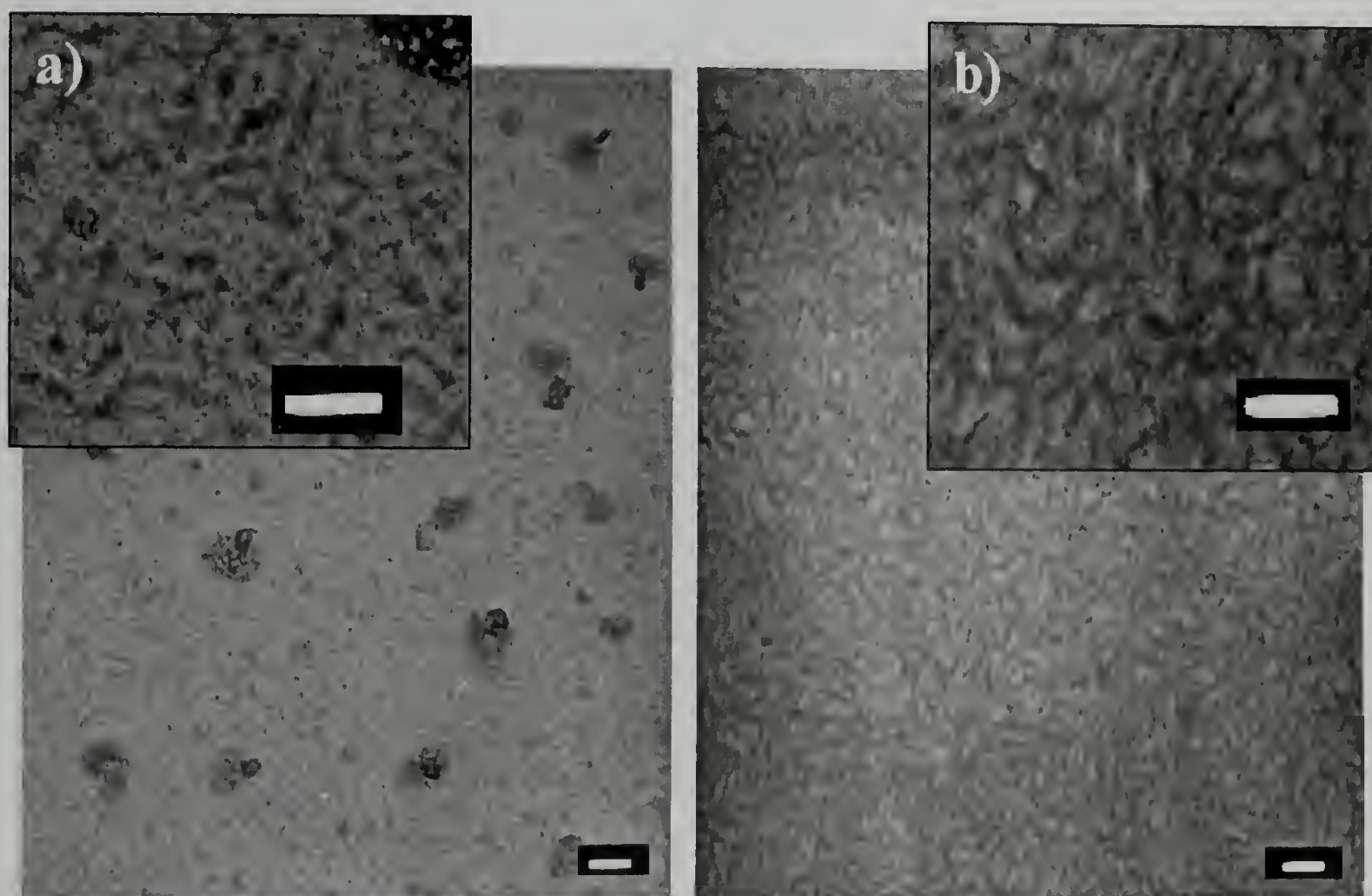


Thin films of PS-*b*-PAN were used for the TEM studies, so that microtoming was not necessary. Thin films were spin-coated at 1000–3000 rpm from either 1% w/w or 5% w/w DMF, DMAc, or DMSO solutions onto silicon wafers having a 200 nm silicon oxide layer. The casting conditions for these polymer solutions were extremely important due to the hygroscopic nature of the solvents. Therefore, the wafer was heated using a hot air gun just prior to spin-coating to facilitate the evaporation of the solvent. An alternate method that proved to be equally effective was to pass a light stream of dry nitrogen over the wafer during the spin-coating process. If neither of these approaches was used, the result was a very rough film that appeared hazy or opaque due to large aggregates of the polymer.

After the films were cast, they could be removed from the silicon oxide substrate using an aqueous HF (5%) solution and floated onto a copper grid. TEM done on the

as-cast PS-*b*-PAN thin film samples (~30 nm thick) showed no indication of the microphase-separated morphology, due to insufficient electron density contrast, so staining was needed. Upon staining with RuO<sub>4</sub> for 30 minutes to selectively stain the PS domains<sup>112</sup>, the microphase separation was evident. However, if the as-cast samples were heated at 250 °C for 2 hours in air, the cyclization reaction of the nitrile groups, provided enough electron density contrast to see the morphology clearly (see Figure 3.8).

**Figure 3.8. TEM images looking down through films of PS-*b*-PAN (SANA3), (a) as-cast from DMF then stained with RuO<sub>4</sub>, and (b) Stabilized at 250 °C. The stained sample shows PS as the dark regions, and the stabilized sample shows PAN as the dark regions. Large dark spots are from contamination during the RuO<sub>4</sub> staining process. Overlays are “zoomed in” regions of the underlying TEM images. Scale bars= 50 nm.**



It is evident that there is no preferred orientation of the morphology under these casting conditions. Studies using other solvents, such as DMSO and DMAC were also



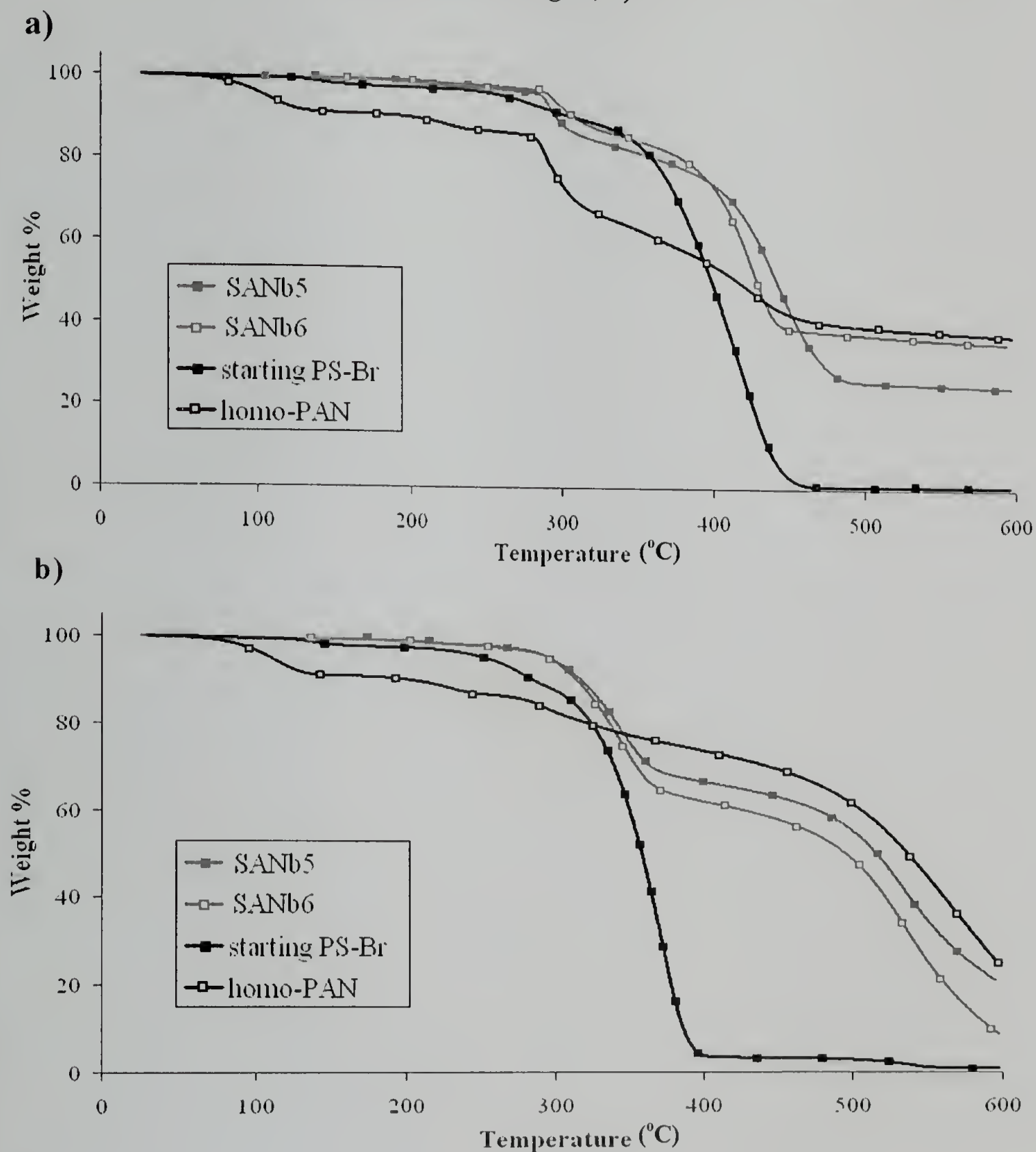
performed and gave similar results. The pyrolysis behavior of the thin films cast from various solvents, and the effects of thermal annealing are shown under the “template preparation” section. The values for the domain spacing from TEM on the thin films, agrees with the values obtained from the SAXS measurements.

### 3.4.2 Thermal Degradation

The bulk thermal degradation of PS-*b*-PAN, PS and PAN polymers was studied using TGA. The polymers were studied under nitrogen and air up to 600 °C, (see Figure 3.9). Between 250 °C–300 °C there was a loss in weight when the PAN-containing diblock copolymers and homopolymer were degraded under nitrogen. This is consistent with what has been observed, and can be attributed to the random chain scission of the polymer, corresponding to a loss of hydrocarbons, such as AN or propionitrile.<sup>83</sup> This weight loss is not seen in the air-degraded samples, since heating PAN in the presence of air stabilizes the polymer, promoting the cyclization of the nitrile groups, so the only degradation seen in the 250 °C–300 °C range is from the uncyclized portions of the PAN<sup>83</sup> (see Figure 3.1). Further heating under air, however, results in the complete degradation of the polymers, whereas, heating to higher temperatures under nitrogen results in a char yield that is proportional to the amount of PAN present in the polymer. The initial weight loss in the PAN homopolymer sample was most likely due to residual solvent or adsorbed water. It is also important to note that the PS homopolymer does not begin degrading until ~300 °C and by 400 °C it is completely degraded by random chain scission<sup>113</sup>. Since this temperature is well below the pyrolysis conditions used to convert the PAN structure into carbon at 600 °C, it

guarantees that the PS domains in the PS-*b*-PAN microphase separated structure are completely degraded by the time the PAN domains are converted to carbon.

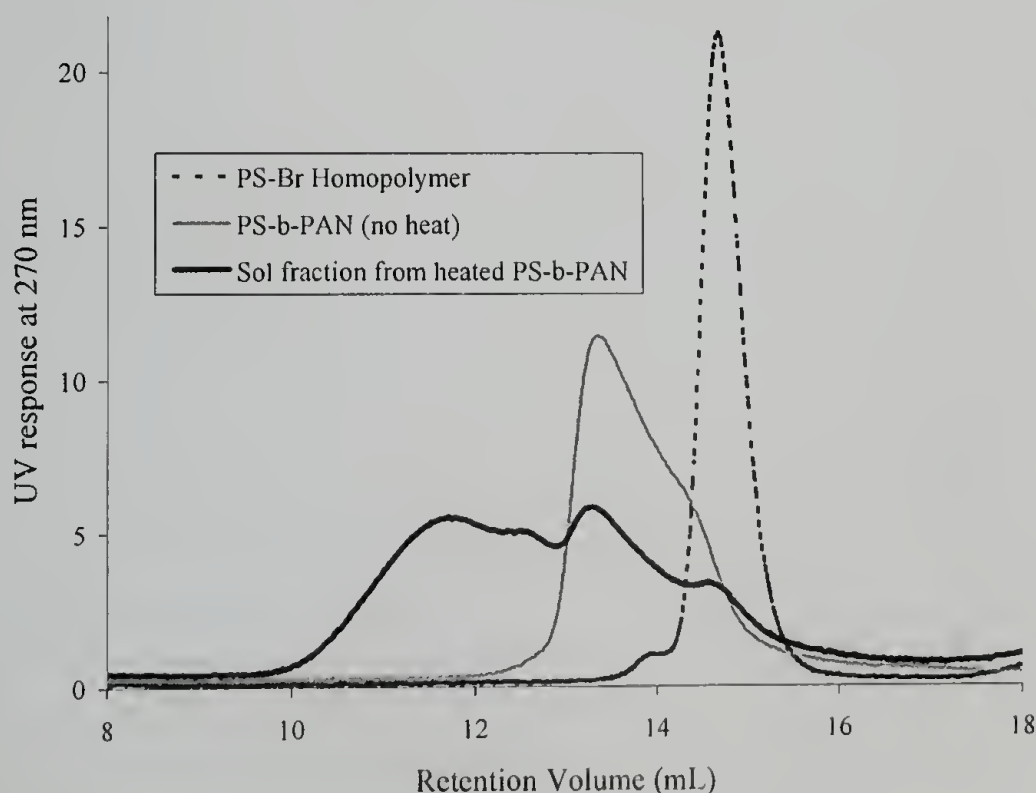
**Figure 3.9. TGA studies of PS-*b*-PAN and homopolymers heated at 5 °C/min, under a) nitrogen, b) air.**



The TGA studies show the weight loss resulting from the formation of volatile products. However, the data does not indicate whether or not the diblock copolymer has a thermally cleavable junction point. Since the junction between the two blocks is

an ester, the thermal stability of that point is in question. A higher molecular weight PS-*b*-PAN diblock copolymer sample (25 kg/mol total, PDI= 1.25, 43% v/v PAN, notebook JML-3-27) synthesized using the same method as outlined previously, was drop cast onto a silicon wafer and heated to 250 °C for 2 hours under nitrogen. The heated sample was extracted with DMF (with 0.01 M LiCl), and SEC was used to check for homopolymer PS. The majority of the heated diblock copolymer did not dissolve in the DMF. SEC done on the sol portion shows a broadening of the diblock copolymer peak, consistent with the stabilization of the PAN block (see Figure 3.10). The starting homopolymer PS-Br (13 kg/mol, PDI= 1.06, JML-1-89) is also shown for comparison. The SEC data does not show the evolution of a PS homopolymer peak, which would be prominent in the chromatogram if the diblock copolymer junction point were thermally labile. Also, since the sol fraction can be seen using the UV detector, it is a strong indication that the PS is still attached to the crosslinked diblock copolymer.

**Figure 3.10. SEC of the sol fraction of stabilized PS-*b*-PAN heated to 250 °C for 2 hours under nitrogen. PS-Br and PS-*b*-PAN were dissolved at 1 mg/mL in DMF, and the heated sample (2 mg) was extracted with 1 mL of DMF. Chromatograms are not normalized.**



## 3.5 Nanoporous Template Preparation

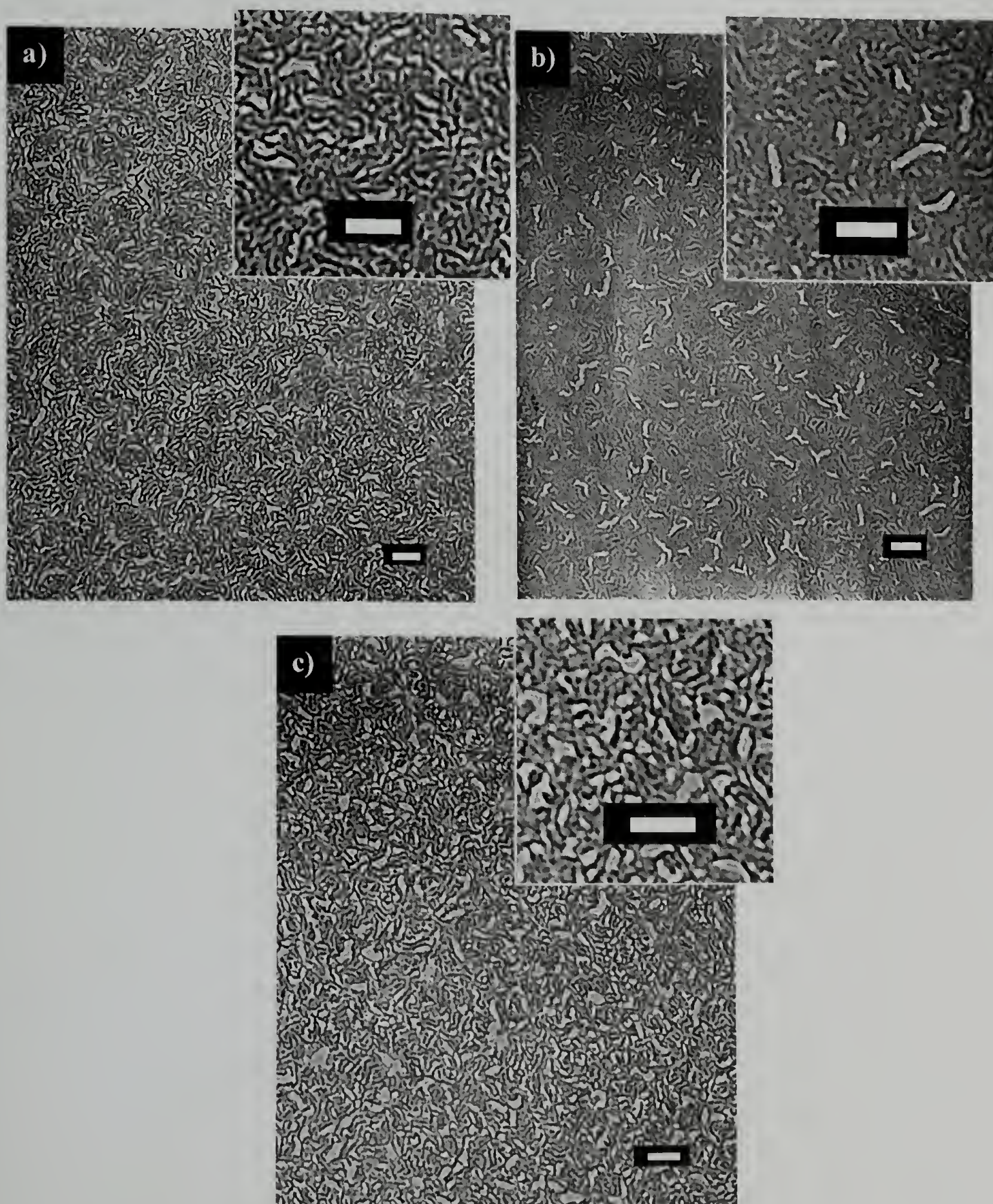
### 3.5.1 Template Pyrolysis

As was discussed in the background section, the formation of carbon fibers only occurs under a strict process of stabilization followed by pyrolysis. A similar heat treatment was applied here to convert the microphase separated film into a carbonaceous template. First, thin films of PS-*b*-PAN were heated at 250 °C under air for two hours on a hot plate, then cooled and placed into a TGA furnace. Pyrolysis was done in the TGA, under nitrogen, by heating the films at 20 °C/min from room temperature to 600 °C and holding the temperature at 600 °C for ten minutes. This heat treatment converts the PAN domains to carbon and degrades the PS domains (see Figure 3.9), leaving holes in place of the PS. The microphase separation and pyrolysis behavior of thin films of three of the PS-*b*-PAN diblock copolymers were studied in detail; SANa2 and SANb5 (54% v/v PAN), and SANa3 (62% v/v PAN). Microphase separation of these polymers occurs on the ~10 nm size-scale, due to the large value of  $\chi$  and low molecular weight.

Finding a solvent that dissolves both the PS and PAN blocks was challenging due to the limited solubility of PAN. The images in Figure 3.8 are from thin film samples of PS-*b*-PAN that were spin-coated from DMF. Similar films were prepared using DMSO or DMAC, 1 % solutions. Sample thicknesses before stabilization and pyrolysis, ranged from 18 nm – 46 nm (depending on the spinning speed). All three solvents have varying polarities and vapor pressures, but under the same casting conditions, gave similar results. Several films were spin-coated onto silicon wafers having a 200 nm layer of oxide, stabilized and then pyrolyzed (see Figure 3.11). Since

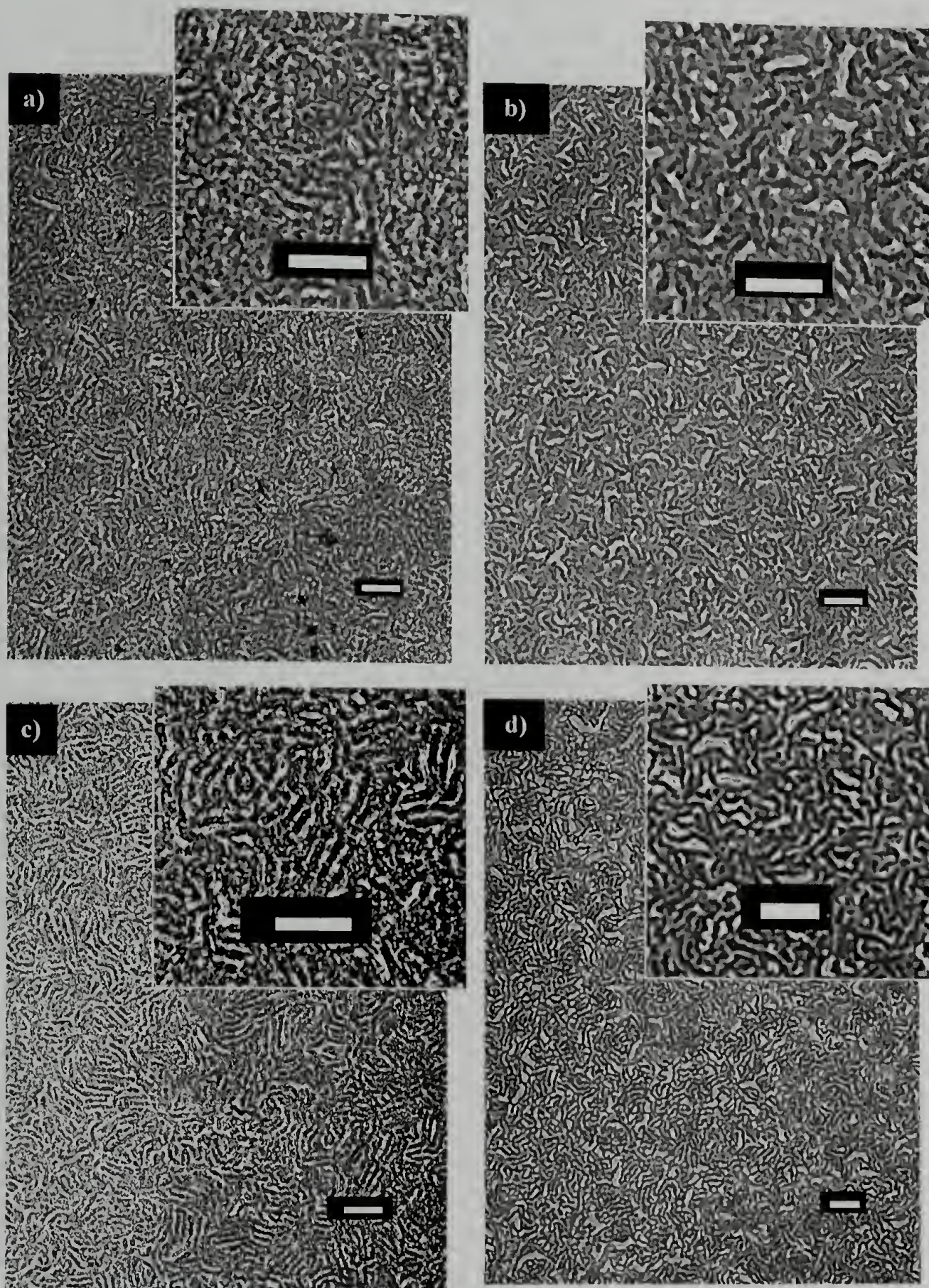
stabilization and pyrolysis increases the electron density contrast by stabilizing the PAN and removing the PS, no stain was needed for these samples.

**Figure 3.11.** The effect of different casting solvents on the morphology of the carbonaceous films. Thin films were spin-coated using SANa2 from (a) DMF, and SANb5 from (b)DMAc and (b) DMSO solutions, all stabilized at 250 °C for 2 hours, and pyrolyzed. Insets are of expanded areas of the underlying TEM micrographs. Scale bars = 100 nm.



For all the solvents used, the morphology does not appear to orient in a preferred direction. Attempts were made to orient the microphase-separated structure by thermal annealing (see Figure 3.12). Solutions of polymer SANa2 in DMF were spin-coated onto 200 nm SiO substrates, annealed at 150 °C for 18 hours under vacuum, stabilized for 2 hours at 250 °C, then pyrolyzed. Even annealing at temperatures above the glass transitions of PS ( $T_g \sim 80$  °C) and PAN ( $T_g \sim 100$  °C)<sup>114</sup> did not result in a preferred orientation or rearrangement of the morphology. This is expected, however, since the PAN may contain crystalline regions, with a melting temperature ( $T_m \sim 320$  °C)<sup>114</sup>. This is above the decomposition temperature of PAN. It has been shown, however, that rapid heating to this temperature can result in the melting transition with little to no decomposition of the PAN, then after a certain period of time at that temperature decomposition occurs.<sup>115</sup> Therefore, the thermal energy needed to create the mobility to anneal the structure, competes with the cyclization (“decomposition”) of the nitrile side-groups. Further studies need to be done to optimize the casting and annealing conditions to afford an ordered array of microphase-separated polymer domains with preferred orientation either perpendicular or parallel to the substrate.

Figure 3.12. Thermal annealing of PS-*b*-PAN polymers. SANA2 spin-coated using, a) 5% DMF, b) 1% DMF solutions, annealed, stabilized, then pyrolyzed. c) and d) are comparable films without annealing to a) and b) respectively. Insets are of expanded areas of the underlying TEM micrographs. Scale bars = 100 nm.

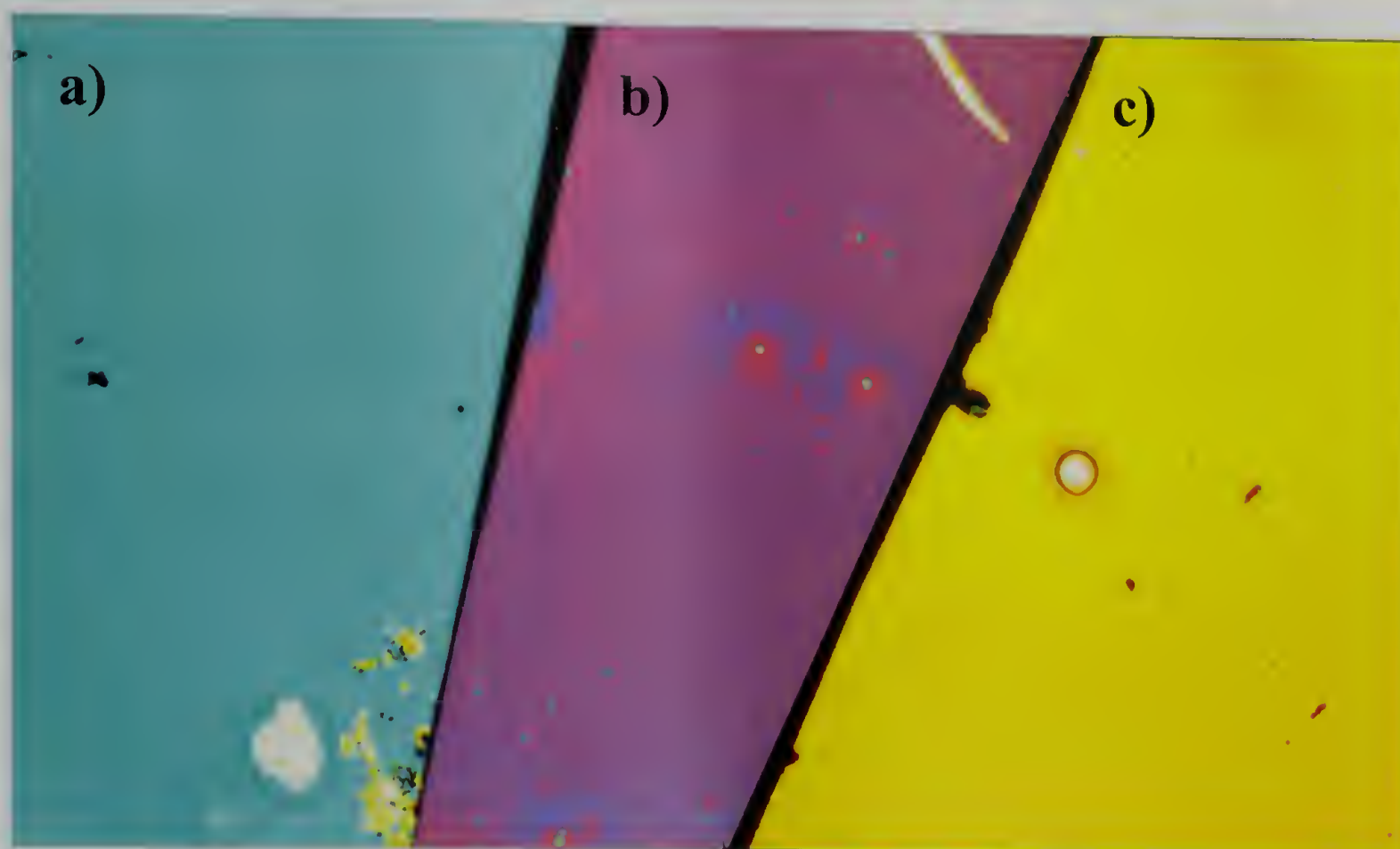


The thin films that were studied all show the presence of a few “holes” or voids after stabilization and pyrolysis, as can be seen in the TEM images (see Figures 3.11

and 3.12). While some of these holes can be attributed to the removal of the PS sacrificial block, larger holes are more likely due to volume contraction of the film during stabilization and pyrolysis, (further supported in the “Stabilization” section of this chapter). Studies on the pyrolysis of PAN to create carbon films and fibers have shown that ~50% of the polymer weight is lost during the carbonization process; two-thirds of which is lost during the initial stabilization process.<sup>83,90,116</sup> This loss of weight also corresponds to a significant volume change for the carbon fibers and films, with a volume shrinkage of ~25% between 200 °C–300 °C.<sup>117</sup> PS-*b*-PAN thin films coated on 200 nm SiO substrates also undergo a change in volume. During this volume shrinkage, the film remains adhered to the substrate, so that only the thickness of the film changes. Optical microscopy was used to study this thickness change after stabilization and pyrolysis (see Figure 3.13). The films in Figure 3.13 were lightly scratched and SFM measurements were done to monitor the change in thickness. The as-cast samples were 100 nm and after stabilization at 250°C were 70 nm. After the final pyrolysis step, the resulting film was 32 nm thick. These volume shrinkages are larger than what has been seen for PAN, which may be due to additional volume contraction from the removal of the PS domains.



**Figure 3.13. Optical microscopy images of thicker films of SANa2 cast from DMF onto 200 nm SiO. (a) as-cast (b) stabilized at 250 °C for 2 hours under air (c) pyrolyzed at 600 °C under nitrogen. The image shows a distinct color change due to the change in film thickness and no cracking of the films upon heating.**

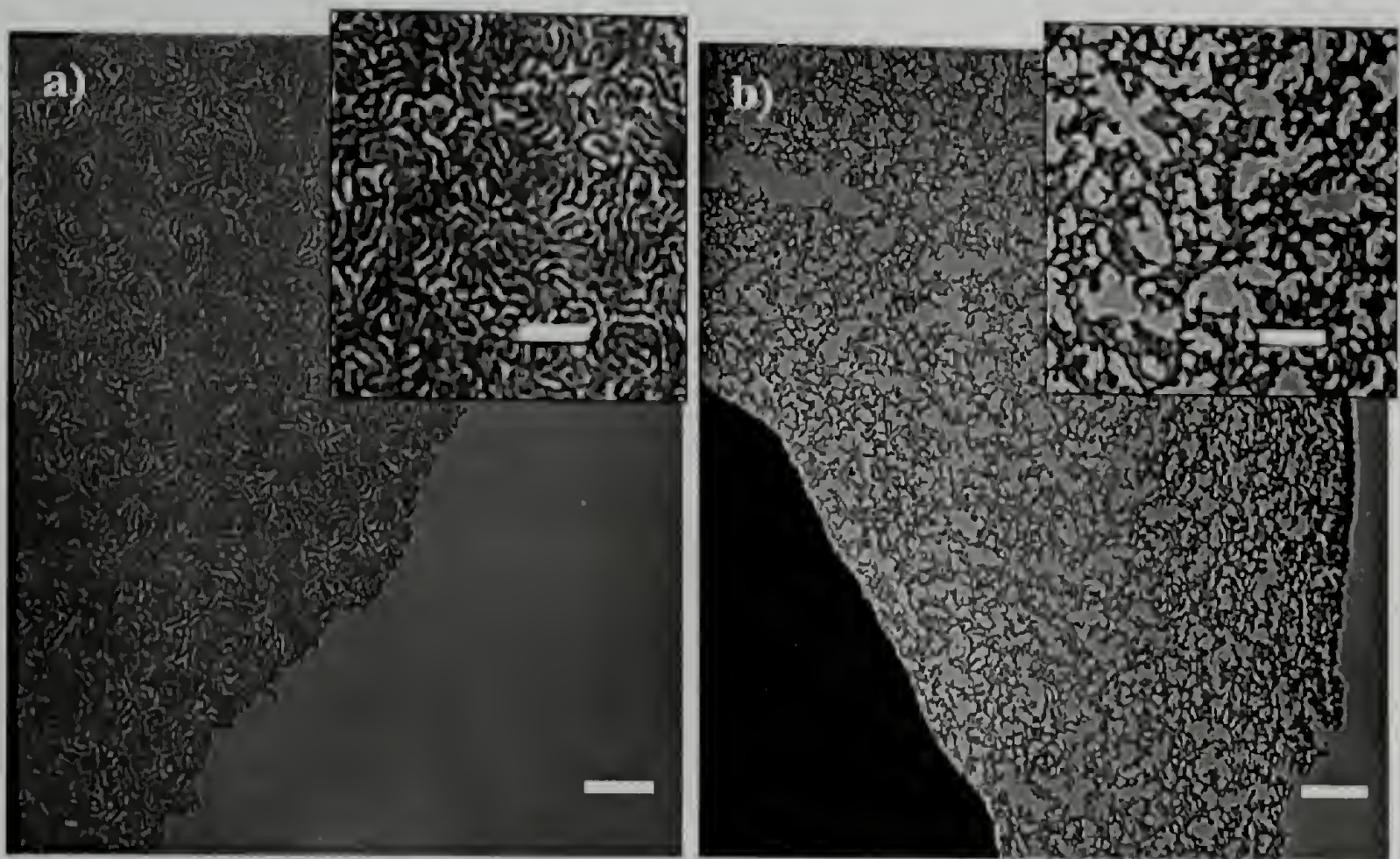


### 3.5.2 Effect of Stabilization

As was stated earlier, the stabilization and pyrolysis conditions were used based on similar methods used for the creation of carbon fibers. A quick study was done using the PS-*b*-PAN polymers to probe if the stabilization prior to pyrolysis is necessary for the replication of the microphase-separated structure into a carbonaceous template. The stabilization step starts the intra- and intermolecular reactions that are needed to stabilize the structure prior to pyrolysis (see Figure 3.1). Without this initial stabilization step, the competition between chain scission and cyclization during the pyrolysis step (at 600 °C under nitrogen) would lead to the destruction of the thin film. This can be seen in Figure 3.14, where a thin film sample (~30 nm) of SANa2 (54% PAN) was broken into two pieces: one half was stabilized then pyrolyzed, and another

half was just pyrolyzed. The sample that was quickly heated to 600 °C shows gaping holes in the film and no preservation of the microphase separated morphology. The stabilized, then pyrolyzed samples, however, show that the morphology remains, now in a carbonaceous form, and the sacrificial PS domains have been removed.

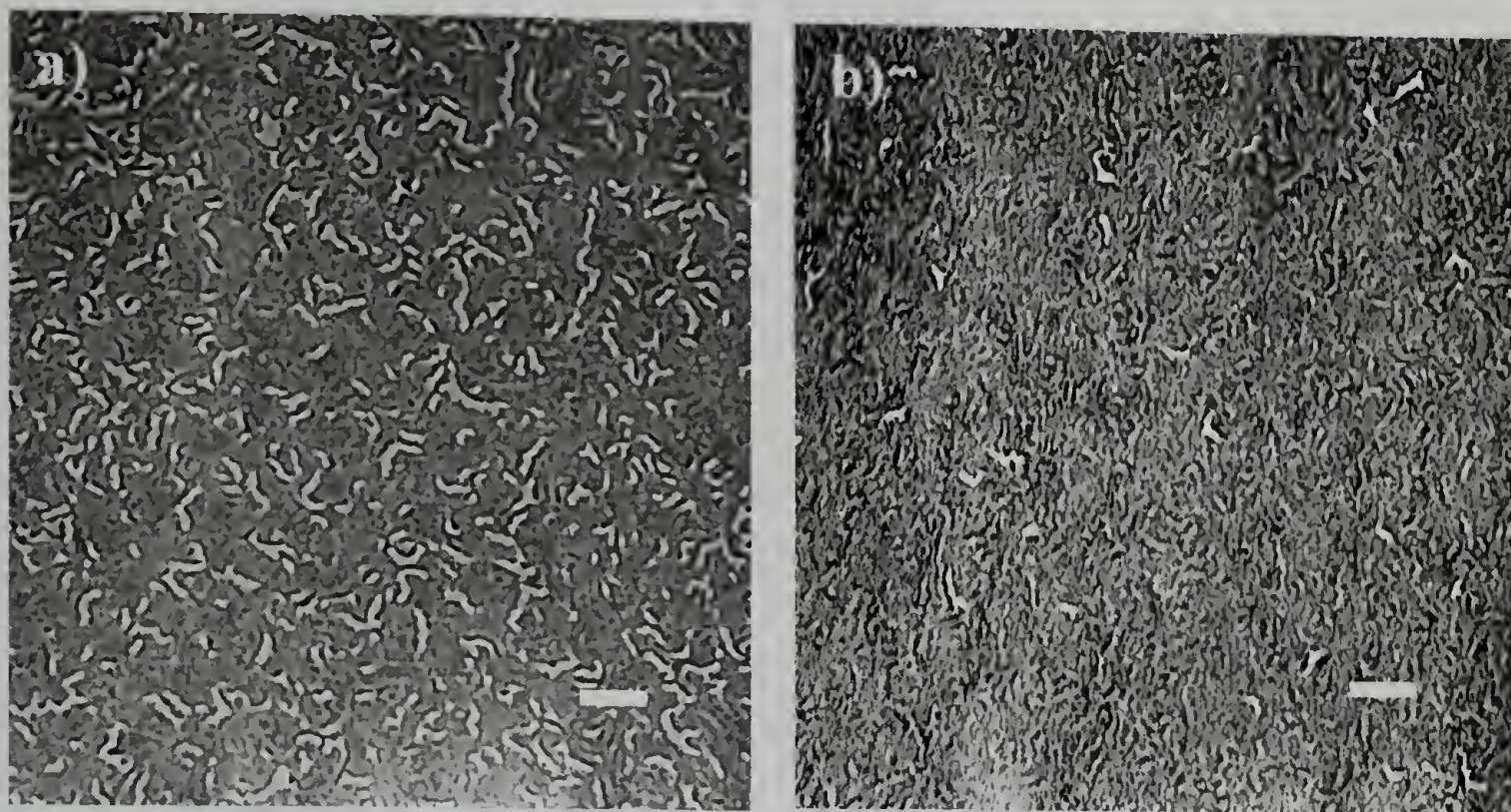
**Figure 3.14. Carbonaceous film formation using thin films of SANa2 cast from DMF (a) stabilized and pyrolyzed, (b) unstabilized and pyrolyzed. Overlays are “zoomed-in” regions of the underlying TEM images. Scale bars= 200 nm, inset scale bars= 100 nm.**



According to this data, there is a possibility that the holes seen in Figure 3.11 are due to insufficient stabilization. To test this, samples similar to those in Figure 3.11 were stabilized in air for 4 hours (instead of 2 hours), then pyrolyzed (see Figure 3.15). The resulting films, however, still show the presence of small holes, even though there was an increase in stabilization time, indicating the holes are caused from volume contraction. The films shown in Figure 3.12 also support this conclusion, since the thicker films show less holes than their thinner counterparts, indicating that the thicker

films are less prone to cracks and holes from volume contraction due to a greater amount of material.

**Figure 3.15. Effect of increased stabilization time. Both films were spin-coated, then stabilized for 4 hours, and pyrolyzed. A) cast from DMF, b) cast from DMAC.**



### 3.6 Conclusions

Diblock copolymers containing PS-*b*-PAN were synthesized by a combination of living anionic and ATRP polymerization techniques, and were shown to phase separate for low molecular weights. SAXS and TEM data indicate poor lateral ordering, but distinctive phase separation. Attempts to orient the microphase-separated structure by using different casting solvents and thermal annealing, gave the same results as the unannealed counterparts. The PAN domains could be successfully converted to carbon, through stabilization and pyrolysis, while the sacrificial PS domains were thermally degraded. This is a promising method to obtain nanoporous (<10 nm) carbonaceous films using diblock copolymers that have strong microphase separation behavior.

## APPLICATIONS AND FUTURE DIRECTIONS

4.1 PSBCB-*b*-PLA Project

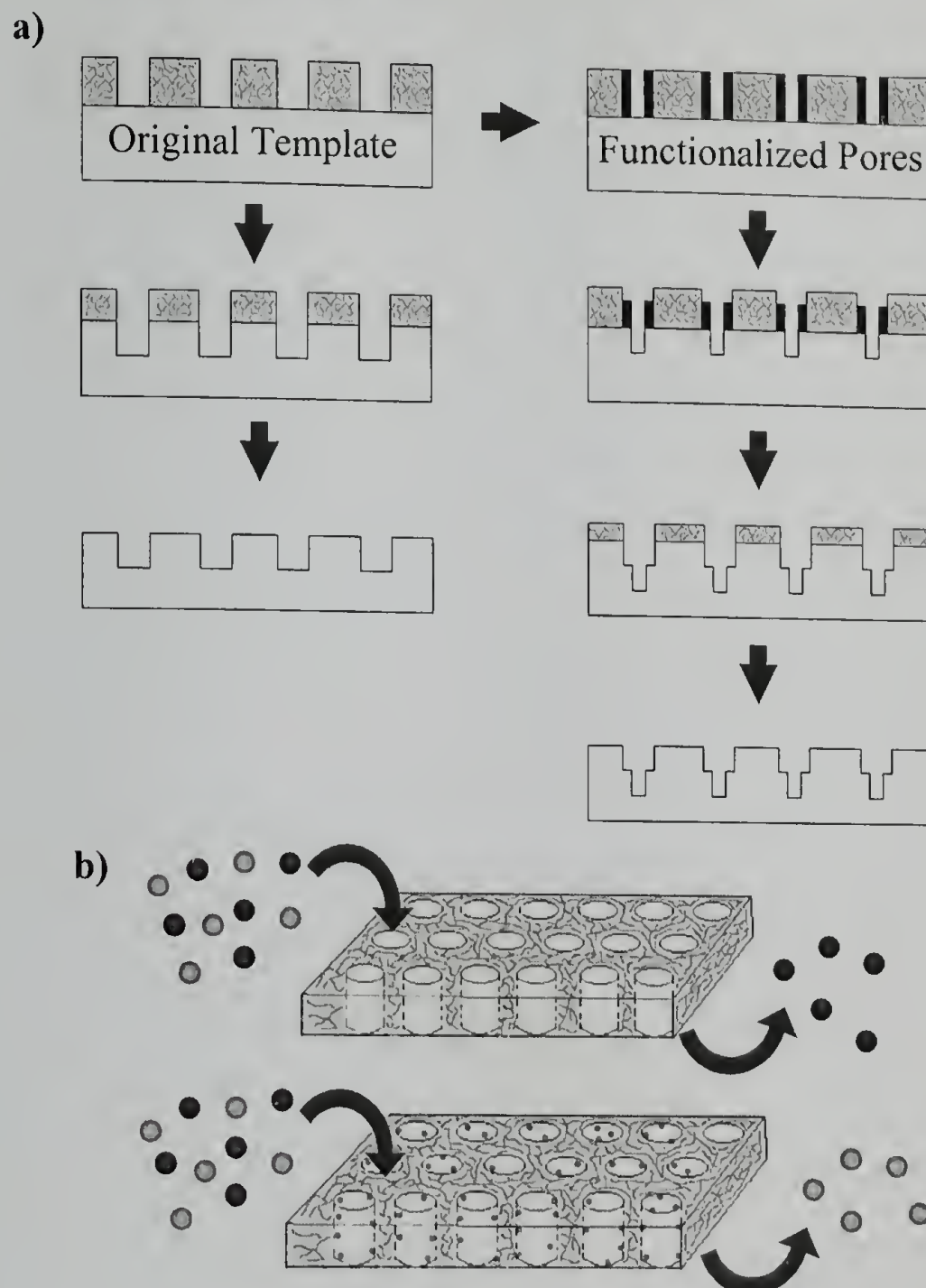
The PSBCB-*b*-PLA project, as discussed in Chapter 2, shows a process by which thermally stable nanoporous templates can be created.<sup>58</sup> The process presented here for the fabrication of nanoporous templates eliminates the need for UV irradiation, ion etching or secondary chemical modification to remove the minor component. In addition, the amount of crosslinking can be “dialed-in” at the start, through modification of the number of crosslinkable groups on the polymer and/or tailoring the crosslinking conditions. The majority of the work done on this project focused on the use of thin films for the generation of these templates. Future work in this area could focus on the use of thicker films, to create nanopores with higher aspect ratios. Preliminary work, as shown in Chapter 2 (see Figure 2.17), indicates that the electric field alignment of these polymers is possible for thicker films of PSBCB-*b*-PLA to generate the perpendicular alignment of the PLA domains (with respect to the substrate).

In addition, these nanoporous films contain hydroxyl groups, remaining after the degradation of the PLA, which should be located along the pore walls. Attempts were made to address these hydroxyl groups, but the characterization met with difficulty due to the small amount and low density of hydroxyl groups along the pore walls (see Appendix B). Typical methods of characterization gave results that were inconclusive, since the sensitivity of these instruments was pushed to their limits. Future work on this could involve using nanoparticles to address whether or not the functionality is

accessible, although even this will have its own challenges (refer to Challenges section of Appendix B).

If addressable, the hydroxyl functionality within the crosslinked nanopores provides a versatile tool for incorporating and exploring chemical reactions in constrained geometries. Since these nanoporous templates resist collapse under thermal and solvent treatments, a vast library of chemical reactions could potentially be used to address the hydroxyl-lined pore walls. Modification of the pores could have potential applications in such areas as lithography, where the template is used as a mask, or in selective filtration, where the nanoporous film is placed onto another microporous support to enhance filtration of smaller/chemically specific particles (see Figure 4.1).

**Figure 4.1. Possible applications for modified nanoporous crosslinked templates. a) lithographic methods with or without pore functionalization, b) selective filtration via pore wall functionalization.**



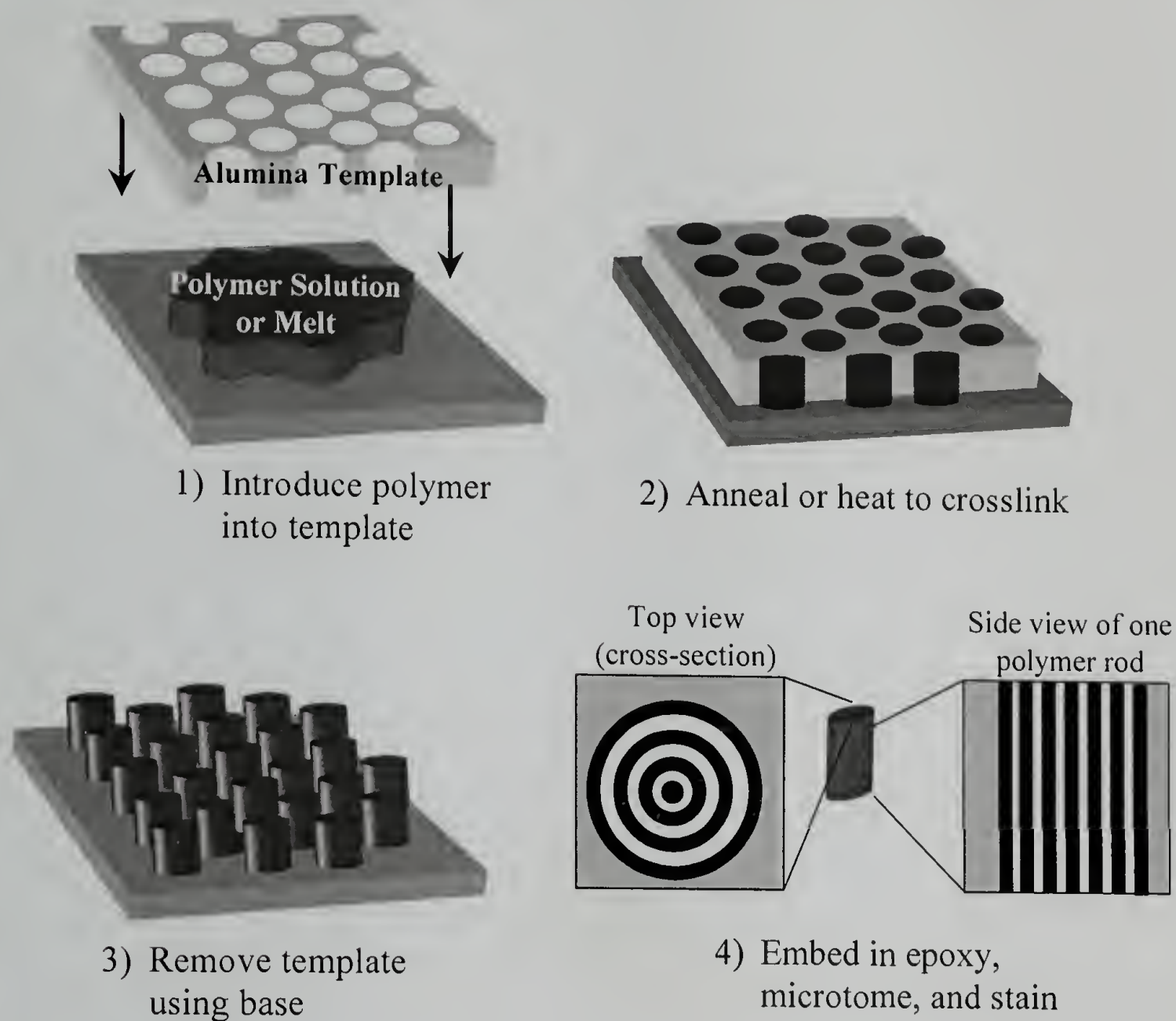
From a commercial standpoint, it is nice that the amount of crosslinking can be dialed-in from the start and that subsequent degradation can be done using a commercially available developer (MF-319™, Rohm and Haas), as mentioned in Chapter 2. However, there are some challenges that need to be addressed before this polymer can be used for the aforementioned applications. The first challenge, as previously mentioned, is the difficulty in proving the addressibility of the hydroxyl groups in the porous structure. The second challenge is that this polymer can only be

made using a two-step polymerization method, whereas, for example, PS-*b*-PMMA can be made in “one-pot”. The third challenge is the lack of availability of the monomer. It is not commercially available (yet) and involves either complex synthesis or flash-vacuum pyrolysis. Once these limitations are overcome or accepted, this method to create nanoporous templates becomes easier to scale-up for the exploration of its potential uses.

#### 4.2 PS-*b*-PAN Project

The PS-*b*-PAN project, as discussed in Chapter 3, provides a completely thermal route to the generation of stable nanoporous templates using thin films.<sup>118</sup> While the microphase separation behavior is maintained and can be converted into carbon, the microphase-separated morphology lacks orientation. Future work on this project may involve finding ways to orient the morphology, such as solvent annealing or electric field. A more promising method, however, for the orientation of these polymers is to use confined geometries. It has been previously shown that the microphase separation of diblock copolymers is maintained within the porous structure of alumina membranes.<sup>119,120</sup> Not only does this result in the orientation of the microdomains of the polymer over microns, but it also allows for unique microphase separation behavior, such as the formation of concentric cylinders<sup>120</sup> or helices<sup>121</sup> (see Figure 4.2). In addition, theoretical calculations support the morphologies seen, and suggest other distinct morphologies based on the degree of confinement, volume fraction of the two blocks and surface energies of the two blocks.<sup>122</sup>

**Figure 4.2. Introduction of diblock copolymers into confined geometries. Cross-sections shown are for the concentric cylinder morphology.**



This method is currently being applied to the PS-*b*-PAN polymers to produce unique carbonaceous structures, such as amorphous carbon nanotubes.<sup>123</sup> In addition, these carbonaceous structures can, theoretically, be turned into graphitic structures with the application of heat  $>1600$  °C. Future work on this project will use PS-*b*-PAN to attempt to produce unique graphitic structures.

In addition to using PAN to create carbonaceous structures, there are also other random copolymers of PAN that can be used to the same end. The use of random copolymers, typically acrylic based, imparts favorable processing properties, such as



increased solubility in a variety of solvents and reduced melting temperature.<sup>82</sup>

Copolymers of PAN containing MA, MMA, VA, and VBr have been studied for their use as carbon precursors.<sup>83</sup> There is a point of diminishing returns, however, since the incorporation of too many non-acrylonitrile units in the copolymer actually decreases the mechanical properties of the resulting carbon structure, as was noted in the case of carbon fibers.<sup>83</sup> Random copolymers of PAN also require increased and gradual stabilization when compared to their PAN homopolymer counterparts. Therefore, the synthesis of random copolymers to help with the processing properties would be a favorable route to pursue for the confinement studies described in Figure 4.2, as well as for the studies of thin film behavior.

## APPENDIX A

### EXPERIMENTAL SECTION

#### A.1 PSBCB-*b*-PLA Project

##### A.1.1 Materials

Tetrahydrofuran (THF) and benzene were dried over sodium and benzophenone, and distilled under nitrogen just prior to use. Dimethylformamide (DMF) was distilled under reduced pressure over magnesium sulfate. 3-Bromobenzocyclobutene (BrBCB) was provided by the DOW Chemical Company. The hydroxy-functionalized alkoxyamine initiator was provided by Dr. Eric Drockenmuller (IBM Almaden Research Center), made using established procedures.<sup>53</sup> Styrene, chlorobenzene (Aldrich), tetra-*n*-butyl ammonium fluoride (Aldrich), *n*-butyllithium (2.89 M in hexanes, Alfa Aesar), methyltriphenylphosphonium bromide (Alfa Aesar, 98+%), magnesium turnings (Fisher), and triethyl aluminum (Aldrich, 1.0M in hexanes) were used as received. D,L-lactide (Aldrich) was recrystallized from ethyl acetate. All glassware, unless otherwise mentioned, was dried in an oven at 250 °C overnight, and cooled under dry nitrogen just prior to use.

##### A.1.2 Synthesis

###### A.1.2.1 Benzocyclobutene Carbaldehyde (ald-BCB)

The ald-BCB was made based on established procedures.<sup>53</sup> Magnesium turnings (2.88 g, 120 mmol) were added to a 500 mL round-bottom flask, containing THF (50 mL) under nitrogen. To this mixture, 4 drops of 1,2-dibromoethane were added. Using

an addition funnel, BrBCB (20.0 g, 109 mmol) and 25 mL THF were added dropwise. The resulting exothermic reaction, caused the THF to reflux. After this initial addition, THF (25 mL) was used to rinse the addition funnel, and was added to the reaction mixture. The flask was then heated at reflux, under nitrogen, for an additional 45 minutes, until the solution was greenish-brown. The reaction was then cooled to 0 °C, and DMF (15.0 mL, 210 mmol, distilled over MgSO<sub>4</sub>) was added dropwise. The reaction was then once again heated to reflux for 15 minutes, and cooled. The reaction solution was then poured over 150 g of ice, and acidified to pH = 4 using HCl (aq), to react with all the remaining magnesium. The solution was then neutralized using a saturated sodium bicarbonate solution, and extracted with 3 x 200 mL of diethyl ether. The ether was collected, dried over MgSO<sub>4</sub>, filtered, and evaporated to yield the crude product (15.3 g). The reaction progress was checked using TLC with 10% diethyl ether in petroleum ether ( $R_{f \text{ Ald-BCB}} = 0.25$ ,  $R_{f \text{ BrBCB}} = 0.65$ ). The ald-BCB was purified using a silica column with 10% diethyl ether in petroleum ether, with the unreacted starting material (BrBCB) eluting first. Yield= 9.88 g, 68%. [Note: The ald-BCB must be kept in the freezer, since it decomposes readily at room temperature to an insoluble white solid. This solid can be removed from the ald-BCB by filtration.] <sup>1</sup>H NMR, (300 MHz, CDCl<sub>3</sub>),  $\delta = 9.94$  (s, 1H, CHO), 7.73 (d, 1H, Ar-H), 7.57 (s, 1H, Ar-H), 7.21 (d, 1H, Ar-H), 3.24 (br s, 4H, CH<sub>2</sub>).

#### A.1.2.2 Vinyl Benzocyclobutene (vinyl-BCB)

The vinyl-BCB was made based on established procedures.<sup>53</sup>

Methyltriphenylphosphonium bromide (32.4 g, 90.9 mmol, Ph<sub>3</sub>PCH<sub>3</sub>Br) was added to a 500 mL round-bottom flask equipped with glass stir bar (shown in Figure 3.4b). The

flask was sealed and heated gently using a heat gun, under vacuum, to remove moisture. Freshly distilled THF (150 mL) was added, and the flask was backfilled with nitrogen. The solution was cooled to  $-78\text{ }^{\circ}\text{C}$  using a dry ice/acetone bath, and *n*-butyllithium (30.6 mL, 88 mmol) was added dropwise. The reaction was then warmed to room temperature to destroy any unreacted *n*-butyllithium. The resulting yellow/orange solution was then cooled back down to  $-78\text{ }^{\circ}\text{C}$ . The ald-BCB (9.55 g, 72.3 mmol) was diluted in dry THF (45.4 mL) and added to the reaction. After addition the reaction was allowed to warm to room temperature, and stirred for two hours. The reaction was then treated with saturated ammonium chloride and saturated sodium bicarbonate, filtered over Celite, and washed with petroleum ether. This was evaporated to remove the majority of the petroleum ether and THF. More petroleum ether was added to precipitate the phosphorous salts, followed by filtration and further evaporation. A silica gel column, with 10% ether in petroleum ether as eluent, was used to purify the vinyl-BCB ( $R_{f\text{ vinyl-BCB}} = 0.75$ ). After the vinyl-BCB was retrieved, the eluent was switched to pure ether to recover the unreacted ald-BCB.  $^1\text{H NMR}$  (300 MHz,  $\text{CDCl}_3$ ),  $\delta = 7.25$  (d, 1H, Ar-H), 7.18 (s, 1H, Ar-H), 7.03 (d, 1H, Ar-H), 6.73 (dd, 1H,  $\text{CH}=\text{CH}_2$ ), 5.70 (d, 1H,  $\text{CH}=\text{CH}_2$ ), 5.18 (d, 1H,  $\text{CH}=\text{CH}_2$ ), 3.19 (s, 4H,  $\text{CH}_2$ ).

### A.1.2.3 PSBCB-OH and PS-OH Homopolymers

Hydroxy-terminated poly(styrene-*r*-benzocyclobutene) (PSBCB-OH) was made using established procedures.<sup>53</sup> Vinyl-BCB (1.30 g), styrene (5.0 mL, 4.52 g), and initiator (128 mg) were added, in bulk, to a polymerization tube, freeze/pump/thawed for 3 cycles, then sealed. Polymerization was done at  $120\text{ }^{\circ}\text{C}$ , between 11- 16 hours, or to approximately 75% conversion. The resulting polymer contained 16 mol% BCB

groups. The hydroxy-terminated polystyrene (PS-OH) analog was made using the exact same procedure as outlined above, omitting the vinyl-BCB monomer, and using styrene instead. The molecular weights and PDI information are summarized in Table 2.1.  $^1\text{H}$  NMR (300 MHz,  $\text{CDCl}_3$ ),  $\delta = 6.2 - 7.3$  (m, 5H from styrene, 3H from BCB units, Ar-H), 3.1 (br s, 4H,  $\text{CH}_2$  from the cyclobutene ring), 1.2 – 2.2 (m, 3H, CH- $\text{CH}_2$  from PSBCB backbone).

#### A.1.2.4 PSBCB-*b*-PLA and PS-*b*-PLA Diblock Copolymers

For polymer G (see Table 2.1), the tert-butyldimethylsilyl (TBDMS) protecting group was removed using 1.0 M tetra-*n*-butyl ammonium fluoride (TBAF) in THF. The TBAF solution (0.5 mL) was added to a solution containing the protected polymer (1.0g) in THF (4.0 mL) and stirred at room temperature for 24 hours. Acidic methanol was added to quench the reaction and the polymer was precipitated into methanol and filtered. The synthesis of the diblock copolymer does not require protecting the hydroxyl group, so preparation of subsequent diblock copolymers was done without the protection/deprotection step.

The PLA block was grown using D,L-lactide and  $\text{AlEt}_3$  in benzene, adapted from a previous procedure.<sup>26</sup> For a typical reaction, a polymerization tube with a Teflon stopcock was charged with PSBCB-OH (0.3 g), heated briefly with a heat gun under vacuum, and backfilled with nitrogen. This was repeated three times. Then under positive nitrogen flow, with the stopcock completely loosened,  $\text{AlEt}_3$  (25  $\mu\text{L}$  of 1.0 M, Aldrich) and benzene (5.0 mL, distilled over sodium and benzophenone) were carefully added via gas-tight glass syringes. The polymerization tube was then quickly vented through a bubbler, sealed, covered in aluminum foil, and allowed to react overnight at

room temperature (see Figure 2.4). This method was preferred over a septum-sealed flask, to prevent contamination from the septa, as well as to achieve a tighter seal to prevent the introduction of air or moisture.

The following day, D,L-lactide (0.625 g, Aldrich, recrystallized from ethyl acetate and stored in a desiccator under nitrogen) was added to the polymerization tube in a glove bag under a nitrogen atmosphere. The tube was sealed, removed from the glove bag, and heated at 80 °C for 7 hours. The polymers were isolated by precipitation into acidic methanol (MeOH/HCl). After drying and preliminary characterization, unreacted PSBCB homopolymer was removed using cyclohexane (~30 mL for each 0.5 g of polymer) at room temperature, followed by centrifugation. Characterization of the diblocks was done using NMR and size exclusion chromatography (SEC). <sup>1</sup>H NMR (300 MHz, CDCl<sub>3</sub>), δ = 6.2–7.3 (m, 5H from styrene, 3H from BCB units, Ar-H), 5.2 (m, 1H, CH from PLA), 3.1 (br s, 4H, CH<sub>2</sub> from the cyclobutene ring), 1.2–2.2 (m, 3H, CH-CH<sub>2</sub> from PSBCB backbone), 1.6 (m, 3H, CH<sub>3</sub> from PLA). The molecular weights and PDI information are summarized in Table 2.1.

## A.2 PS-*b*-PAN Project

### A.2.1 Materials

Styrene (Fluka) was distilled over calcium hydride and stored under nitrogen immediately before polymerization. *sec*-butyllithium (1.4 M in hexanes) and ethylene oxide were obtained from Aldrich and used without further purification. Benzene was distilled over sodium/benzophenone. Acrylonitrile (AN) (Aldrich, 99+%) was passed through a plug of basic alumina (Alfa Aesar, activated, basic, 96%) prior to use.

Dimethylformamide (DMF) was distilled under reduced pressure over magnesium sulfate or used directly from a bottle of anhydrous DMF. Copper (I) bromide (Aldrich, 99.999%) and 4,4'-dinonyl-2,2'-dipyridyl (dNbpy) (Aldrich, 97%) were used as received.

## A.2.2 Synthesis

### A.2.2.1 PS-Br Macroinitiator

Benzene (300 mL) was added to a flame-dried flask (see Figure 3.4b) equipped with glass stir bar, nitrogen inlet/outlet and Teflon stopcock. Addition of reagents was done under a positive nitrogen flow. Sec-butyllithium solution (actual 1.2 M, 0.75 mL) was added via syringe to the stirring solution. Styrene (20.0 mL), distilled just prior to use (see Figure 3.4a) was added via syringe to the reaction flask that was cooled in an ice bath due to exothermic initiation. After 10 minutes the ice bath was removed to prevent benzene freezing. The reaction flask was sealed and the reaction was allowed to proceed for 3 hours at room temperature. Ethylene oxide was bubbled through the reaction until the color associated with the living anion vanished (~5 minutes).

[CAUTION: Ethylene oxide is very toxic!] The reaction flask was then sealed, and stirred overnight (~16 hours). An excess of 2-bromoisobutyryl bromide (1.6 mL) was added to the reaction flask and the polymer was precipitated in methanol and dried under vacuum overnight. The macroinitiator was characterized by SEC in THF with:  $M_w = 2.1 \times 10^3$ ,  $M_n = 2.0 \times 10^3$ , and a PDI = 1.09. The higher molecular weight macroinitiators were made using the same procedure, with less initiator.  $^1\text{H}$  NMR (in  $\text{CDCl}_3$ ) end group analysis: 3.93 (br m, 6H, PS- $\text{CH}_2\text{-CH}_2\text{-O-CO-C}(\text{CH}_3)_2\text{-Br}$ ), 3.73 (br

m, 2H, PS-CH<sub>2</sub>-CH<sub>2</sub>-O-CO-C(CH<sub>3</sub>)<sub>2</sub>-Br), 3.30 (br m, 2H, PS-CH<sub>2</sub>-CH<sub>2</sub>-OH, from aliquot before acid halide addition).

#### A.2.2.2 PS-*b*-PAN Low Molecular Weight Diblock Copolymers

The polystyrene macroinitiator (0.50 g), CuBr (30 mg) and dNbpy (160 mg) were added to an oven dried polymerization tube equipped with Teflon stir bar. The polymerization tube was backfilled with nitrogen 3 times, and then DMF (4.0 mL) and AN (2.0 mL) were added. The tube was then freeze/pump/thawed 3 times, backfilled with nitrogen and reacted at 70°C for varying times (see Table 3.1). The polymer was precipitated into methanol and characterized with DMF (0.01 M LiCl) SEC and NMR. <sup>1</sup>H NMR (300 MHz, DMSO-d<sub>6</sub>), δ = 6.28–7.38 (br m, 5H, Ar-H), 3.13 (br m, 1H, PAN), 2.00 (br m, 2H, PAN), 0.45–2.3 (br m, 3H from PS).

#### A.2.2.3 PS-*b*-PAN Higher Molecular Weight Diblock Copolymers

Higher molecular weight diblock copolymers (such as JML-3-27 from section 3.4.2, and JML-3-30 from Appendix C) were made using a similar method. The polystyrene macroinitiator (JML-1-89, 13 kg/mol, PDI = 1.06, 0.50 g), CuBr (5.1 mg) and dNbpy (29.2 mg) were added to an oven dried polymerization tube equipped with Teflon stir bar. The polymerization tube was backflushed with nitrogen 3 times, and then DMF (4.0 mL) and AN (2.0 mL) were added. The tube was then freeze/pump/thawed 3 times, backfilled with nitrogen and reacted at 70°C for 2 days. The polymer was precipitated into methanol and characterized with DMF (0.01 M LiCl) SEC and NMR. <sup>1</sup>H NMR (300 MHz, DMF-d<sub>7</sub>), δ = 6.42–7.39 (br m, 5H, Ar-H), 3.30 (br m, 1H, PAN), 2.29 (br m, 2H, PAN), 1.1–2.6 (br m, 3H from PS). The resulting



polymers were JML-3-27 (25 kg/mol total, PDI = 1.25, 43% v/v PAN) and JML-3-30 (28 kg/mol total, PDI = 1.33, 52% v/v PAN). [Note: Higher concentrations of AN were attempted to obtain a greater conversion of PAN in a shorter time, but the polymer precipitated readily in the reaction media, even at low conversions.]

## APPENDIX B

# HYDROXYL FUNCTIONALITY ACCESSIBILITY IN NANOPOROUS PSBCB-*B*-PLA FILMS

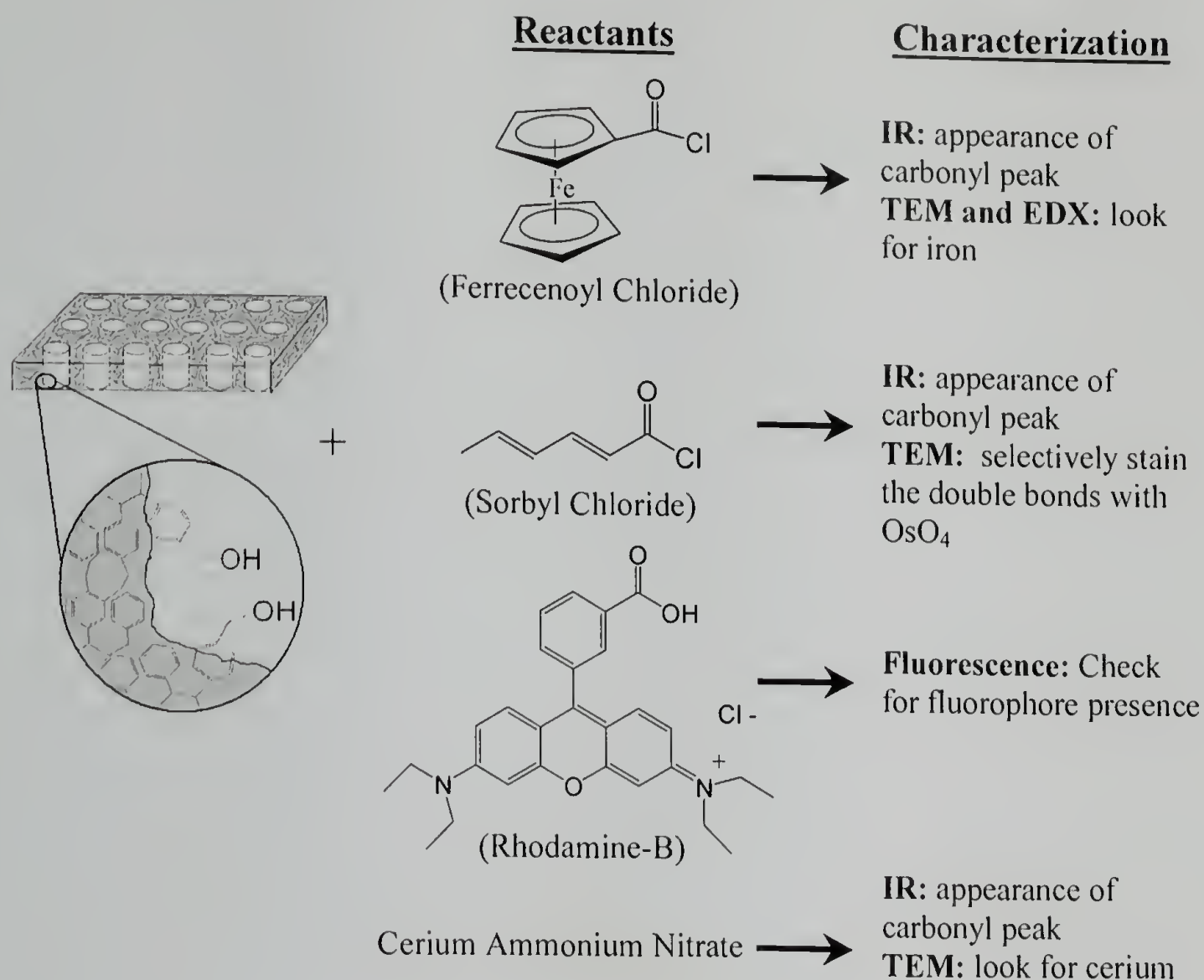
### B.1 Overview

Several reactions were explored in order to address the hydroxyl functionality of 30 nm films with aligned pores. All of the reactions that were attempted gave inconclusive results. This was most likely due to the sensitivity limits of the instruments used for the characterization, since these reactions are done on relatively thin films. Similar reactions have been done on soluble PS-*b*-PLA bulk monoliths, characterized by NMR, and have shown that the hydroxyl groups resulting from PLA degradation are accessible.<sup>26</sup> Here, the attempts to prove the addressibility of the hydroxyl groups in thin films are explained in detail, as well as the challenges that are faced when trying to characterize reactions within crosslinked thin films.

### B.2 Reactions Attempted

Several different reactions were attempted, keeping in mind the best methods of characterization. For example, carbonyl groups were added since they absorb strongly in IR and electron dense transition metals were chosen for TEM. These reactions were done using ferrocene (for IR, TEM, and EDX measurements), sorbyl chloride or low molecular weight polyisoprene (IR and to stain with OsO<sub>4</sub> for TEM), and rhodamine (for fluorescence) (see Figure B.1).

**Figure B.1. Attempts to address the hydroxyl functionality within the pores. List of reactions attempted and characterization used. All results were inconclusive.**



Attempts to anchor ferrocene on the pore walls was done using benzene (distilled over sodium and benzophenone), and ferrocene carboxylic acid (Lancaster, 98%). The ferrocene carboxylic acid was converted to the acid chloride using oxalyl chloride, based on a previous procedure.<sup>124</sup> The acid chloride (26 mg, deep red crystals), was added to 10 mL of benzene in a polymerization tube under nitrogen, resulting in a 0.01 M solution. The concentration of ferrocene was chosen arbitrarily, since in order to achieve a ratio of 1:1 of acid halide:hydroxyl group, a very small ( $\sim 10^{-8}$  g) amount would be needed, and would have resulted in a very dilute solution. A 1 cm x 1 cm wafer with a crosslinked nanoporous template on its surface was dropped into the reaction flask. A similar wafer was placed into another flask, for the control, containing

a 0.01 M solution of ferrocene (unfunctionalized) in benzene. Both were sealed and heated at 64 °C for 4 hours, without stirring, then removed from the flasks, and subjected to several benzene washes. The films were dried, removed from the substrate using an iodine etch and looked at under TEM. The nanoporous template did not show any increase in electron density around the pores, in either sample. Another batch of films was analyzed, while on the substrate, using EDX, but a peak corresponding to iron was not seen. The reaction was repeated using a higher concentration of acid halide in benzene (0.04 M) for the reaction, but still gave the same results. Thin films were also analyzed by IR using PM-IRRAS, while still on the gold substrate, but no signal for the carbonyl peak was seen.

Another approach to addressing the pore walls would be to use a reagent containing double bonds that could be selectively stained using osmium tetroxide ( $\text{OsO}_4$ ). This would result in enhanced electron density contrast for TEM measurements. For this, sorbyl chloride and low molecular weight hydroxy-terminated polyisoprene (PI-OH) were used. The PI-OH reaction was not straightforward, since it required the transformation of the hydroxyl groups on the pore walls to carboxylic acid halides in order to couple the PI-OH to the pore walls. Attempts were made to convert the hydroxyl functionality within the pores to the acid halide, using succinic anhydride, followed by oxalyl chloride. Preliminary studies using a low molecular weight PS-OH, suggested that the reaction with succinic anhydride did indeed give carboxylic acid terminated polymer, as confirmed via MALDI-ToF mass spectrometry. However, characterizing several reactions in a row within the pore was not feasible, and the supply of PI-OH was limited. The attempts using the sorbyl chloride were also

inconclusive. Sorbyl chloride was synthesized using oxalyl chloride, based on a modified procedure<sup>125</sup>, from the sorbic acid precursor. In a typical reaction, benzene (5.0 mL, distilled over sodium/benzophenone) and sorbyl chloride (1.0 mL) were added to a polymerization tube under nitrogen. A 1 cm x 2 cm wafer containing the crosslinked nanoporous template was added to the tube, which was sealed, heated to 65 °C, and reacted for 3 hours. The film was then removed from the reaction and washed several times in benzene, dried, then removed from the substrate using the iodine etch, and floated onto a copper grid for TEM analysis. Staining of the film was attempted using OsO<sub>4</sub> vapor, but, again, the results were inconclusive. Films still on the substrate were sent for analysis by PM-IRRAS, but there was no carbonyl peak present.

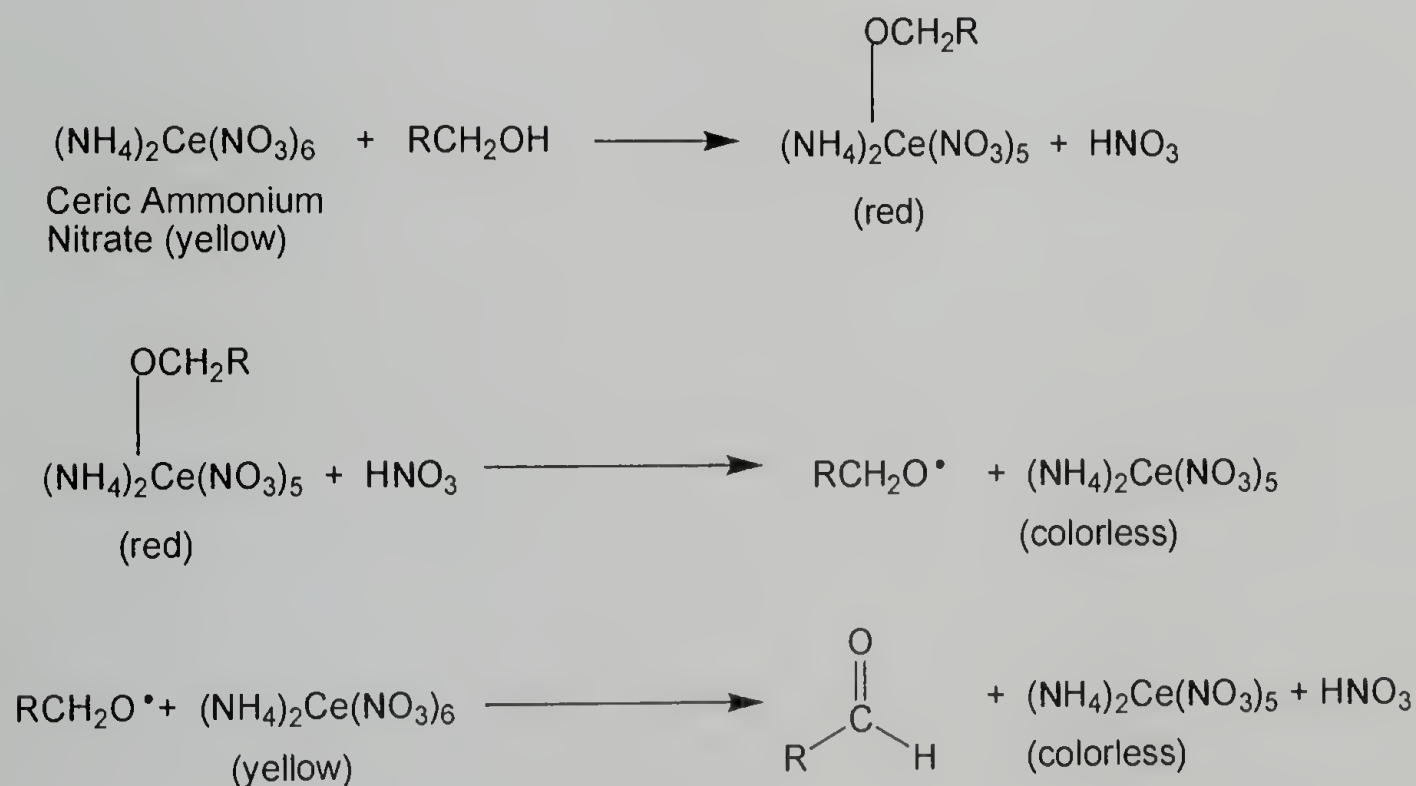
Fluorescence studies were also attempted, where rhodamine-b was reacted with the hydroxyl functionality, while still on the substrate. In a typical reaction, DMF (5 mL, anhydrous) was added to N, N'-diisopropylcarbodiimide (DIC)(3.2 mg), 1-hydroxybenzotriazole (HOBT)(3.8 mg), and rhodamine-b (2.4 mg) in a vial. A control vial containing DMF and rhodamine-6G was also prepared, since this fluorophore lacks the carboxylic acid group to react. The films were removed from the reactions after 24 hours at room temperature. The emission maximum for Rhodamine-b is at 625 nm, with an excitation maximum at 543 nm. Fluorescence measurements were done on the 30 nm film, still on the gold substrate, at 500 nm, with 5 nm slit widths, but no fluorescence was seen.

In addition, thin films (~30 nm) with aligned pores and thicker films (~200 nm) with parallel pore orientation (with respect to the substrate), were studied using a cerium ammonium nitrate reagent<sup>126</sup> to convert the primary hydroxyl groups to

aldehydes (see Figure B.2). This reaction has the added feature that there is a cerium intermediate that is bonded to the oxygen tethered to the pore wall. For a benzyl alcohol, this cerium intermediate persists (in solution) for ~4 hours, until all the material is converted to the aldehyde, releasing a colorless cerium salt. For the thin films, TEM was done to see the cerium on the pore walls, but due to a low concentration of the hydroxyl functionality, no contrast was seen. A control film that used cerium chloride, which would not react, also showed no cerium when analyzed by TEM. The thin films were also analyzed by PM-IRRAS, but no signal for the carbonyl was seen.

In the thicker films, the cerium ammonium nitrate reaction was allowed to proceed to completion (~ 5 hours), to create the aldehyde, and ATR-IR was used to check for the appearance of the carbonyl peak associated with the aldehyde. The thick film was scratched off the substrate and analyzed, but no carbonyl peak was seen.

**Figure B.2. Cerium ammonium nitrate reaction to convert primary alcohols to aldehydes.**<sup>126</sup>



Another method that can be used to address the functionality would be to initiate another PLA polymerization from the hydroxyl functionality. This also has its own

challenges, since PLA polymerization could be initiated from any hydroxyl functionality, potentially even the silicon substrate, and the concentration of catalyst has to be carefully controlled.

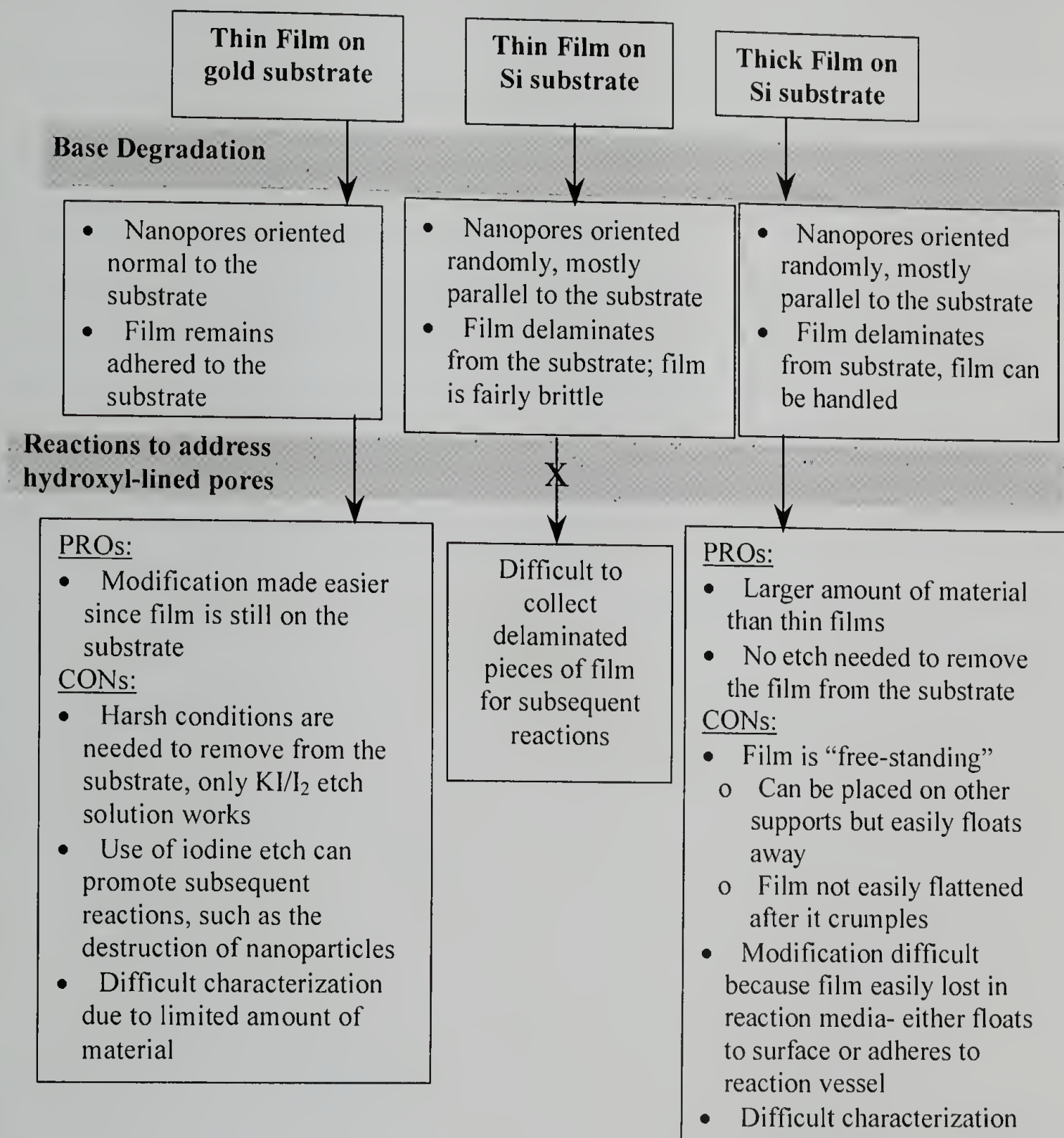
While these may seem like failed reactions that would support the inaccessibility of the hydroxyl groups, it is more than likely it is just hard to detect such a low concentration of functional groups. If the hydroxyl groups are accessible, there are a variety of parameters that need to be taken into consideration, not only for the reactions conditions used, but for the characterization conditions as well.

### **B.3 Challenges**

There are challenges in designing a method to address the limited functionality on the pore wall. One challenge is the low concentration of hydroxyl groups lining the pore walls. The number and concentration of end groups in the nanoporous films can be calculated using the observed domain sizes in Table 2.2. For example, for a 30 nm film of polymer "K", the volume of one pore (14 nm x 30 nm) is 4600 nm<sup>3</sup>. Using the density of PLA = 1.26 g/cm<sup>3</sup>, there is 5.8E-18 g (7.3E-22 mol) of PLA in each pore, and therefore, there are 440 hydroxyl groups. The surface area of the pore is 1300 nm<sup>2</sup>, which means that there is 1 hydroxyl group for every 3 nm<sup>2</sup>. The concentration of end groups within the film is calculated using the volume fractions established in Table 2.1. The volume fraction of PLA (0.36), means that there is 8200 nm<sup>3</sup> of PSBCB associated with each 4600 nm<sup>3</sup> pore. The moles of hydroxyl groups for each pore divided by the total volume of PSBCB and PLA associated with one pore (~13000 nm<sup>3</sup>), gives a concentration of 0.057 M. While this concentration is reasonable, the small amount of material from the thin films still pushes the sensitivity limits of the instruments used.

Additional challenges are summarized in Figure B.3, and are complicated by not only the low concentration of hydroxyl groups, but also by the limited methods available to align the porous structure and to remove the film from the substrate.

**Figure B.3. Challenges associated with the modification of nanoporous templates.**



Furthermore, the sensitivity of the instrumentation used for characterization has to be taken into consideration. The most promising methods of characterization would be elemental analysis (if enough material could be collected), IR, and TEM. Of course



TEM has the added advantage that if a reaction occurs, one can directly observe where the reaction took place, provided, of course, that the reaction results in a large electron density contrast. Functionalized nanoparticles could be used, but care would need to be exercised, since the etching solution needed to remove the film from the gold substrate, may also destroy the nanoparticles. For example, the destruction of cobalt nanoparticles was observed when they were placed into the iodine etch solution, resulting in a black precipitate over a short period of time.

Further attempts to address the hydroxyl groups should keep the above challenges in mind. Such parameters as instrumental sensitivity and sample preparation need to be adjusted if thin films are to be characterized reproducibly and accurately. Future experiments could circumvent the sensitivity issues by exploring larger probes and larger amounts of material, if possible.

## APPENDIX C

### SOLUTION BEHAVIOR OF ACRYLONITRILE DIBLOCK COPOLYMERS

#### C.1 Overview

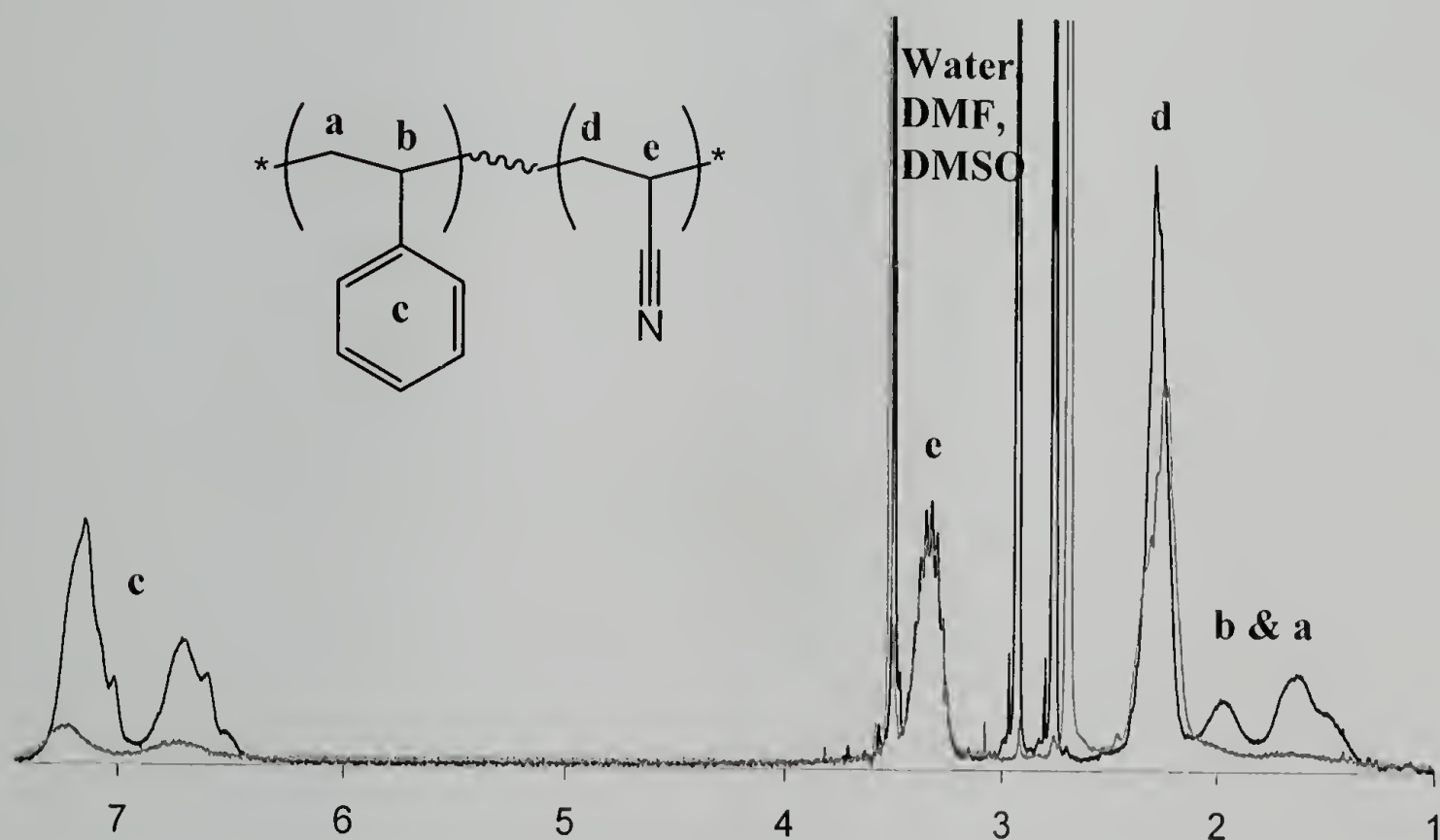
As discussed in Chapter 4, the use of alumina templates is a route by which unique morphologies can be obtained from confined diblock copolymers. In order to explore the effect of confinement on PS-*b*-PAN, it was determined that using higher molecular weight diblock copolymers would be a better starting point, since the domain sizes would be larger and, therefore, confinement would play a larger role in determining the resultant morphology. However, when these higher molecular weight polymers were characterized using the same methods as their lower molecular weight counterparts, some interesting solution properties appeared. While low molecular weight PS-*b*-PAN is soluble in DMSO, higher molecular weight polymers aggregate in solution, since the PS polymer is not soluble in DMSO. Understanding this solution behavior plays an important role in future experimentation with these higher molecular weight diblock copolymers.

#### C.2 Characterization

As noted in Chapter 3, the ~5 kg/mol PS-*b*-PAN diblock copolymers were characterized by <sup>1</sup>H NMR in DMSO-d<sub>6</sub>. When this solvent was used to characterize higher molecular weight PS-*b*-PAN, it appeared as though the conversion of PAN was abnormally large and that the PS block was almost non-existent. When the PS homopolymer, PS-Br (13 kg/mol, PDI= 1.06, JML-1-89), was placed into DMSO-d<sub>6</sub>, it

became evident that polystyrene was insoluble. Therefore the PS-*b*-PAN was characterized using  $^1\text{H}$  NMR with DMF- $\text{d}_7$  and was found to be 28 kg/mol total with a PDI= 1.33 and 52% v/v PAN (notebook JML-3-30). When the same polymer was characterized by DMSO- $\text{d}_6$ , ( $\sim 8$  mg/mL) it appeared as though the PAN block was 81 kg/mol (81 %v/v PAN), using the PS-Br aromatic peaks as an internal standard. The distinct difference in solution behavior can be seen in Figure C.1.

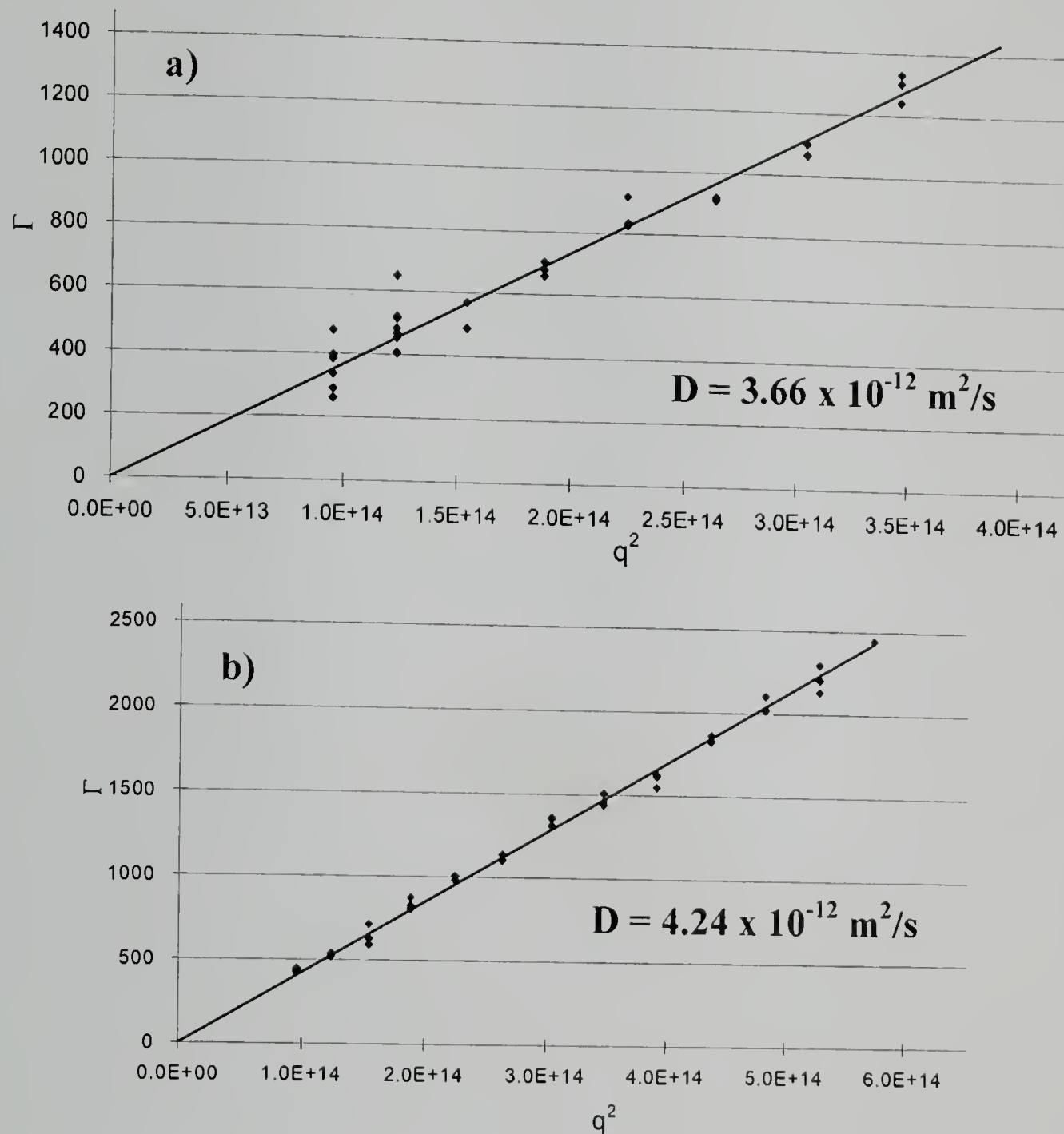
**Figure C.1. Comparison of PS-*b*-PAN behavior in DMSO- $\text{d}_6$  (gray line) and DMF- $\text{d}_7$  (black line).**



This NMR data indicates that aggregation is taking place. It is important to note that the solutions are clear, even though the PS block is apparently not soluble in DMSO. Dynamic light scattering (DLS) was done on dilute solutions of PS-*b*-PAN (JML-3-30) (0.31 g/L – 5.0 g/L), in both DMSO and DMF to determine the hydrodynamic radii ( $R_h$ ) of the aggregates. In DMF there are two populations, where  $R_h \sim 4$  nm and 74 nm, whereas in DMSO,  $R_h \sim 26$  nm. These were determined from the

diffusion data shown Figure C.2, (diffusion data for  $R_h \sim 4$  nm not shown), using the viscosities<sup>127</sup> for DMSO, 1.98 cp (at 25 °C) and DMF, 0.796 cp (at 25 °C).

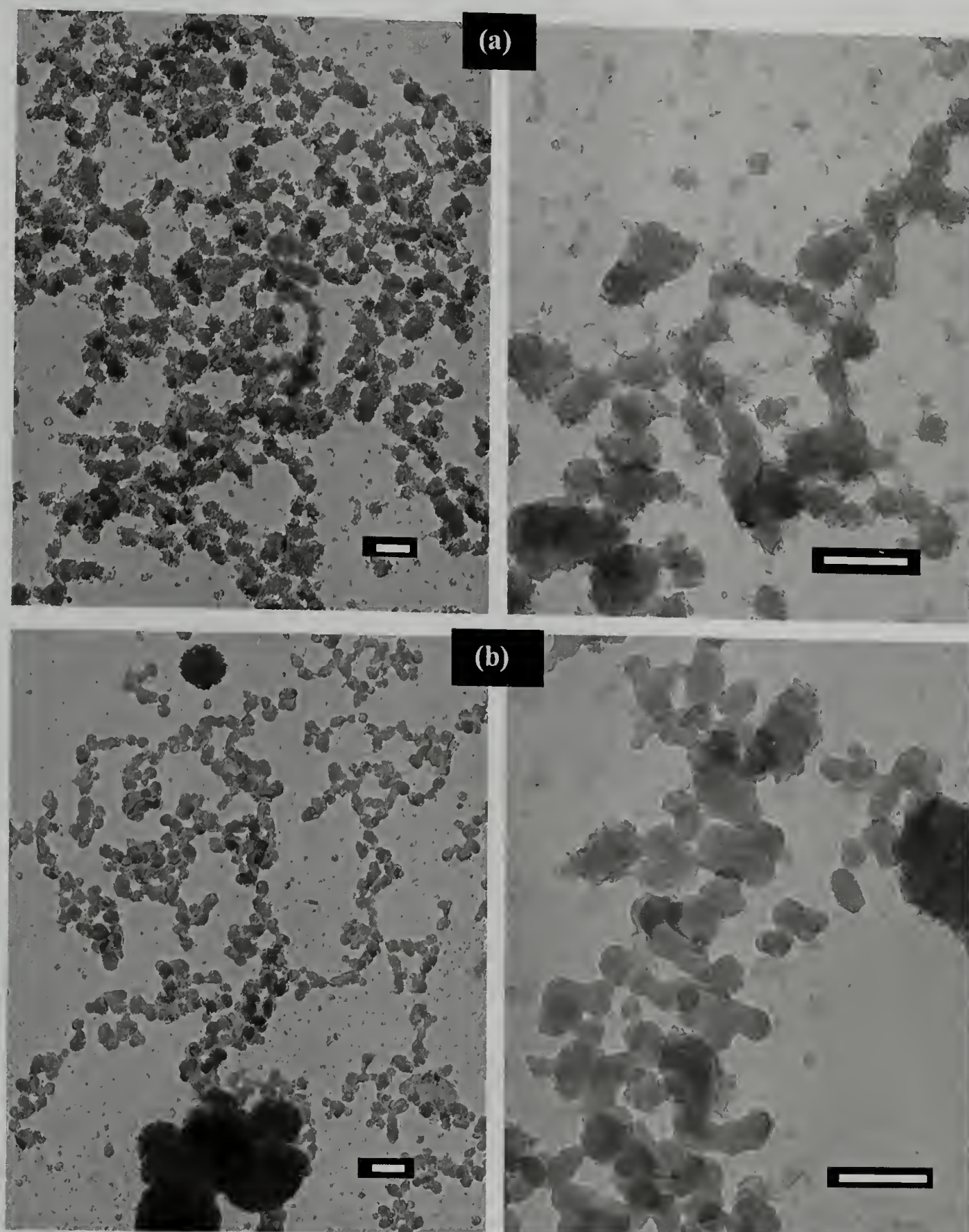
**Figure C.2. Representative DLS data for PS-*b*-PAN in a) DMF and b) DMSO.**



A couple of the solutions used for the DLS studies (both 5 mg/mL in either DMF or DMSO) were used for TEM studies. A drop of this solution was placed onto a carbon-coated copper grid and dried overnight at ambient conditions. The results, shown in Figure C.3, show the aggregates, without staining, under TEM. The DMF aggregates appear to be wrinkled more than the DMSO aggregates. This can be

attributed to the fact that the PS core(s) swell in DMF, so that when the DMF evaporates the aggregates wrinkle. In addition, DMF has a higher vapor pressure than DMSO, and therefore evaporates more rapidly. The DMSO aggregates, on the other hand, have only a minimal amount of DMSO in the PS center. These conclusions are further supported by the NMR data (see Figure C.1), because the PS peaks "disappear" in DMSO, indicating that the PS core is "solid-like". Although the sizes of the aggregates are consistent with those found in solution, there appears to be a larger distribution of sizes. This is most likely due to the aggregation of the particles as the film dried, as well as the introduction of moisture as the film dried under ambient conditions.

Figure C.3. TEM of PS-*b*-PAN aggregates from a) DMF and b) DMSO solutions at various magnifications. Scale bars = 200 nm.

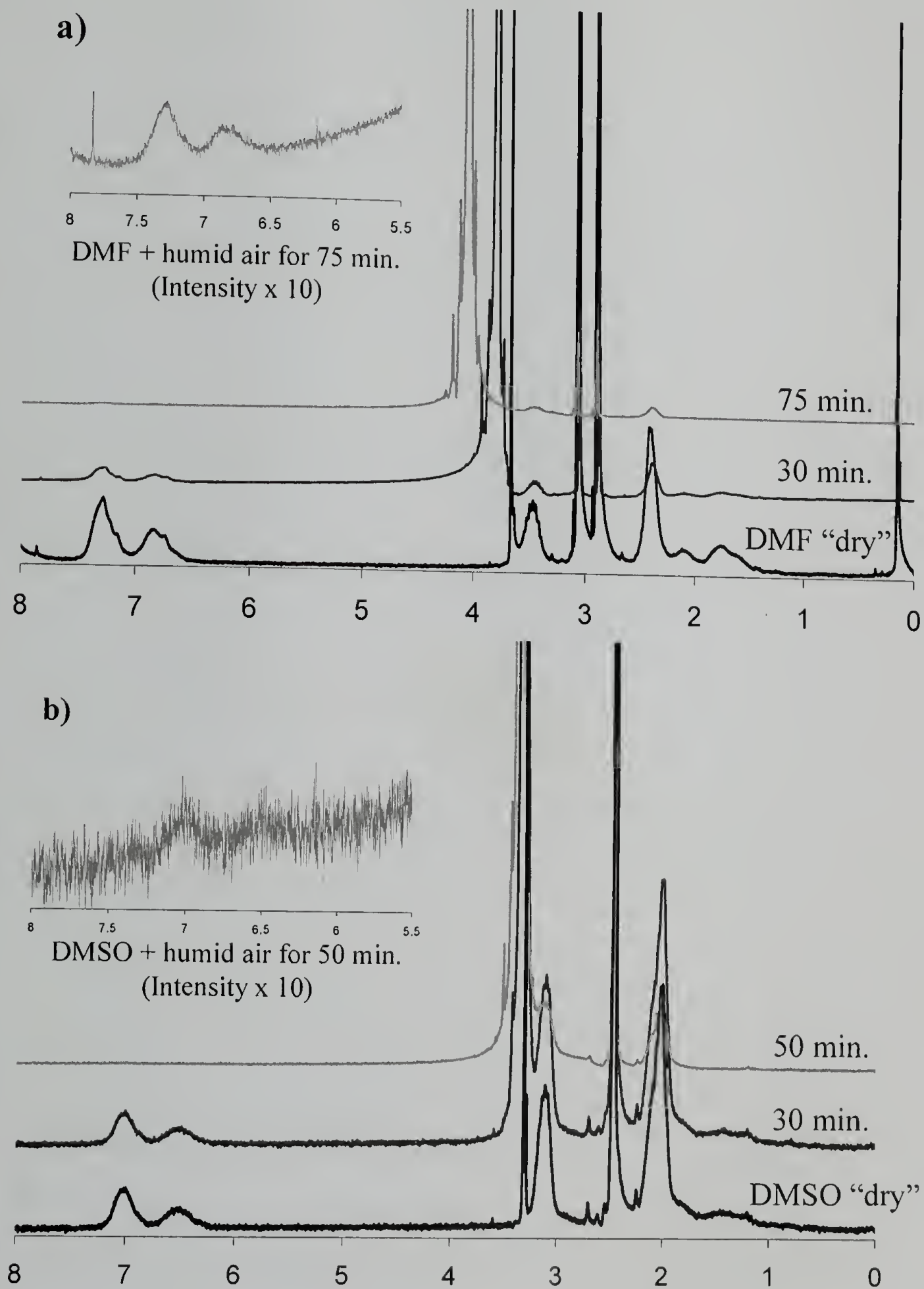


Since the solvents used were very hygroscopic, the role of water in the formation of these aggregates was explored. Instead of preparing the TEM grids by placing a drop of DMF or DMSO solution on a carbon-coated copper grid, and letting it evaporate under ambient conditions, it was allowed to dry overnight under a nitrogen

atmosphere at 0% humidity. Similar films were also prepared by drop-casting the solutions onto carbon-coated silicon wafers (to mimic the carbon coated copper grids) and silicon wafers with native oxide (to rule out the effect of the substrate). It was found, for all of the samples dried under ambient conditions, aggregates formed. For those dried at 0% humidity, no aggregates were formed, and in the case of the silicon wafers, smooth films were seen. This supports the earlier conclusions in Chapter 3 that the elimination of water when casting films of PS-*b*-PAN, is the key to smooth, reproducible films.

Since water has such a profound effect on the aggregation behavior of PS-*b*-PAN, the addition of water and its effect on the aggregates in solution was studied. Solutions of PS-*b*-PAN (JML-3-30) in either DMF- $d_7$  or DMSO- $d_6$  were prepared, as dry as possible, and  $^1\text{H}$  NMR was immediately taken. The “dry” results are similar to those shown in the initial NMR studies in Figure C.1. A stream of air saturated with water (via a bubbler) was passed over the solution in the NMR tube for 30 min and 50 min. Bubbling through the solutions was attempted, but resulted in very foamy solutions. The NMR data shows the disappearance of the PS peaks almost entirely, which is clearly seen in the aromatic region of the NMR spectra (see Figure C.4). It is important to note that the solutions were all clear, indicating the aggregates were still smaller than the wavelength of light. The addition of water to the solutions has the effect of causing the PS cores to apparently expel the solvent, as the solvent/water mixture becomes less miscible.

Figure C.4. Effect of water on the aggregation behavior of PS-*b*-PAN in solution.  
a) DMF- $d_7$  and b) DMSO- $d_6$ . Humid air was passed over the solutions for the times shown. Figures are offset vertically for clarity.

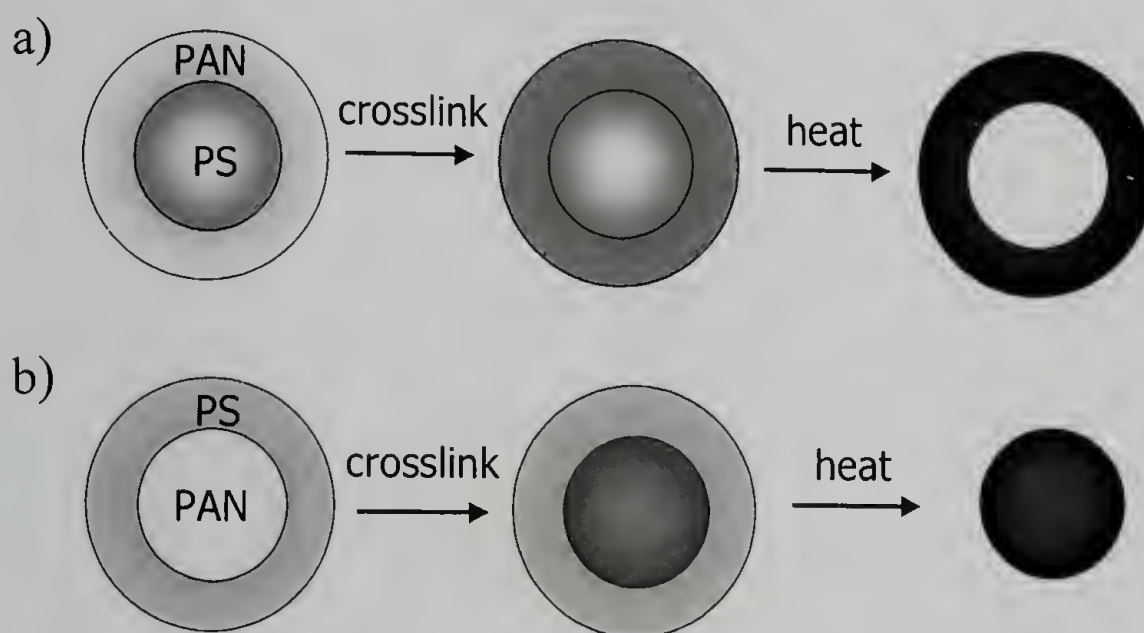




### C.3 Challenges and Future Directions

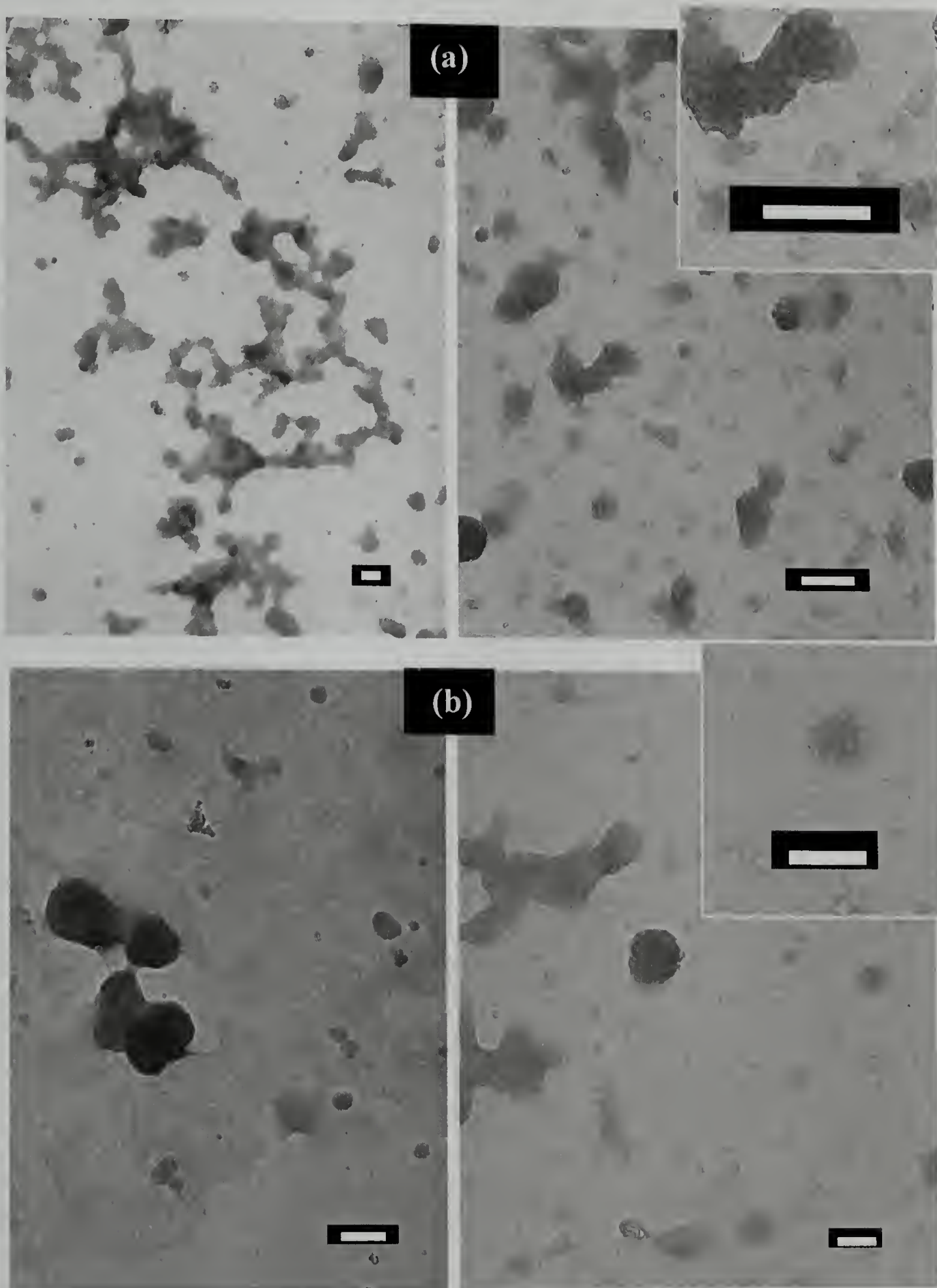
It would be interesting if the aforementioned aggregates could be converted into carbonaceous structures. If the aggregates were micelles, then this would allow for either the creation of “solid” carbon balls or hollow carbon spheres, depending upon the nature of the solvent. If the solvent prefers the PAN block, as the case is for DMSO, then the result would be a hollow sphere (see Figure C.5).

**Figure C.5. Creation of carbon nanostructures from solution aggregates. a) PAN selective solvent, b) PS selective solvent.**



As is suggested by Figure C.5, the first step in the creation of these structures involves crosslinking. In order to achieve this, base-induced cyclization was attempted<sup>128,129</sup> using KOH while the polymer was in solution. However, this resulted in an orange-colored solution that, when cast onto a carbon-coated copper grid, showed no aggregates. Optimization of this technique by using various bases and various solvents may lead to better results. In addition, thermal crosslinking of the aggregates, while on the TEM grid was attempted. The samples shown in Figure C.3 were heated to 250 °C for 2 hours. While this heating may have induced crosslinking of the PAN domains, it also flattened and coalesced the aggregates (see Figure C.6).

Figure C.6. Thermal treatment of PS-*b*-PAN aggregates from a)DMF and b) DMSO on carbon-coated TEM grids at 250 °C for 2 hours in air.



Future directions for this project should focus on quantifying the amount of water and its effect on the aggregation behavior, since studies up to this point have

focused on the qualitative trends. In addition, attempting other means to crosslink the aggregates may be worthwhile, such as UV irradiation, small molecule crosslinking or thermal crosslinking in solution using higher boiling solvents such as sulfolane.

Understanding the solution behavior of PS-*b*-PAN will aid in other projects where the higher molecular weight polymers are used, and will allow for the potential creation of carbonaceous nanostructures with tuneable sizes.

## REFERENCES

- (1) Edwards, E. W.; Montague, M. F.; Solak, H. H.; Hawker, C. J.; Nealey, P. F. *Adv. Mater.* **2004**, *16*, 1315.
- (2) Stoykovich, M. P.; Muller, M.; Kim, S. O.; Solak, H. H.; Edwards, E. W.; de Pablo, J. J.; Nealey, P. F. *Science* **2005**, *308*, 1442–1446.
- (3) Hawker, C. J.; Russell, T. P. *MRS Bulletin* **2005**, *30*, 952–966.
- (4) Huggins, M. L. *J. Chem. Phys.* **1941**, *9*, 440.
- (5) Flory, P. J. *Principles of Polymer Chemistry*; Cornell University Press: Ithaca, NY, 1953.
- (6) Leibler, L. *Macromolecules* **1980**, *13*, 1602–1617.
- (7) Krishnamoorti, R.; Graessley, W. W.; Dee, G. T.; Walsh, D. J.; Fetters, L. J.; Lohse, D. J. *Macromolecules* **1996**, *29*, 367–376.
- (8) Van Krevelen, D. W.; Hoftyzer, P. J. *Properties of Polymers: Correlation with Chemical Structure*; Elsevier: New York, 1972.
- (9) Ruzette, A. V. G.; Mayes, A. M. *Macromolecules* **2001**, *34*, 1894–1907.
- (10) Ruzette, A. V. G.; Banerjee, P.; Mayes, A. M.; Russell, T. P. *J. Chem. Phys.* **2001**, *114*, 8205–8209.
- (11) Matsen, M. W.; Bates, F. S. *Macromolecules* **1996**, *29*, 1091–1098.
- (12) Gupta, V. K.; Krishnamoorti, R.; Chen, Z.-R.; Kornfield, J. A.; Smith, S. D.; Satkowski, M. M.; Grothaus, J. T. *Macromolecules* **1996**, *29*, 875–884.
- (13) Kimura, M.; Misner, M. J.; Xu, T.; Kim, S. H.; Russell, T. P. *Langmuir* **2003**, *19*, 9910–9913.
- (14) Segalman, R. A.; Hexemer, A.; Kramer, E. J. *Macromolecules* **2003**, *36*, 6831–6839.
- (15) Kim, S. H.; Misner, M. J.; Xu, T.; Kimura, M.; Russell, T. P. *Adv. Mater.* **2004**, *16*, 226–231.
- (16) Morkved, T. L.; Lu, M.; Urbas, A. M.; Ehrichs, E. E.; Jaeger, H. M.; Mansky, P.; Russell, T. P. *Science* **1996**, *273*, 931–933.
- (17) Mansky, P.; Liu, Y.; Huang, E.; Russell, T. P.; Hawker, C. *Science* **1997**, *275*, 1458–1460.
- (18) Thurn-Albrecht, T.; DeRouchey, J.; Russell, T. P. *Macromolecules* **2000**, *33*, 3250–3253.
- (19) Mansky, P.; DeRouchey, J.; Russell, T. P. *Macromolecules* **1998**, *31*, 4399–4401.
- (20) Ryu, D. Y.; Shin, K.; Drockenmuller, E.; Hawker, C. J.; Russell, T. P. *Science* **2005**, *308*, 236–239.
- (21) Park, M.; Harrison, C.; Chaikin, P. M.; Register, R. A.; Adamson, D. H. *Science* **1997**, *276*, 1401–1404.
- (22) Lammertink, R. G. H.; Hempenius, M. A.; van den Enk, J. E.; Chan, V. Z. H.; Thomas, E. L.; Vancso, G. J. *Adv. Mater.* **2000**, *12*, 98–103.
- (23) Cavicchi, K. A.; Zalusky, A. S.; Hillmyer, M. A.; Lodge, T. P. *Macromol. Rapid Commun.* **2004**, *25*, 704–709.
- (24) Hansen, M. S.; Vigild, M. E.; Berg, R. H.; Ndoni, S. *Polym. Bull.* **2004**, *51*, 403–409.

- (25) Olayo-Valles, R.; Lund, M. S.; Leighton, C.; Hillmyer, M. A. *J. Mater. Chem.* **2004**, *14*, 2729–2731.
- (26) Zalusky, A. S.; Olayo-Valles, R.; Wolf, J. H.; Hillmyer, M. A. *J. Am. Chem. Soc.* **2002**, *124*, 12761–12773.
- (27) Guarini, K. W.; Black, C. T.; Zhang, Y.; Kim, H.; Sikorski, E. M.; Babich, I. V. *J. Vac. Sci. Technol., B* **2002**, *20*, 2788–2792.
- (28) Lazzari, M.; Lopez-Quintela, M. A. *Adv. Mater.* **2003**, *15*, 1583–1594.
- (29) Shin, K.; Leach, K. A.; Goldbach, J. T.; Kim, D. H.; Jho, J.-Y.; Tuominen, M.; Hawker, C. J.; Russell, T. P. *Nano Lett.* **2002**, *2*, 933–936.
- (30) Thurn-Albrecht, T.; Schotter, J.; Kastle, G. A.; Emley, N.; Shibauchi, T.; Krusin-Elbaum, L.; Guarini, K.; Black, C. T.; Tuominen, M. T.; Russell, T. P. *Science* **2000**, *290*, 2126–2129.
- (31) Lopes, W. A.; Jaeger, H. M. *Nature* **2001**, *414*, 735–738.
- (32) Li, M.; Douki, K.; Goto, K.; Li, X.; Coenjarts, C.; Smilgies, D. M.; Ober, C. K. *Chem. Mater.* **2004**, *16*, 3800–3808.
- (33) Wolf, J. H.; Hillmyer, M. A. *Langmuir* **2003**, *19*, 6553–6560.
- (34) Noro, A.; Cho, D.; Takano, A.; Matsushita, Y. *Macromolecules* **2005**, *38*, 4371–4376.
- (35) Lynd, N. A.; Hillmyer, M. A. *Macromolecules* **2005**, *38*, 8803–8810.
- (36) Matsushita, Y.; Noro, A.; Iinuma, M.; Suzuki, J.; Ohtani, H.; Takano, A. *Macromolecules* **2003**, *36*, 8074–8077.
- (37) Burger, C.; Ruland, W.; Semenov, A. N. *Macromolecules* **1990**, *23*, 3339–3346.
- (38) Burger, C.; Ruland, W.; Semenov, A. N. *Macromolecules* **1991**, *24*, 816.
- (39) Quirk, R. P.; Lee, B. *Polym. Int.* **1992**, *27*, 359–367.
- (40) Yakimansky, A. V. *Poly. Sci. Series C* **2005**, *C47*, 1–49.
- (41) Solomon, D. H.; Rizzardo, E.; Cacioli, P. *U.S. Patent # 4581429*, **1986**.
- (42) Veregin, R. P.; Michael, G. K.; Kazmaier, P. M.; Hamer, G. K. *Macromolecules* **1993**, *26*, 5316–5320.
- (43) Hsieh, H. L.; Quirk, R. P. *Anionic Polymerization: Principles and Practical Applications*; Marcel Dekker, Inc.: New York, 1996.
- (44) Kricheldorf, H. R.; Kreiseraunders, I.; Boettcher, C. *Polymer* **1995**, *36*, 1253–1259.
- (45) Dubois, P.; Jerome, R.; Teyssie, P. *Makromol. Chem., Macromol. Symp.* **1991**, *42-3*, 103–116.
- (46) Dechy-Cabaret, O.; Martin-Vaca, B.; Bourissou, D. *Chem. Rev.* **2004**, *104*, 6147–6176.
- (47) Matyjaszewski, K.; Xia, J. *Chem. Rev.* **2001**, *101*, 2921–2990.
- (48) Szwarc, M. *Nature* **1956**, *178*, 1168–1169.
- (49) Szwarc, M.; Levy, M.; Milkovich, R. *J. Am. Chem. Soc.* **1956**, *78*, 2656–2657.
- (50) Fetters, L. J. *J. Polym. Sci., Part C* **1969**, *26*, 1–35.
- (51) Morton, M. *Anionic Polymerization: Principles and Practice*; Academic Press: New York, 1993.
- (52) Hawker, C. J.; Hedrick, J. L.; Miller, R. D.; Volksen, W. *U.S. Patent # US Patent 20010040294*, **2001**.
- (53) Harth, E.; Van Horn, B.; Lee, V. Y.; Germack, D. S.; Gonzales, C. P.; Miller, R. D.; Hawker, C. J. *J. Am. Chem. Soc.* **2002**, *124*, 8653–8660.

- (54) Johnson, R. W.; Phillips, T. L.; Weidner, W. K.; Hahn, S. F.; Burdeaux, D. C.; Townsend, P. H. *IEEE Trans. Compon. Hyb.* **1990**, *13*, 347–352.
- (55) Burdeaux, D.; Townsend, P.; Carr, J.; Garrou, P. *J. Electron. Mater.* **1990**, *19*, 1357–1364.
- (56) Ohba, K. *J. Photopolym. Sci. Technol.* **2002**, *15*, 177–182.
- (57) Drockenmuller, E.; Li, L. Y. T.; Ryu, D. Y.; Harth, E.; Russell, T. P.; Kim, H. C.; Hawker, C. J. *J. Polym. Sci., Part A: Polym. Chem.* **2005**, *43*, 1028–1037.
- (58) Leiston-Belanger, J. M.; Russell, T. P.; Drockenmuller, E.; Hawker, C. J. *Macromolecules* **2005**, *38*, 7676–7683.
- (59) Barton, J. W.; Howard, J. A. K.; Shepherd, M. K.; Stringer, A. M. *J. Chem. Soc., Perkin Trans. 1* **1987**, 2443–2445.
- (60) Lloyd, J. B. F.; Ongley, P. A. *Tetrahedron* **1965**, *21*, 245.
- (61) Tan, L. S.; Arnold, F. E. *J. Polym. Sci., Part A: Polym. Chem.* **1988**, *26*, 1819–1834.
- (62) Bubb, W. A.; Sternhell, S. *Aust. J. Chem.* **1976**, *29*, 1685–1697.
- (63) Durr, H.; Nickels, H.; Pacala, L. A.; Jones, M. *J. Org. Chem.* **1980**, *45*, 973–980.
- (64) Jones, M.; Levin, R. H. *J. Am. Chem. Soc.* **1969**, *91*, 6411.
- (65) Sadana, A. K.; Saini, R. K.; Billups, W. E. *Chem. Rev.* **2003**, *103*, 1539–1602.
- (66) Schiess, P.; Heitzmann, M.; Rutschmann, S.; Staeheli, R. *Tet. Lett.* **1978**, *46*, 4569–4572.
- (67) McKean, D. R.; Parrinello, G.; Renaldo, A. F.; Stille, J. K. *J. Org. Chem.* **1987**, *52*, 422–424.
- (68) Sheffy, F. K.; Godschalx, J. P.; Stille, J. K. *J. Am. Chem. Soc.* **1984**, *106*, 4833–4840.
- (69) Labadie, J. W.; Stille, J. K. *J. Am. Chem. Soc.* **1983**, *105*, 6129–6137.
- (70) Blomberg, S.; Ostberg, S.; Harth, E.; Bosman, A. W.; Van Horn, B.; Hawker, C. J. *J. Polym. Sci., Part A: Polym. Chem.* **2002**, *40*, 1309–1320.
- (71) Buffeteau, T.; Desbat, B.; Turlet, J. M. *Appl. Spectrosc.* **1991**, *45*, 380–389.
- (72) Toomey, R.; Freidank, D.; Ruhe, J. *Macromolecules* **2004**, *37*, 882–887.
- (73) Flory, P. J.; Rehner, J. R. *J. Chem. Phys.* **1943**, *11*, 521.
- (74) Flory, P. J. *J. Chem. Phys.* **1950**, *18*, 108.
- (75) Gonzalez-Leon, J. A.; Mayes, A. M. *Macromolecules* **2003**, *36*, 2508–2515.
- (76) Muralidharan, V.; Hui, C. Y. *Macromol. Rapid Commun.* **2004**, *25*, 1487–1490.
- (77) Wu, S. *J. Phys. Chem.* **1970**, *74*, 632–638.
- (78) Rodlert, M.; Harth, E.; Rees, I.; Hawker, C. J. *J. Polym. Sci., Part A: Polym. Chem.* **2000**, *38*, 4749–4763.
- (79) Xu, T. *Electric Field Alignment of Diblock Copolymer Thin Films*. Ph.D. Dissertation, University of Massachusetts Amherst, MA, 2004.
- (80) Xu, T.; Goldbach, J. T.; Leiston-Belanger, J. M.; Russell, T. P. *Colloid Polym. Sci.* **2004**, *282*, 927–931.
- (81) Wang, J.; Xu, T.; Leiston-Belanger, J. M.; Gupta, S.; Russell, T. P. *Phys. Rev. Lett.* **2006**, *96*, 128301/128301–128301/128304.
- (82) Ham, G. E. *Copolymerization: High Polymers: Chapter IX*; Interscience Publishers: New York, 1964.
- (83) Henrici-Olive, G.; Olive, S. *Adv. Polym. Sci.* **1983**, *51*, 1–60.

- (84) Surianarayanan, M.; Vijayaraghavan, R.; Raghavan, K. V. *J. Polym. Sci., Part A: Polym. Chem.* **1998**, *36*, 2503–2512.
- (85) Xue, T. J.; McKinney, M. A.; Wilkie, C. A. *Polym. Deg. Stab.* **1997**, *58*, 193–202.
- (86) Monahan, A. R. *J. Polym. Sci., Part A-1* **1966**, *4*, 2391–2399.
- (87) Minagawa, M.; Onuma, H.; Ogita, T.; Uchida, H. *J. Appl. Polym. Sci.* **2000**, *79*, 473–478.
- (88) Chatterjee, N.; Basu, S.; Palit, S. K.; Maiti, M. M. *J. Polym. Sci., Part B: Polym. Phys.* **1995**, *33*, 1705–1712.
- (89) Linnemayr, K.; Vana, P.; Allmaier, G. *Rapid Comm. Mass. Spec.* **1998**, *12*, 1344–1350.
- (90) Chung, T. C.; Schlesinger, Y.; Etemad, S.; Macdiarmid, A. G.; Heeger, A. J. *J. Polym. Sci., Part B: Polym. Phys.* **1984**, *22*, 1239–1246.
- (91) Overberger, C. G.; Moore, J. A. *Adv. Polym. Sci.* **1970**, *7*, 113–150.
- (92) Kowalewski, T.; Tsarevsky, N. V.; Matyjaszewski, K. *J. Am. Chem. Soc.* **2002**, *124*, 10632–10633.
- (93) Kowalewski, T.; McCullough, R. D.; Matyjaszewski, K. *Eur. Phys. J., Sect. E* **2003**, *10*, 5–16.
- (94) Tang, C.; Kowalewski, T.; Matyjaszewski, K. *Macromolecules* **2003**, *36*, 1465–1473.
- (95) Liang, C. D.; Hong, K. L.; Guiochon, G. A.; Mays, J. W.; Dai, S. *Angew. Chem., Int. Ed.* **2004**, *43*, 5785–5789.
- (96) Ono, H.; Hisatani, K.; Kamide, K. *Polym. J.* **1993**, *25*, 245–265.
- (97) Perry, E. *J. Appl. Polym. Sci.* **1964**, *8*, 2605–2618.
- (98) Claes, P.; Smets, G. *Makromol. Chem.* **1961**, *44*, 212–220.
- (99) Wachter, U.; Morgenstern, U.; Berger, W.; Dreyer, R. *Acta Polym.* **1991**, *42*, 300–304.
- (100) Kolesnikov, G. S.; Yaralov, L. K. *Vysokomol. Soedin.* **1966**, *8*, 2018–2023.
- (101) Sui, K. Y.; Gu, L. X. *J. Appl. Polym. Sci.* **2003**, *89*, 1753–1759.
- (102) Xu, X.; Xiao, W.; Chen, K. *Eur. Polym. J.* **1994**, *30*, 1439–1442.
- (103) Mu Jo, S.; Gaynor, S. G.; Matyjaszewski, K. *Polym. Prepr. (Am. Chem. Soc., Div. Polym. Chem.)* **1996**, *37*, 272–273.
- (104) Lazzari, M.; Chiantore, O.; Mendichi, R.; Lopez-Quintela, M. A. *Macromol. Chem. Phys.* **2005**, *206*, 1382–1388.
- (105) Priddy, D. B. *Adv. Polym. Sci.* **1995**, *121*, 124–154.
- (106) Matyjaszewski, K.; Mu Jo, S.; Paik, H. J.; Shipp, D. A. *Macromolecules* **1999**, *32*, 6431–6438.
- (107) Acar, M. H.; Matyjaszewski, K. *Macromol. Chem. Phys.* **1999**, *200*, 1094–1100.
- (108) Hadjichristidis, N.; Iatrou, H.; Pispas, S.; Pitsikalis, M. *J. Polym. Sci., Part A: Polym. Chem.* **2000**, *38*, 3211–3234.
- (109) Goldbach, J. T. *Synthesis, Characterization and Thin Film Morphology of Poly(Styrene-block-Methyl Methacrylate) Containing UV Photolabile Junction Points*. Ph.D. Dissertation, University of Massachusetts Amherst, MA, 2004.
- (110) Azuma, C.; Dias, M. L.; Mano, E. B. *Polym. Bull.* **1995**, *34*, 585–592.
- (111) Azuma, C.; Dias, M. L.; Mano, E. B. *Polym. Bull. (Berlin)* **1995**, *34*, 593–598.

- (112) Trent, J. S.; Scheinbeim, J. I.; Couchman, P. R. *Macromolecules* **1983**, *16*, 589–598.
- (113) Reich, L.; Stivala, S. S. *Elements of Polymer Degradation*; McGraw-Hill Book Co.: New York, 1971.
- (114) Mark, J. E. *Polymer Data Handbook*; Oxford University Press: New York, 1999.
- (115) Dunn, P.; Ennis, B. C. *J. Appl. Polym. Sci.* **1970**, *14*, 1795–1798.
- (116) Semsarzadeh, M. A.; Molaei, A. *Iran. Polym. J.* **1997**, *6*, 113–119.
- (117) Fitzer, E.; Muller, D. J. *Makromol. Chem.* **1971**, *144*, 117.
- (118) Leiston-Belanger, J. M.; Penelle, J.; Russell, T. P. *Macromolecules* **2006**, *39*, 1766–1770.
- (119) Xiang, H.; Shin, K.; Kim, T.; Moon, S.; McCarthy, T. J.; Russell, T. P. *J. Polym. Sci., Part B: Polym. Phys.* **2005**, *43*, 3377–3383.
- (120) Shin, K.; Xiang, H.; Moon, S.; Kim, T.; McCarthy, T. J.; Russell, T. P. *Science* **2004**, *306*, 76.
- (121) Xiang, H.; Shin, K.; Kim, T.; Moon, S.; McCarthy, T. J.; Russell, T. P. *Macromolecules* **2005**, *38*, 1055–1056.
- (122) Li, W.; Wickham, R. A.; Garbary, R. A. *Macromolecules* **2006**, *39*, 806–811.
- (123) Chen, J.-T.; Shin, K.; Leiston-Belanger, J. M.; Zhang, M.; Russell, T. P. *Adv. Mater.* **2006**, *in press*.
- (124) Rolfes, J.; Andersson, J. T. *Anal. Comm.* **1996**, *33*, 429–432.
- (125) Cartwright, D.; Lee, V. J.; Rinehart, K. L. *J. Am. Chem. Soc.* **1978**, *100*, 4237–4239.
- (126) Shriner, R. L.; Hermann, C. K. F.; Morrill, T. C.; Curtin, D. Y.; Fuson, R. C. *The Systematic Identification of Organic Compounds: 7th ed.*; John Wiley and Sons, Inc.: New York, 1998.
- (127) Gordon, A. J.; Ford, R. A. *The Chemist's Companion: A Handbook of Practical Data, Techniques and References*; John Wiley and Sons: New York, 1972.
- (128) Bashir, Z.; Manns, G.; Service, D. M.; Bott, D. C.; Herbert, I. R.; Ibbett, R. N.; Church, S. P. *Polymer* **1991**, *32*, 1826–1833.
- (129) Andreeva, O. A.; Burkova, L. A. *J. Macromol. Sci. Phys.* **1998**, *B37*, 773–782.



## BIBLIOGRAPHY

- Acar, M. H.; Matyjaszewski, K. "Block Copolymers by Transformation of Living Anionic Polymerization into Controlled/"Living" Atom Transfer Radical Polymerization", *Macromol. Chem. Phys.* **1999**, *200*, 1094–1100.
- Andreeva, O. A.; Burkova, L. A. "PMAN Coloration Due to Carboxylate and Acidic Group Clustering on Alkali and Thermal Treatment", *J. Macromol. Sci. Phys.* **1998**, *B37*, 773–782.
- Arduengo, A. J.; Krafczyk, R.; Schmutzler, R. "Imidazolylidenes, Imidazolinylienes and Imidazolidines", *Tetrahedron* **1999**, *55*, 14523–14534.
- Askadskii, A. A. *Physical Properties of Polymers: Prediction and Control*; Gordon and Breach Publishers: Amsterdam, 1996.
- Azuma, C.; Dias, M. L.; Mano, E. B. "Size Exclusion Behavior of Polymers in amide solvents", *Polym. Bull.* **1995**, *34*, 585–592.
- Azuma, C.; Dias, M. L.; Mano, E. B. "Size exclusion behavior of polymers in amide solvents. II. Molecular weight determination of acrylonitrile polymers in N,N-dimethylformamide", *Polym. Bull. (Berlin)* **1995**, *34*, 593–598.
- Barboiu, B.; Percec, V. "Metal Catalyzed Living Radical Polymerization of Acrylonitrile Initiated with Sulfonyl Chlorides", *Macromolecules* **2001**, *34*, 8626–8636.
- Barton, J. W.; Howard, J. A. K.; Shepherd, M. K.; Stringer, A. M. "The Rearrangement of a Tetrahydrobiphenylene Derivative to a Bridged Benzocycloheptene", *J. Chem. Soc., Perkin Trans. 1* **1987**, 2443–2445.
- Bashir, Z.; Manns, G.; Service, D. M.; Bott, D. C.; Herbert, I. R.; Ibbett, R. N.; Church, S. P. "Investigation of Base Induced Cyclization and Methine Proton Abstraction in Polyacrylonitrile Solutions", *Polymer* **1991**, *32*, 1826–1833.
- Beevers, R. B. "Dependence of the Glass Transition Temperature of Polyacrylonitrile on Molecular Weight", *J. Appl. Polym. Sci., Part A* **1964**, *2*, 5257–5265.
- Benoit, D.; Chaplinski, V.; Braslau, R.; Hawker, C. J. "Development of a Universal Alkoxyamine for "Living" Free Radical Polymerizations", *J. Am. Chem. Soc.* **1999**, *121*, 3904–3920.
- Bercea, M.; Morariu, S.; Ioan, C.; Ioan, S.; Simionescu, B. C. "Viscometric Study of Extremely Dilute Polyacrylonitrile Solutions", *Eur. Polym. J.* **1999**, *35*, 2019–2024.

- Bicerano, J. *Prediction of Polymer Properties*; M. Dekker: New York, 1996.
- Blomberg, S.; Ostberg, S.; Harth, E.; Bosman, A. W.; Van Horn, B.; Hawker, C. J. "Production of Crosslinked, Hollow Nanoparticles by Surface-Initiated Living Free-Radical Polymerization", *J. Polym. Sci., Part A: Polym. Chem.* **2002**, *40*, 1309–1320.
- Bubb, W. A.; Sternhell, S. "Proton Nmr-Spectra of 1-Substituted Benzocyclobutenes (Bicyclo[4,2,0]Octa-1,3,5-Trienes)", *Aust. J. Chem.* **1976**, *29*, 1685–1697.
- Buffeteau, T.; Desbat, B.; Turllet, J. M. "Polarization modulation FT-IR spectroscopy of surfaces and ultra-thin films: experimental procedure and quantitative analysis", *Appl. Spectrosc.* **1991**, *45*, 380–389.
- Burdeaux, D.; Townsend, P.; Carr, J.; Garrou, P. "Benzocyclobutene (Bcb) Dielectrics for the Fabrication of High-Density, Thin-Film Multichip Modules", *J. Electron. Mater.* **1990**, *19*, 1357–1364.
- Burger, C.; Ruland, W.; Semenov, A. N. "Polydispersity Effects on the Microphase-Separation Transition in Block Copolymers", *Macromolecules* **1990**, *23*, 3339–3346.
- Burger, C.; Ruland, W.; Semenov, A. N. "Corrections to 1990 paper", *Macromolecules* **1991**, *24*, 816.
- Caillol, S.; Lecommandoux, S.; Mingotaud, A.-F.; Schappacher, M.; Soum, A.; Meyrueix, R. "Synthesis and Self-Assembly Properties of Peptide-Poly lactide Block Copolymers", *Macromolecules* **2003**, *36*, 1118–1124.
- Cartwright, D.; Lee, V. J.; Rinehart, K. L. "3-Acyl tetramic acids. 7. Synthesis of 3-Acyl Tetramic Acids Via Aspartamide Rearrangement", *J. Am. Chem. Soc.* **1978**, *100*, 4237–4239.
- Cavicchi, K. A.; Zalusky, A. S.; Hillmyer, M. A.; Lodge, T. P. "An Ordered Nanoporous Monolith from an Elastomeric Crosslinked Block Copolymer Precursor", *Macromol. Rapid Commun.* **2004**, *25*, 704–709.
- Chatterjee, N.; Basu, S.; Palit, S. K.; Maiti, M. M. "An XRD Characterization of the Thermal Degradation of Polyacrylonitrile", *J. Polym. Sci., Part B: Polym. Phys.* **1995**, *33*, 1705–1712.
- Chen, J.-T.; Shin, K.; Leiston-Belanger, J. M.; Zhang, M.; Russell, T. P. "Amorphous Carbon Nanotubes with Tunable Properties via Template Wetting", *Adv. Mater.* **2006**, *in press*.

- Chung, T. C.; Schlesinger, Y.; Etemad, S.; Macdiarmid, A. G.; Heeger, A. J. "Optical Studies of Pyrolyzed Polyacrylonitrile", *J. Polym. Sci., Part B: Polym. Phys.* **1984**, *22*, 1239–1246.
- Claes, P.; Smets, G. "Anionic Polymerization initiated by Sodium Naphthalene and Synthesis of Block Copolymers", *Makromol. Chem.* **1961**, *44*, 212–220.
- Connor, E. F.; Nyce, G. W.; Myers, M.; Mock, A.; Hedrick, J. L. "First Example of N-Heterocyclic Carbenes as Catalysts for Living Polymerization: Organocatalytic Ring-Opening Polymerization of Cyclic Esters", *J. Am. Chem. Soc.* **2002**, *124*, 914–915.
- Dechy-Cabaret, O.; Martin-Vaca, B.; Bourissou, D. "Controlled ring-opening polymerization of lactide and glycolide", *Chem. Rev.* **2004**, *104*, 6147–6176.
- Djuric, S.; Venit, J.; Magnus, P. "Silicon in Synthesis: Stabase Adducts- A New Primary Amine Protecting Group: Alkylation of Ethyl Glycinate", *Tet. Lett.* **1981**, *22*, 1787–1790.
- Drockenmuller, E.; Li, L. Y. T.; Ryu, D. Y.; Harth, E.; Russell, T. P.; Kim, H. C.; Hawker, C. J. "Covalent Stabilization of Nanostructures: Robust Block Copolymer Templates from Novel Thermoreactive Systems", *J. Polym. Sci., Part A: Polym. Chem.* **2005**, *43*, 1028–1037.
- Dubois, P.; Jerome, R.; Teyssie, P. "Aluminum Alkoxides - a Family of Versatile Initiators for the Ring-Opening Polymerization of Lactones and Lactides", *Makromol. Chem., Macromol. Symp.* **1991**, *42-3*, 103–116.
- Dunn, P.; Ennis, B. C. "Thermal Analysis of Polyacrylonitrile. Part I. The Melting of Polyacrylonitrile", *J. Appl. Polym. Sci.* **1970**, *14*, 1795–1798.
- Durr, H.; Nickels, H.; Pacala, L. A.; Jones, M. "Benzocyclobutenylidene-Cycloadditions, Reactivity, and Multiplicity", *J. Org. Chem.* **1980**, *45*, 973–980.
- Edwards, E. W.; Montague, M. F.; Solak, H. H.; Hawker, C. J.; Nealey, P. F. "Precise control over molecular dimensions of block-copolymer domains using the interfacial energy of chemically nanopatterned substrates", *Adv. Mater.* **2004**, *16*, 1315.
- Endo, T.; Koizumi, T.; Takata, T.; Chino, K. "Synthesis of Poly(4-vinylbenzocyclobutene) and Its Reaction with Dienophiles", *J. Polym. Sci., Part A: Polym. Chem.* **1995**, *33*, 707–715.
- Fetters, L. J. "Synthesis of Block Copolymers by Homogeneous Anionic Polymerization", *J. Polym. Sci., Part C* **1969**, *26*, 1–35.

- Fitzer, E.; Muller, D. J. "Formation of Angled Ladder Structure in Polyacrylic Nitrile Fibers", *Makromol. Chem.* **1971**, *144*, 117.
- Flory, P. J. "Statistical Mechanics of Swelling of Network Structures", *J. Chem. Phys.* **1950**, *18*, 108.
- Flory, P. J. *Principles of Polymer Chemistry*; Cornell University Press: Ithaca, NY, 1953.
- Flory, P. J.; Rehner, J. R. "Statistical Mechanics of Cross-Linked Polymer Networks II. Swelling", *J. Chem. Phys.* **1943**, *11*, 521.
- Frick, E. M.; Zalusky, A. S.; Hillmyer, M. A. "Characterization of Poly(lactide)-b-Poly(isoprene)-b-Poly(lactide) Thermoplastic Elastomers", *Biomacromolecules* **2003**, *4*, 216–223.
- Goldbach, J. T. *Synthesis, Characterization and Thin Film Morphology of Poly(Styrene-block-Methyl Methacrylate) Containing UV Photolabile Junction Points*. Ph.D. Dissertation, University of Massachusetts Amherst, MA, 2004.
- Gonzalez-Leon, J. A.; Mayes, A. M. "Phase behavior of Ternary Polymer Mixtures", *Macromolecules* **2003**, *36*, 2508–2515.
- Gordon, A. J.; Ford, R. A. *The Chemist's Companion: A Handbook of Practical Data, Techniques and References*; John Wiley and Sons: New York, 1972.
- Gravert, D. J.; Janda, K. D. "Bifunctional Initiators for Free Radical Polymerization of Non-Crosslinked Block Copolymers", *Tet. Lett.* **1998**, *39*, 1513–1516.
- Greenler, R. G. "Infrared Study of Adsorbed Molecules on Metal Surfaces by Reflection Techniques", *J. Chem. Phys.* **1966**, *44*, 310–315.
- Guarini, K. W.; Black, C. T.; Zhang, Y.; Kim, H.; Sikorski, E. M.; Babich, I. V. "Process Integration of Self-Assembled Polymer Templates into Silicon Nanofabrication", *J. Vac. Sci. Technol., B* **2002**, *20*, 2788–2792.
- Gupta, V. K.; Krishnamoorti, R.; Chen, Z.-R.; Kornfield, J. A.; Smith, S. D.; Satkowski, M. M.; Grothaus, J. T. "Dynamics of Shear Alignment in a Lamellar Diblock Copolymer: Interplay of Frequency, Strain Amplitude and Temperature", *Macromolecules* **1996**, *29*, 875–884.
- Hadjichristidis, N.; Iatrou, H.; Pispas, S.; Pitsikalis, M. "Anionic Polymerization: High Vacuum Techniques", *J. Polym. Sci., Part A: Polym. Chem.* **2000**, *38*, 3211–3234.

- Hakem, I. F.; Lal, J. "Polyelectrolyte-like Behaviour of Poly(Ethylene-oxide) Solutions with Added Monovalent Salt", *Europhys. Lett.* **2003**, *64*, 204–210.
- Hakem, I.-F.; Lal, J. "Evidence of Solvent-Dependent Complexation in Non-ionic Polymer-salt Systems", *Appl. Phys.* **2002**, *A74*, S531–S533.
- Ham, G. E. *Copolymerization: High Polymers: Chapter IX*; Interscience Publishers: New York, 1964.
- Hansen, C. M. *Hansen Solubility Parameters: A User's Handbook*; CRC Press: Boca Raton, Fla., 2000.
- Hansen, M. S.; Vigild, M. E.; Berg, R. H.; Ndoni, S. "Nanoporous Crosslinked Polyisoprene from polyisoprene - Polydimethylsiloxane Block Copolymer", *Polym. Bull.* **2004**, *51*, 403–409.
- Harth, E.; Van Horn, B.; Lee, V. Y.; Germack, D. S.; Gonzales, C. P.; Miller, R. D.; Hawker, C. J. "A Facile Approach to Architecturally Defined Nanoparticles via Intermolecular Chain Collapse", *J. Am. Chem. Soc.* **2002**, *124*, 8653–8660.
- Hawker, C. J.; Barclay, G. G.; Orellana, A.; Dao, J.; Devonport, W. "Initiating Systems for Nitroxide-Mediated "Living" Free Radical Polymerizations: Synthesis and Evaluation", *Macromolecules* **1996**, *29*, 5245–5254.
- Hawker, C. J.; Elce, E.; Dao, J.; Volksen, W.; Russell, T. P.; Barclay, G. G. "Well-Defined Random Copolymers by a "Living" Free-Radical Polymerization Process", *Macromolecules* **1996**, *29*, 2686–2688.
- Hawker, C. J.; Hedrick, J. L.; Malmstrom, E. E.; Trollsas, M.; Mecerreyes, D.; Moineau, G.; Dubois, P.; Jerome, R. "Dual Living Free Radical and Ring Opening Polymerizations from a Double-Headed Initiator", *Macromolecules* **1998**, *31*, 213–219.
- Hawker, C. J.; Hedrick, J. L.; Miller, R. D.; Volksen, W. *U.S. Patent # US Patent 20010040294*, **2001**.
- Hawker, C. J.; Russell, T. P. "Block Copolymer Lithography- Merging "Bottom-Up" with "Top-down" processes", *MRS Bulletin* **2005**, *30*, 952–966.
- Henrici-Olive, G.; Olive, S. "The Chemistry of Carbon Fiber Formation from Polyacrylonitrile", *Adv. Polym. Sci.* **1983**, *51*, 1–60.
- Hsieh, H. L.; Quirk, R. P. *Anionic Polymerization: Principles and Practical Applications*; Marcel Dekker, Inc.: New York, 1996.

- Hua, F. J.; Chen, S. M.; Lee, D. S.; Yang, Y. L. "Nitroxide-Controlled Free Radical Copolymerization of Styrene and Acrylonitrile Monitored by Electron Spin Resonance and Fourier Transform Infrared Technique in situ", *Appl. Magn. Reson.* **2001**, *21*, 49–62.
- Huang, J.; Huang, X.; Hu, W.; Lou, W. "Block Copolymerization of Ethylene Oxide and Acrylonitrile and the Influence of Block length of Polyacrylonitrile on the Thermal Behavior and Morphology of Block Copolymer", *J. Polym. Sci., Part A: Polym. Chem.* **1996**, *34*, 1317–1324.
- Huggins, M. L. "Solutions of Long Chain Compounds", *J. Chem. Phys.* **1941**, *9*, 440.
- Hulteen, J. C.; Chen, H. X.; Chambliss, C. K.; Martin, C. R. "Template Synthesis of Carbon Nanotubule and Nanofiber Arrays", *Nanostruct. Mater.* **1997**, *9*, 133–136.
- Jamshidi, K.; Hyon, S.-H.; Ikada, Y. "Thermal Characterization of Polylactides", *Polymer* **1988**, *29*, 2229–2234.
- Jenkins, A. D. "Acrylonitrile Block and Graft Copolymers", *Pure Appl. Chem.* **1976**, *46*, 45–48.
- Johnson, R. W.; Phillips, T. L.; Weidner, W. K.; Hahn, S. F.; Burdeaux, D. C.; Townsend, P. H. "Benzocyclobutene Interlayer Dielectrics for Thin-Film Multichip Modules", *IEEE Trans. Compon. Hyb.* **1990**, *13*, 347–352.
- Jones, M.; Levin, R. H. "Stereochemistry of 2+2 and 2+4 Cycloadditions of Benzyne", *J. Am. Chem. Soc.* **1969**, *91*, 6411.
- Kim, S. H.; Misner, M. J.; Xu, T.; Kimura, M.; Russell, T. P. "Highly Oriented and Ordered Arrays from Block Copolymers via Solvent Evaporation", *Adv. Mater.* **2004**, *16*, 226–231.
- Kimura, M.; Misner, M. J.; Xu, T.; Kim, S. H.; Russell, T. P. "Long-Range Ordering of Diblock Copolymers Induced by Droplet Pinning", *Langmuir* **2003**, *19*, 9910–9913.
- Kobatake, S.; Harwood, H. J.; Quirk, R. P.; Priddy, D. B. "Synthesis of Nitroxide-Functionalized Polybutadiene Using Halogen-Containing Benzyloxyamine as Terminators for Anionic Polymerization", *Macromolecules* **1999**, *32*, 10–13.
- Kolesnikov, G. S.; Yaralov, L. K. "Synthesis of Block Copolymers of Polystyrene and Polyacrylonitrile", *Vysokomol. Soedin.* **1966**, *8*, 2018–2023.

- Kowalewski, T.; McCullough, R. D.; Matyjaszewski, K. "Complex Nanostructured Materials from Segmented Copolymers Prepared by ATRP", *Eur. Phys. J., Sect. E* **2003**, *10*, 5–16.
- Kowalewski, T.; Tsarevsky, N. V.; Matyjaszewski, K. "Nanostructured Carbon Arrays from Block Copolymers of Polyacrylonitrile", *J. Am. Chem. Soc.* **2002**, *124*, 10632–10633.
- Kowalski, A.; Duda, A.; Penczek, S. "Kinetics and Mechanism of Cyclic Esters Polymerization Initiated with Tin (II) Octoate. 3. Polymerization of L,L-Dilactide", *Macromolecules* **2000**, *33*, 7359–7370.
- Kowalski, A.; Duda, A.; Penczek, S. "Mechanism of Cyclic Ester Polymerization Initiated with Tin (II) Octoate. 2. Macromolecules Fitted with Tin (II) Alkoxide Species Observed Directly in MALDI-TOF Spectra", *Macromolecules* **2000**, *33*, 689–695.
- Kressler, J.; Rudolf, B. "Cyclization Reaction of Polyacrylonitrile and Poly(Styrene-co-Acrylonitrile) Studied by PVT Measurements", *Macromol. Rapid Commun.* **1995**, *16*, 631–636.
- Krevelen, D. W. v. In *Properties of Polymers: Their Correlation with Chemical Structure, Their Numerical Estimation and Prediction from Additive Group Contributions*; Elsevier: Amsterdam, N.Y., 1990; p 875.
- Kricheldorf, H. R.; Kreiseraunders, I.; Boettcher, C. "Polylactones .31. Sn(II)Octoate-Initiated Polymerization of L-Lactide - a Mechanistic Study", *Polymer* **1995**, *36*, 1253–1259.
- Krishnamoorti, R.; Graessley, W. W.; Dee, G. T.; Walsh, D. J.; Fetters, L. J.; Lohse, D. J. "Pure Component Properties and Mixing Behavior in Polyolefin Blends", *Macromolecules* **1996**, *29*, 367–376.
- Labadie, J. W.; Stille, J. K. "Mechanisms of the Palladium-Catalyzed Couplings of Acid-Chlorides with Organotin Reagents", *J. Am. Chem. Soc.* **1983**, *105*, 6129–6137.
- Lammertink, R. G. H.; Hempenius, M. A.; van den Enk, J. E.; Chan, V. Z. H.; Thomas, E. L.; Vancso, G. J. "Nanostructured thin films of organic-organometallic block copolymers: One-step lithography with poly(ferrocenylsilanes) by reactive ion etching", *Adv. Mater.* **2000**, *12*, 98–103.
- Lazzari, M.; Chiantore, O.; Mendichi, R.; Lopez-Quintela, M. A. "Synthesis of Polyacrylonitrile-*block*-Polystyrene Copolymers by Atom Transfer Radical Polymerization", *Macromol. Chem. Phys.* **2005**, *206*, 1382–1388.

- Lazzari, M.; Lopez-Quintela, M. A. "Block copolymers as a Tool for Nanomaterial Fabrication", *Adv. Mater.* **2003**, *15*, 1583–1594.
- Lee, S.-H.; Kim, S. H.; Han, Y.-K.; Kim, Y. H. "Synthesis and Degradation of End-Group-Functionalized Polylactide", *J. Polym. Sci., Part A: Polym. Chem.* **2001**, *39*, 973–985.
- Leibler, L. "Theory of Microphase Separation in Block Copolymers", *Macromolecules* **1980**, *13*, 1602–1617.
- Leiston-Belanger, J. M.; Penelle, J.; Russell, T. P. "Synthesis and Microphase Separation Behavior of Poly(Styrene-*b*-Acrylonitrile) Prepared by Sequential Anionic and ATRP Techniques", *Macromolecules* **2006**, *39*, 1766–1770.
- Leiston-Belanger, J. M.; Russell, T. P.; Drockenmuller, E.; Hawker, C. J. "A Thermal and Manufacturable Approach to Stabilized Diblock Copolymer Templates", *Macromolecules* **2005**, *38*, 7676–7683.
- Li, M.; Douki, K.; Goto, K.; Li, X.; Coenjarts, C.; Smilgies, D. M.; Ober, C. K. "Spatially Controlled Fabrication of Nanoporous Block Copolymers", *Chem. Mater.* **2004**, *16*, 3800–3808.
- Li, W.; Wickham, R. A.; Garbary, R. A. "Phase Diagram for a Diblock Copolymer Melt under Cylindrical Confinement", *Macromolecules* **2006**, *39*, 806–811.
- Liang, C. D.; Hong, K. L.; Guiochon, G. A.; Mays, J. W.; Dai, S. "Synthesis of a Large-Scale Highly Ordered Porous Carbon Film by Self-Assembly of Block Copolymers", *Angew. Chem., Int. Ed.* **2004**, *43*, 5785–5789.
- Linnemayr, K.; Vana, P.; Allmaier, G. "Time-Delayed Extraction Matrix-Assisted Laser Desorption/Ionization Time-of-Flight Mass Spectrometry of Polyacrylonitrile and Other Synthetic Polymers with the Matrix 4-Hydroxybenzylidene Malononitrile", *Rapid Comm. Mass. Spec.* **1998**, *12*, 1344–1350.
- Lloyd, J. B. F.; Ongley, P. A. "Electrophilic Substitution of Benzocyclobutene .2. Benzoylation Sulphonation Bromination and Chlorination", *Tetrahedron* **1965**, *21*, 245.
- Lopes, W. A.; Jaeger, H. M. "Hierarchical Self-Assembly of Metal Nanostructures on Diblock Copolymer Scaffolds", *Nature* **2001**, *414*, 735–738.
- Lynd, N. A.; Hillmyer, M. A. "Influence of Polydispersity on the Self-Assembly of Diblock Copolymers", *Macromolecules* **2005**, *38*, 8803–8810.
- Mailhot, B.; Gardette, J.-L. "Mechanism of Poly(Styrene-co-Acrylonitrile) Photooxidation", *Polym. Deg. Stab.* **1994**, *44*, 237–247.



- Malmstrom, E.; Miller, R. D.; Hawker, C. J. "Development of a New Class of Rate-Accelerating Additives for Nitroxide-Mediated 'Living' Free Radical Polymerization", *Tetrahedron* **1997**, *53*, 15225–15236.
- Malz, H.; Komber, H.; Voigt, D.; Pionteck, J. "Reactions for the Selective Elimination of TEMPO End Groups in Polystyrene", *Macromol. Chem. Phys.* **1998**, *199*, 583–588.
- Mansky, P.; DeRouchey, J.; Russell, T. P. "Large-area Domain Alignment in Block Copolymer Thin Films Using Electric Fields", *Macromolecules* **1998**, *31*, 4399–4401.
- Mansky, P.; Liu, Y.; Huang, E.; Russell, T. P.; Hawker, C. "Controlling Polymer-Surface Interactions with Random Copolymer Brushes", *Science* **1997**, *275*, 1458–1460.
- Mark, J. E. *Polymer Data Handbook*; Oxford University Press: New York, 1999.
- Matsen, M. W.; Bates, F. S. "Unifying Weak- and Strong-Segregation Block Copolymer Theories", *Macromolecules* **1996**, *29*, 1091–1098.
- Matsen, M. W.; Bates, F. S. "Origins of Complex Self-Assembly in Block Copolymers", *Macromolecules* **1996**, *29*, 7641–7644.
- Matsushita, Y.; Noro, A.; Iinuma, M.; Suzuki, J.; Ohtani, H.; Takano, A. "Effect of Composition Distribution on Microphase-Separated Structure from Diblock Copolymers", *Macromolecules* **2003**, *36*, 8074–8077.
- Matyjaszewski, K.; Mu Jo, S.; Paik, H. J.; Gaynor, S. G. "Synthesis of Well-Defined Polyacrylonitrile by Atom Transfer Radical Polymerization", *Macromolecules* **1997**, *30*, 6398–6400.
- Matyjaszewski, K.; Mu Jo, S.; Paik, H. J.; Shipp, D. A. "An Investigation into the CuX/2,2'-bipyridine (X=Br or Cl) Mediated Atom Transfer Radical Polymerization of Acrylonitrile", *Macromolecules* **1999**, *32*, 6431–6438.
- Matyjaszewski, K.; Patten, T. E.; Xia, J. "Controlled/"Living" Radical Polymerization. Kinetics of the Homogenous Atom Transfer Radical Polymerization of Styrene", *J. Am. Chem. Soc.* **1997**, *119*, 674–680.
- Matyjaszewski, K.; Xia, J. "Atom Transfer Radical Polymerization", *Chem. Rev.* **2001**, *101*, 2921–2990.

- McKean, D. R.; Parrinello, G.; Renaldo, A. F.; Stille, J. K. "Synthesis of Functionalized Styrenes Via Palladium-Catalyzed Coupling of Aryl Bromides with Vinyl Tin Reagents", *J. Org. Chem.* **1987**, *52*, 422–424.
- Minagawa, M.; Onuma, H.; Ogita, T.; Uchida, H. "Pyrolysis Gas Chromatographic Analysis of Polyacrylonitrile", *J. Appl. Polym. Sci.* **2000**, *79*, 473–478.
- Monahan, A. R. "Thermal Degradation of Polyacrylonitrile in the Temperature Range 280- 450°C", *J. Polym. Sci., Part A-1* **1966**, *4*, 2391–2399.
- Morkved, T. L.; Lu, M.; Urbas, A. M.; Ehrichs, E. E.; Jaeger, H. M.; Mansky, P.; Russell, T. P. "Local Control of Microdomain Orientation in Diblock Copolymer Thin Films with Electric Fields", *Science* **1996**, *273*, 931–933.
- Morton, M. *Anionic Polymerization: Principles and Practice*; Academic Press: New York, 1993.
- Mu Jo, S.; Gaynor, S. G.; Matyjaszewski, K. "Homo- and ABA Block polymerization of Acrylonitrile, n-butyl acrylate and 2-ethylhexyl acrylate using ATRP", *Polym. Prepr. (Am. Chem. Soc., Div. Polym. Chem.)* **1996**, *37*, 272–273.
- Muralidharan, V.; Hui, C. Y. "Stability of Nanoporous Materials", *Macromol. Rapid Commun.* **2004**, *25*, 1487–1490.
- Nederberg, F.; Connor, E. F.; Moller, M.; Glauser, T.; Hedrick, J. L. "New Paradigms for Organic Catalysts: The First Organocatalytic Living Polymerization", *Angew. Chem., Int. Ed.* **2001**, *40*, 2712–2715.
- Noro, A.; Cho, D.; Takano, A.; Matsushita, Y. "Effect of Molecular Weight Distribution on Microphase-Separated Structures from Block Copolymers", *Macromolecules* **2005**, *38*, 4371–4376.
- Nyce, G. W.; Glauser, T.; Connor, E. F.; Mock, A.; Waymouth, R. M.; Hedrick, J. L. "In Situ Generation of Carbenes: A General and Versatile Platform for Organocatalytic Living Polymerization", *J. Am. Chem. Soc.* **2003**, *125*, 3046–3056.
- Ohba, K. "Overview of Photo-definable Benzocyclobutene Polymer", *J. Photopolym. Sci. Technol.* **2002**, *15*, 177–182.
- Olayo-Valles, R.; Lund, M. S.; Leighton, C.; Hillmyer, M. A. "Large Area Nanolithographic Templates by Selective Etching of Chemically Stained Block Copolymer Thin Films", *J. Mater. Chem.* **2004**, *14*, 2729–2731.
- Ono, H.; Hisatani, K.; Kamide, K. "NMR Spectroscopic Study of Side Reactions in Anionic Polymerization of Acrylonitrile", *Polym. J.* **1993**, *25*, 245–265.

- Overberger, C. G.; Moore, J. A. "Ladder Polymers", *Adv. Polym. Sci.* **1970**, *7*, 113–150.
- Pantazis, D.; Chalari, I.; Hadjichristidis, N. "Anionic Polymerization of Styrenic Macromonomers", *Macromolecules* **2003**, *36*, 3783–3785.
- Park, M.; Harrison, C.; Chaikin, P. M.; Register, R. A.; Adamson, D. H. "Block Copolymer Lithography: Periodic Arrays of ~10(11) Holes in 1 Square Centimeter", *Science* **1997**, *276*, 1401–1404.
- Parthasarathy, R. V.; Phani, K. L. N.; Martin, C. R. "Template Synthesis of Graphitic Nanotubules", *Adv. Mater.* **1995**, *7*, 896–897.
- Patten, T. E.; Matyjaszewski, K. "Atom Transfer Radical Polymerization and the Synthesis of Polymeric Materials", *Adv. Mater.* **1998**, *10*, 901–915.
- Perry, E. "Block Copolymers of Styrene and Acrylonitrile", *J. Appl. Polym. Sci.* **1964**, *8*, 2605–2618.
- Podesva, J.; Doskocilova, D. "1H NMR Study of Random and Alternating Styrene/n-Alkyl Methacrylate Copolymers", *Makromol. Chem.* **1977**, *178*, 2383–2392.
- Polavarapu, P. L. *Principles and Applications of Polarization Division Interferometry*; John Wiley and Sons Ltd.: West Sussex, England, 1998.
- Priddy, D. B. "Thermal Discoloration Chemistry of Styrene-co-Acrylonitrile", *Adv. Polym. Sci.* **1995**, *121*, 124–154.
- Qiu, J.; Charleux, B.; Matyjaszewski, K. "Controlled/living Radical Polymerization in Aqueous Media: Homogeneous and Heterogeneous Systems", *Prog. Polym. Sci.* **2001**, *26*, 2083–2134.
- Quirk, R. P. *Comprehensive Polymer Science, 1st Suppl.*; Pergamon, 1992.
- Quirk, R. P.; Lee, B. "Experimental Criteria for Living Polymerizations", *Polym. Int.* **1992**, *27*, 359–367.
- Reich, L.; Stivala, S. S. *Elements of Polymer Degradation*; McGraw-Hill Book Co.: New York, 1971.
- Rodlert, M.; Harth, E.; Rees, I.; Hawker, C. J. "End-Group Fidelity in Nitroxide-Mediated Living Free-Radical Polymerizations", *J. Polym. Sci., Part A: Polym. Chem.* **2000**, *38*, 4749–4763.

- Rolfes, J.; Andersson, J. T. "Determination of Trace Amounts of Alcohols and Phenols in Complex Mixtures as Ferrocenecarboxylic Acid Esters With Gas Chromatography-Atomic Emission Detection", *Anal. Comm.* **1996**, *33*, 429–432.
- Ruzette, A. V. G.; Banerjee, P.; Mayes, A. M.; Russell, T. P. "A Simple Model for Baroplastic Behavior in Block Copolymer Melts", *J. Chem. Phys.* **2001**, *114*, 8205–8209.
- Ruzette, A. V. G.; Mayes, A. M. "Simple Free Energy Model for Weakly Interacting Polymer Blends", *Macromolecules* **2001**, *34*, 1894–1907.
- Ryu, D. Y.; Shin, K.; Drockenmuller, E.; Hawker, C. J.; Russell, T. P. "A Generalized Approach to the Modification of Solid Surfaces", *Science* **2005**, *308*, 236–239.
- Rzayev, J.; Hillmyer, M. A. "Nanoporous Polystyrene Containing Hydrophilic Pores from an ABC Triblock Copolymer Precursor", *Macromolecules* **2005**, *38*, 3–5.
- Sadana, A. K.; Saini, R. K.; Billups, W. E. "Cyclobutarenes and Related Compounds", *Chem. Rev.* **2003**, *103*, 1539–1602.
- Sanchez-Soto, P. J.; Aviles, M. A.; del Rio, J. C.; Gines, J. M.; Perez-Rodriguez, J. L. "Thermal Stability of the Effect of Several Solvents on Polymerization of Acrylonitrile and their Subsequent Pyrolysis", *J. Anal. Apply. Phys.* **2001**, *58-59*, 155–172.
- Schellekens, M. A. J.; de Wit, F.; Klumperman, B. "Effect of the Copper Counterion on the Activation Rate Parameter in Atom Transfer Radical Polymerization", *Macromolecules* **2001**, *34*, 7961–7966.
- Schiess, P.; Heitzmann, M.; Rutschmann, S.; Staeheli, R. "Preparation of Benzocyclobutenes by Flash Vacuum Pyrolysis", *Tet. Lett.* **1978**, *46*, 4569–4572.
- Schmidt, S. C.; Hillmyer, M. A. "Synthesis and Characterization of Model Polyisoprene-Polylactide Diblock Copolymers", *Macromolecules*, *32*, 4794–4801.
- Segalman, R. A.; Hexemer, A.; Kramer, E. J. "Effects of Lateral Confinement on order in Spherical Domain Block Copolymer Thin Films", *Macromolecules* **2003**, *36*, 6831–6839.
- Semsarzadeh, M. A.; Molaei, A. "Thermal Reactions and Analysis of Polyacrylonitrile Films", *Iran. Polym. J.* **1997**, *6*, 113–119.
- Sheffy, F. K.; Godschalx, J. P.; Stille, J. K. "Palladium-Catalyzed Cross Coupling of Allyl Halides with Organotin Reagents - a Method of Joining Highly

- Functionalized Partners Regioselectively and Stereospecifically", *J. Am. Chem. Soc.* **1984**, *106*, 4833–4840.
- Shin, K.; Leach, K. A.; Goldbach, J. T.; Kim, D. H.; Jho, J.-Y.; Tuominen, M.; Hawker, C. J.; Russell, T. P. "A Simple Route to Metal Nanodots and Nanoporous Metal Films", *Nano Lett.* **2002**, *2*, 933–936.
- Shin, K.; Xiang, H.; Moon, S.; Kim, T.; McCarthy, T. J.; Russell, T. P. "Curving and Frustrating Flatland", *Science* **2004**, *306*, 76.
- Shriner, R. L.; Hermann, C. K. F.; Morrill, T. C.; Curtin, D. Y.; Fuson, R. C. *The Systematic Identification of Organic Compounds: 7th ed.*; John Wiley and Sons, Inc.: New York, 1998.
- Solomon, D. H.; Rizzardo, E.; Cacioli, P. *U.S. Patent # 4581429*, **1986**.
- Stoykovich, M. P.; Muller, M.; Kim, S. O.; Solak, H. H.; Edwards, E. W.; de Pablo, J. J.; Nealey, P. F. "Directed Assembly of Block Copolymer Blends into Nonregular Device-Oriented Structures", *Science* **2005**, *308*, 1442–1446.
- Studer, A.; Harms, K.; Knoop, C.; Muller, C.; Schulte, T. "New Sterically Hindered Nitroxides for the Living Free Radical Polymerization: X-ray Structure of an alpha-H-bearing Nitroxide", *Macromolecules* **2004**, *37*, 27–34.
- Sui, K. Y.; Gu, L. X. "Preparation and Characterization of Amphiphilic Block Copolymer of Polyacrylonitrile-block-Poly(ethylene oxide)", *J. Appl. Polym. Sci.* **2003**, *89*, 1753–1759.
- Surianarayanan, M.; Vijayaraghavan, R.; Raghavan, K. V. "Spectroscopic Investigations of Polyacrylonitrile Thermal Degradation", *J. Polym. Sci., Part A: Polym. Chem.* **1998**, *36*, 2503–2512.
- Szwarc, M. "Living Polymers", *Nature* **1956**, *178*, 1168–1169.
- Szwarc, M.; Levy, M.; Milkovich, R. "Polymerization Initiated by Electron Transfer to Monomer. A New Method of Formation of Block Polymers", *J. Am. Chem. Soc.* **1956**, *78*, 2656–2657.
- Tan, L. S.; Arnold, F. E. "Benzocyclobutene in Polymer Synthesis .1. Homopolymerization of Bisbenzocyclobutene Aromatic Imides to Form High-Temperature Resistant Thermosetting Resins", *J. Polym. Sci., Part A: Polym. Chem.* **1988**, *26*, 1819–1834.
- Tan, L. S.; Venkatasubramanian, N.; Mather, P. T.; Houtz, M. D.; Benner, C. L. "Synthesis and Thermal Properties of Thermosetting Bis-benzocyclobutene-

- terminated Arylene Ether Monomers", *J. Polym. Sci., Part A: Polym. Chem.* **1998**, *36*, 2637–2651.
- Tang, C.; Kowalewski, T.; Matyjaszewski, K. "Preparation of Polyacrylonitrile-*block*-poly(*n*-butyl acrylate) Copolymers Using Atom Transfer Free Radical Polymerization and Nitroxide mediated Polymerization Processes", *Macromolecules* **2003**, *36*, 1465–1473.
- Tang, C.; Kowalewski, T.; Matyjaszewski, K. "RAFT Polymerization of Acrylonitrile and Preparation of Block Copolymers Using 2-Cyanoethyl Dithiobenzoate as the Transfer Agent", *Macromolecules* **2003**, *36*, 8587–8539.
- Tao, L.; Luan, B.; Pan, C.-Y. "Block and Star Block Copolymers by Mechanism Transformation. VIII Synthesis and Characterization of Triblock Poly(LLA-*b*-St-*b*-MMA) by Combination of ATRP and ROP", *Polymer* **2003**, *44*, 1013–1020.
- Thurn-Albrecht, T.; DeRouchey, J.; Russell, T. P. "Overcoming Interfacial Interactions with Electric Fields", *Macromolecules* **2000**, *33*, 3250–3253.
- Thurn-Albrecht, T.; Schotter, J.; Kastle, G. A.; Emley, N.; Shibauchi, T.; Krusin-Elbaum, L.; Guarini, K.; Black, C. T.; Tuominen, M. T.; Russell, T. P. "Ultrahigh-Density Nanowire Arrays Grown in Self-Assembled Diblock Copolymer Templates", *Science* **2000**, *290*, 2126–2129.
- Todorov, N. G.; Valkov, E. N.; Stoyanova, M. G. "Chemical Modification of Poly(acrylonitrile) with Amines", *J. Polym. Sci., Part A: Polym. Chem.* **1996**, *34*, 863–868.
- Tolstoy, V. P.; Chernyshova, I. V.; Skryshevsky, V. A. *Handbook of Infrared Spectroscopy of Ultrathin Films*; John Wiley and Sons, Inc.: Hoboken, N.J., 2003.
- Toomey, R.; Freidank, D.; Ruhe, J. "Swelling Behavior of Thin, Surface-Attached Polymer Networks", *Macromolecules* **2004**, *37*, 882–887.
- Trent, J. S.; Scheinbeim, J. I.; Couchman, P. R. "Ruthenium Tetraoxide Staining of Polymers for Electron Microscopy", *Macromolecules* **1983**, *16*, 589–598.
- Tsarevsky, N. V.; Sarbu, T.; Gobelt, B.; Matyjaszewski, K. "Synthesis of Styrene-Acrylonitrile Copolymers and Related Block Copolymers by Atom Transfer Radical Polymerization", *Macromolecules* **2002**, *35*, 6142–6148.
- Tsori, Y.; Tournilhac, F.; Andelman, D.; Leibler, L. "Structural Changes in Block Copolymers: Coupling of Electric Field and Mobile Ions", *Phys. Rev. Lett.* **2003**, *90*, 145504.145501–145504.145504.

- Tsori, Y.; Tournilhac, F.; Leibler, L. "Orienting Ion-Containing Block Copolymers Using Ac Electric Fields", *Macromolecules* **2003**, *36*, 5873–5877.
- Tsuji, H.; Nakahara, K. "Poly(L-lactide). IX. Hydrolysis in Acid Media", *J. Appl. Polym. Sci.* **2002**, *86*, 186–194.
- Tung, L. H. "Mathematical Methods of Correcting Instrumental Spreading in GPC", *Sep. Sci.* **1970**, *5*, 429–436.
- Tung, L. H. "Data Treatment in GPC", *Sep. Sci.* **1970**, *5*, 339–347.
- Ueda, K.; Hirao, A.; Nakahara, S. "Synthesis of Polymers with Amino End Groups. 3. Reactions of Anionic Living Polymers with  $\alpha$ -Halo- $\omega$ -Aminoalkanes with a Protected Amino Functionality", *Macromolecules* **1990**, *23*, 939–945.
- Van Krevelen, D. W.; Hoftyzer, P. J. *Properties of Polymers: Correlation with Chemical Structure*; Elsevier: New York, 1972.
- Veregin, R. P.; Michael, G. K.; Kazmaier, P. M.; Hamer, G. K. "Free Radical Polymerizations for Narrow Polydispersity Resins: Electron Spin Resonance Studies of the Kinetics and Mechanism", *Macromolecules* **1993**, *26*, 5316–5320.
- Wachter, U.; Morgenstern, U.; Berger, W.; Dreyer, R. "Investigation of the Anionic Initiated Block copolymerization of polar monomers", *Acta Polym.* **1991**, *42*, 300–304.
- Wang, J.; Xu, T.; Leiston-Belanger, J. M.; Gupta, S.; Russell, T. P. "Ion Complexation: A Route to Enhanced Block Copolymer Alignment with Electric Fields", *Phys. Rev. Lett.* **2006**, *96*, 128301/128301–128301/128304.
- Wang, J.-L.; Grimaud, T.; Matyjaszewski, K. "Kinetic Study of the Homogenous Atom Transfer Radical Polymerization of Methyl Methacrylate", *Macromolecules* **1997**, *30*, 6507–6512.
- Williams, C. K.; Breyfogle, L. E.; Choi, S. K.; Nam, W.; Young, V. G.; Hillmyer, M. A.; Tolman, W. B. "A Highly Active Zinc Catalyst for the Controlled Polymerization of Lactide", *J. Am. Chem. Soc.* **2003**, *125*, 11350–11359.
- Wolf, J. H.; Hillmyer, M. A. "Ordered Nanoporous Poly(cyclohexylethylene)", *Langmuir* **2003**, *19*, 6553–6560.
- Wu, C. R.; Liedberg, B. "Infrared Reflection-Absorption Spectroscopy of Polyacrylonitrile on Copper and Aluminum Surfaces", *J. Polym. Sci., Part B: Polym. Phys.* **1988**, *26*, 1127–1136.

- Wu, S. "Surface and Interfacial Tensions of Polymer Melts:II: Poly(methyl methacrylate), Poly(n-butyl methacrylate) and Polystyrene", *J. Phys. Chem.* **1970**, *74*, 632–638.
- Xiang, H.; Shin, K.; Kim, T.; Moon, S.; McCarthy, T. J.; Russell, T. P. "The Influence of Confinement and Curvature on the Morphology of Block Copolymers", *J. Polym. Sci., Part B: Polym. Phys.* **2005**, *43*, 3377–3383.
- Xiang, H.; Shin, K.; Kim, T.; Moon, S.; McCarthy, T. J.; Russell, T. P. "From Cylinders to Helices Upon Confinement", *Macromolecules* **2005**, *38*, 1055–1056.
- Xu, T. *Electric Field Alignment of Diblock Copolymer Thin Films*. Ph.D. Dissertation, University of Massachusetts Amherst, Amherst, 2004.
- Xu, T.; Goldbach, J. T.; Leiston-Belanger, J. M.; Russell, T. P. "Effect of Ionic Impurities on the Electric Field Alignment of Diblock Copolymer Thin Films", *Colloid Polym. Sci.* **2004**, *282*, 927–931.
- Xu, T.; Zhu, Y.; Gido, S. P.; Russell, T. P. "Electric Field Alignment of Symmetric Diblock Copolymer Thin Films", *Macromolecules* **2004**, *37*, 2625–2629.
- Xu, X.; Xiao, W.; Chen, K. "Morphology and Crystallinity of Particles formed from Dilute Solutions of Poly(vinyl alcohol-b-acrylonitrile), poly(vinyl alcohol) and polyacrylonitrile", *Eur. Polym. J.* **1994**, *30*, 1439–1442.
- Xue, T. J.; McKinney, M. A.; Wilkie, C. A. "The Thermal Degradation of Polyacrylonitrile", *Polym. Deg. Stab.* **1997**, *58*, 193–202.
- Yakimansky, A. V. "Mechanisms of Living Polymerization of Vinyl Monomers", *Polym. Sci. Series C* **2005**, *C47*, 1–49.
- Zalusky, A. S.; Olayo-Valles, R.; Wolf, J. H.; Hillmyer, M. A. "Ordered Nanoporous Polymers from Polystyrene-Polylactide Block Copolymers", *J. Am. Chem. Soc.* **2002**, *124*, 12761–12773.
- Zhu, S.; Paul, D. R. "Evaluation of the Binary Interaction Energy Density between Styrene and Acrylonitrile Units and Its Temperature Dependence", *Macromolecules* **2002**, *35*, 2078–2083.



